REUSE OF FLOWBACK FLUIDS AS HYDRAULIC FRACTURING FLUIDS IN TIGHT GAS SAND RESERVOIRS

A Dissertation

by

ASHKAN HAGHSHENAS

Submitted to the Office of Graduate and Professional Studies of
Texas A&M University
in partial fulfillment of the requirements for the degree of

DOCTOR OF PHILOSOPHY

Chair of Committee,	Hisham A. Nasr-El-Din
Committee Members,	Stephen A. Holditch
	Jerome Schubert
	Mahmoud El-Halwagi
Head of Department,	A. Daniel Hill

May 2015

Major Subject: Petroleum Engineering

ABSTRACT

Hydraulic fracturing fluids are usually prepared in the field using fresh water. High costs of water acquisition and waste water disposal, and the lack of available water resources near operation sites, make the reuse of produced water an unavoidable option. One of the fluid properties to be considered in investigating the applicability of these fluids as the fracturing base fluid is the total dissolved solids (TDS).

The main objectives of the first section of this work are to investigate the feasibility of using produced water in hydraulic fracturing in sandstone fields at reservoir temperatures and study the use of chelating agents to expand the acceptable range of TDS in fracturing base fluids. The effect of salts and chelating agents on the proppant transport and rheological properties of fracturing fluids was examined in detail. A high-pH guar/borate fluid was selected as the base fluid and loaded with different concentrations of sodium, potassium, calcium, magnesium, and ethylenediaminetetraacetic acid, diammonium salt (EDTA). The experiments were conducted at 140, 225, and 305°F and a pressure of 300 psi.

The results show that the presence of 2 wt% EDTA increased the acceptable maximum limit for TDS content of the base hydraulic fracturing fluid without compromising the performance of the fluid. More than 85% of analyzed flowback fluids from the West Texas region (Ozona, Canyon) were suitable to be used in future jobs with no further treatment regarding ion contents.

In the second section, we developed a decision tree to optimize selection of fracturing fluid based on extensive reservoir data obtained from tight sand fields in Texas. We reviewed completion and production reports on 164 wells, from five tight gas sand reservoirs in Texas, that were completed using six different fracturing fluid categories. Bottomhole temperature, reservoir pressure gradient, mechanical strength of barriers above and below the target zone, and pay zone thickness were the six selected variables for this analysis. We could reach the Out-Of-Bag error of 28.54% which seems reasonable with the complex dataset understudy. Bottomhole temperature and Young's modulus of the lower barrier are the most and the least important variables in this process, respectively. CO_2/N_2/foam assisted hybrid fluid was the best predicted by our model with an error of approximately 20%.

DEDICATION

To my parents and my brother for their unconditional love and support

ACKNOWLEDGEMENTS

First and foremost I offer my sincerest gratitude to my supervisor, Dr. Hisham Nasr-El-Din, who has given me the great opportunity and honor to work with him in Texas A&M University. He has supported me throughout my work with his patience and knowledge.

A debt of gratitude is owed to the committee members Dr. Stephen A. Holditch, Dr. Jerome Schubert and Dr. Mahmoud El-Halwagi, who has helped me with their constructive recommendations to improve my work.

I have had a great deal of institutional support as well as interest and assistance from number of individuals in this dissertation completion. The Department of Petroleum Engineering has provided the support and equipment I have needed to produce and complete my dissertation and the Crisman Institute for Petroleum Research has funded my studies. Baker Hughes has provided the chemicals and technical support for my experiments and I had the chance to talk to some of their experts in different occasions and I am very thankful for their help.

I acknowledge Miss Kristina Hansen who proofread my papers and works. I express my appreciation to my colleagues especially, Dr. Ahmed Goma, Dr. Guanqun Wang, Mohammed Sayed, Hayian Jao, and Khatere Sokhanvarian. Thanks also go to the

department faculty and staff for making my time at Texas A&M University a great experience.

Very special thanks go out to Mehrnoosh Saneifar, Vahid Serajian, Simin Sadeghi, and Amir Nikoienejad, who have helped me in the last part of my project in the developing decision tree for fracturing fluid selection.

Finally, I thank my family for supporting me throughout all my studies. Although I didn't have them physically with me during my study in Texas A&M University, I could always feel their presence in my heart. My brother was not only the big brother he was in my whole life, he was also my best friend, motivator, and support during this period of my life.

TABLE OF CONTENTS

Page

ABSTRACT ii

DEDICATION iv

ACKNOWLEDGEMENTS v

TABLE OF CONTENTS vii

LIST OF FIGURES ix

LIST OF TABLES xvi

CHAPTER I INTRODUCTION 1

1.1 Background 2
1.2 Statement of Problem 7
1.3 Research Objectives 8
1.4 Method Overview 8
1.5 Outline of Dissertation 10

CHAPTER II EFFECT OF DISSOLVED SOLIDS ON REUSE OF PRODUCED WATER AT HIGH TEMPERATURE IN HYDRAULIC FRACTURING JOBS* 12

2.1 Introduction 12
2.2 Experimental Studies 14
2.3 Flowback Fluid Analyses 15
2.4 Materials 15
2.5 Procedures 15
2.6 Results and Discussion 18
2.6.1 Viscosity Measurement Tests 18
2.6.2 Effect of Temperature on High-pH Borate Crosslinked Guar-Based Polymer 28
2.6.3 Small-Amplitude Oscillatory Shear (SAOS) Measurements 30
2.6.4 Static Settling Tests 33
2.7 Conclusions 37

CHAPTER III A FEASIBILITY STUDY OF REUSING FLOWBACK FLUIDS IN HYDRAULIC FRACTURING TREATMENTS* 39

3.1 Introduction 39
3.2 Experimental Studies 42

Page

3.3 Materials 43
3.4 Chelating Agent 44
3.5 Preparation of Base Fluids 45
3.6 Results and Discussion 47
3.6.1 Viscosity Measurements 47
3.6.2 Thermal Stability at Bottomhole Temperatures 54
3.6.3 Small-Amplitude Oscillatory Shear (SAOS) Measurements 56
3.6.4 Static Settling Tests 59
3.7 Conclusions 63

CHAPTER IV A ROBUST ADVISORY SYSTEM FOR SELECTION OF FRACTURING FLUID IN TIGHT GAS SAND RESERVOIRS 64

4.1 Introduction 64
4.2 Methodology 65
4.3 Random Forest Algorithm 68
4.4 Data Gathering 70
4.5 Properties and Characteristics of the Selected Reservoirs 72
4.6 Reservoirs Selection 77
4.6.1 Cotton Valley Reservoir 77
4.6.2 Olmos Reservoir 79
4.6.3 Canyon Sand Reservoir 81
4.6.4 Morrow Reservoir 82
4.6.5 Bossier Reservoir 84
4.7 Results and Discussion 85
4.8 Conclusions 92

CHAPTER V CONCLUSIONS AND RECOMMENDATIONS 94

5.1 Effect of Dissolved Solids on Reuse of Produced Water at High Temperature in Hydraulic Fracturing Jobs 94
5.2 A Feasibility Study of Reusing Flowback Fluids in Hydraulic Fracturing Treatments 95
5.3 A Robust Advisory System for Selection of Fracturing Fluid in Tight Gas Sand Reservoirs 97
5.4 Recommendations 98

REFERENCES 100

LIST OF FIGURES

Page

Fig. 2. 1 Precipitation of gel prepared with 35 pptg guar, 4.0 gpt buffer, 1.0 gpt crosslinker loading, and 600 ppm magnesium after a shear viscosity test at 225°F (107°C) and 300 psi (2,068 kPa). In the picture on the left, there are some precipitation on the bob, and in the picture on the right, precipitation can be seen at the bottom of the measuring cup. 20

Fig. 2. 2 Comparison between gels prepared with different concentrations of divalent ions at 40 and 170 s^{-1}, 140°F (60°C), and 300 psi (2,068 kPa). The base fluid was a gel prepared with 20 pptg guar, 1.75 gpt buffer, and 1.0 gpt crosslinker loading. 21

Fig. 2. 3 Comparison between gels prepared with different concentrations of monovalent ions at 40 and 170 s^{-1}, 140°F (60°C), and 300 psi (2,068 kPa). The base fluid was a gel prepared with 20 pptg guar, 1.75 gpt buffer, and 1.0 gpt crosslinker loading. 22

Fig. 2. 4 Comparison between gels prepared with different concentrations of divalent ions at 40 and 170 s^{-1}, 225°F (107°C), and 300 psi (2,068 kPa). The base fluid was a gel prepared with 35 pptg guar, 4 gpt buffer, and 1.0 gpt crosslinker loading. 22

Fig. 2. 5 Comparison between gels prepared with different concentrations of monovalent ions at 40 and 170 s^{-1}, 225°F (107°C), and 300 psi (2,068 kPa). The base fluid was a gel prepared with 35 pptg guar, 4 gpt buffer, and 1.0 gpt crosslinker loading. 23

Fig. 2. 6 Comparison between gels prepared with different concentrations of divalent ions at 40 and 170 s^{-1}, 305°F (152°C), and 300 psi (2,068 kPa). The base fluid was a gel prepared with 50 pptg guar, 4 gpt buffer, and 2.0 gpt crosslinker loading. 23

Fig. 2. 7 Comparison between gels prepared with different concentrations of monovalent ions at 40 and 170 s^{-1}, 305°F (152°C), and 300 psi (2,068 kPa). The base fluid was a gel prepared with 50 pptg guar, 4 gpt buffer, and 2.0 gpt crosslinker loading. 24

Fig. 2. 8 Comparison between gels prepared with DI water and the fluids containing different concentrations of calcium at 225°F (107°C) and 300 psi (2,068 kPa). The base fluid was a gel prepared with 35 pptg guar, 4 gpt buffer, and 1.0 gpt crosslinker loading. 26

Page

Fig. 2. 9 Comparison between gels prepared with DI water and the fluids containing different concentrations of magnesium at 225°F (107°C) and 300 psi (2,068 kPa). The base fluid was a gel prepared with 35 pptg guar, 4 gpt buffer, and 1.0 gpt crosslinker loading. 26

Fig. 2. 10 Comparison between gels prepared with DI water and the fluids containing different concentrations of sodium at 225°F (107°C) and 300 psi (2,068 kPa). The base fluid was a gel prepared with 35 pptg guar, 4 gpt buffer, and 1.0 gpt crosslinker loading.....27

Fig. 2. 11 Comparison between gels prepared with DI water and the fluids containing different concentrations of potassium at 225°F (107°C) and 300 psi (2,068 kPa). The base fluid was a gel prepared with 35 pptg guar, 4 gpt buffer, and 1.0 gpt crosslinker loading. 27

Fig. 2. 12 Single shear rate test to investigate the stability of proposed fluids at 140, 225, and 305°F (60, 107, and 152°C); 170 s^{-1}; and 300 psi (2,068 kPa). The base fluids were gels prepared with 20, 35, and 50 pptg of polymer; 1.75, 4, and 4 gpt buffer, and 1.0, 1.0 and 2.0 gpt crosslinker was selected as the base fluid at 140, 225, and 305°F (60, 107, and 152°C), respectively. 29

Fig. 2. 13 SAOS measurements performed on the gel prepared with fresh water and the fluid loaded with the maximum acceptable dissolved solid contents at 75°F (24°C) and 5% applied strain. The base fluid was a gel prepared with 20 pptg guar, 1.75 gpt buffer, and 1.0 gpt crosslinker loading. 32

Fig. 2. 14 SAOS measurements performed on the gel prepared with fresh water and the fluid loaded with the maximum acceptable dissolved solid contents at 225°F (107°C) and 5% applied strain. The base fluid was a gel prepared with 20 pptg guar, 1.75 gpt buffer, and 1.0 gpt crosslinker loading. 32

Fig. 2. 15 SAOS measurements performed on the gel prepared with fresh water and the fluid loaded with the maximum acceptable dissolved solid contents at 225°F (107°C) and 5% applied strain. The base fluid was a gel prepared with 35 pptg guar, 4.0 gpt buffer, and 1.0 gpt crosslinker loading. 33

Page

Fig. 2. 16 Static proppant settling test on the fluid prepared with maximum acceptable dissolved solid contents which was loaded with 4 lbm/gal of 20/40 Ottawa sand at 225°F (107°C). The base fluid was a gel prepared with 20 pptg guar, 1.75 gpt buffer, and 1.0 gpt crosslinker loading. 35

Fig. 2. 17 Comparison between proppant settling of sample prepared with fresh water and the fluid prepared with the maximum acceptable dissolved solid contents which were loaded with 4 lbm/gal of 20/40 Ottawa sand at 75°F (24°C). The base fluid was a gel prepared with 20 pptg guar, 1.75 gpt buffer, and 1.0 gpt crosslinker loading. 36

Fig. 2. 18 Comparison between proppant settling of sample prepared with fresh water and the fluid prepared with the maximum acceptable dissolved solid contents which were loaded with 4 lbm/gal of 20/40 Ottawa sand at 225°F (107°C). The base fluid was a gel prepared with 20 pptg guar, 1.75 gpt buffer, and 1.0 gpt crosslinker loading. 36

Fig. 2. 19 Comparison between proppant settling of sample prepared with fresh water and the fluid prepared with the maximum acceptable dissolved solid contents which were loaded with 4 lbm/gal of 20/40 Ottawa sand at 225°F (107°C). The base fluid was a gel prepared with 35 pptg guar, 4.0 gpt buffer, and 1.0 gpt crosslinker loading. 37

Fig. 3. 1 Comparison between gels prepared with DI water and the fluids containing different Ca^{++} concentrations at 225°F and 300 psi. The base fluid was a gel prepared with 30 pptg guar, 2 wt% EDTA, 19 gpt buffer, and 1.25 gpt crosslinker loading. 49

Fig. 3. 2 Comparison between gels prepared with DI water and fluids containing different Mg^{++} concentrations at 225°F and 300 psi. The base fluid was a gel prepared with 30 pptg guar, 2 wt% EDTA, 19 gpt buffer, and 1.25 gpt crosslinker loading. 49

Fig. 3. 3 Comparison between gels prepared with DI water and fluids containing different Na^{+} concentrations at 225°F and 300 psi. The base fluid was a gel prepared with 30 pptg guar, 2 wt% EDTA, 19 gpt buffer, and 1.25 gpt crosslinker loading. 50

Fig. 3. 4 Comparison between gels prepared with DI water and fluids containing different K^{+} concentrations at 225°F and 300 psi. The base fluid was a gel prepared with 30 pptg guar, 2 wt% EDTA, 19 gpt buffer, and 1.25 gpt crosslinker loading. 50

Page

Fig. 3. 5 Comparison between gels prepared with different concentrations of divalent ions at 40 s^{-1}, 140°F, and 300 psi. The base fluid was a gel prepared with 20 pptg guar, 2 wt% EDTA, 16 gpt buffer, and 1.0 gpt crosslinker loading. The gels without EDTA were prepared with 20 pptg guar, 2.0 gpt buffer, and 1.0 gpt crosslinker loading. 51

Fig. 3. 6 Comparison between gels prepared with different concentrations of monovalent ions at 40 s^{-1}, 140°F, and 300 psi. The base fluid was a gel prepared with 20 pptg guar, 2 wt% EDTA, 16 gpt buffer, and 1.0 gpt crosslinker loading. The gels without EDTA were prepared with 20 pptg guar, 2.0 gpt buffer, and 1.0 gpt crosslinker loading. 52

Fig. 3. 7 Comparison between gels prepared with different concentrations of divalent ions at 40 s^{-1}, 225°F, and 300 psi. The base fluid was a gel prepared with 30 pptg guar, 2 wt% EDTA, 19 gpt buffer, and 1.25 gpt crosslinker loading. The gels without EDTA were prepared with 35 pptg guar, 4.0 gpt buffer, and 1.0 gpt crosslinker loading. 52

Fig. 3. 8 Comparison between gels prepared with different concentrations of monovalent ions at 40 s^{-1}, 225°F, and 300 psi. The base fluid was a gel prepared with 30 pptg guar, 2 wt% EDTA, 19 gpt buffer, and 1.25 gpt crosslinker loading. The gels without EDTA were prepared with 35 pptg guar, 4.0 gpt buffer, and 1.0 gpt crosslinker loading. 53

Fig. 3. 9 Comparison between gels prepared with different concentrations of divalent ions at 40 s^{-1}, 305°F, and 300 psi. The base fluid was a gel prepared with 50 pptg guar, 2 wt% EDTA, 20 gpt buffer, and 3.0 gpt crosslinker loading. The gels without EDTA were prepared with 50 pptg guar, 4.0 gpt buffer, and 3.0 gpt crosslinker loading. 53

Fig. 3. 10 Comparison between gels prepared with different concentrations of monovalent ions at 40 s^{-1}, 305°F, and 300 psi. The base fluid was a gel prepared with 50 pptg guar, 2 wt% EDTA, 20 gpt buffer, and 3.0 gpt crosslinker loading. The gels without EDTA were prepared with 50 pptg guar, 4.0 gpt buffer, and 3.0 gpt crosslinker loading. 54

Page

Fig. 3. 11 Single shear rate test to investigate the stability of proposed fluids at 140, 225, and 305°F; 170 s^{-1}; and 300 psi. The base fluids were gels prepared with 20, 30, and 50 pptg of polymer; 2 wt% EDTA, 16, 19, and 20 gpt buffer; and 1.0, 1.25 and 3.0 gpt crosslinker was selected as the base fluid at 140, 225, and 305°F, respectively. The gels without EDTA were prepared with 20, 35, and 50 pptg guar, 2.0, 4.0, and 4.0 gpt buffer, and 1.0, 1.0, and 3.0 gpt crosslinker loading at 140, 225, and 305°F, respectively. 55

Fig. 3. 12 SAOS measurements performed on the gel prepared with fresh water and the fluid loaded with the maximum acceptable dissolved solid contents at 75°F and 5% applied strain. The base fluid was a gel prepared with 20 pptg guar, 2 wt% EDTA, 16 gpt buffer, and 1.0 gpt crosslinker loading. 57

Fig. 3. 13 SAOS measurements performed on the gel prepared with fresh water and the fluid loaded with the maximum acceptable dissolved solid contents at 225°F and 5% applied strain. The base fluid was a gel prepared with 20 pptg guar, 2 wt% EDTA, 19 gpt buffer, and 2.0 gpt crosslinker loading. 58

Fig. 3. 14 SAOS measurements performed on the gel prepared with fresh water and the fluid loaded with the maximum acceptable dissolved solid contents at 225°F and 5% applied strain. The base fluid was a gel prepared with 30 pptg guar, 2 wt% EDTA, 19 gpt buffer, and 1.25 gpt crosslinker loading. 58

Fig. 3. 15 Comparison between proppant settling of sample prepared with fresh water and the fluid prepared with the maximum acceptable dissolved solid contents which were loaded with 4 lb_m/gal of 20/40 Ottawa sand at 75°F. The base fluid was a gel prepared with 20 pptg guar, 2 wt% EDTA, 16 gpt buffer, and 1.0 gpt crosslinker loading. 61

Fig. 3. 16 Comparison between proppant settling of sample prepared with fresh water and the fluid prepared with the maximum acceptable dissolved solid contents which were loaded with 4 lb_m/gal of 20/40 Ottawa sand at 225°F. The base fluid was a gel prepared with 20 pptg guar, 2 wt% EDTA, 19 gpt buffer, and 2.0 gpt crosslinker loading. 61

Page

Fig. 3. 17 Comparison between proppant settling of sample prepared with fresh water and the fluid prepared with the maximum acceptable dissolved solid contents which were loaded with 4 lb_m/gal of 20/40 Ottawa sand at 225°F. The base fluid was a gel prepared with 30 pptg guar, 2 wt% EDTA, 19 gpt buffer, and 1.25 gpt crosslinker loading. 62

Fig. 3. 18 Static proppant settling test on the fluid prepared with maximum acceptable dissolved solid contents which was loaded with 4 lbm/gal of 20/40 Ottawa sand at 225°F. The base fluid was a gel prepared with 30 pptg guar, 2 wt% EDTA, 19 gpt buffer, and 1.25 gpt crosslinker loading. 62

Fig. 4. 1 Reservoirs selected for the study (the red stars on the map show the location of the reservoirs). 71

Fig. 4. 2 Distribution of pay zone thickness for all selected wells. 73

Fig. 4. 3 Distribution of pressure gradient for all selected wells. 73

Fig. 4. 4 Distribution of bottomhole pressure for all selected wells. 74

Fig. 4. 5 Distribution of bottomhole temperature for all selected wells. 74

Fig. 4. 6 Cotton Valley reservoir wells snapshot (Thirty one wells were selected from Gregg and Smith Counties in Texas) 79

Fig. 4. 7 Olmos reservoir wells snapshot (Forty wells were selected from Webb County in Texas) 80

Fig. 4. 8 Canyon Sand reservoir wells snapshot (Thirty three wells were selected from Crockett County in Texas) 82

Fig. 4. 9 Morrow reservoir wells snapshot (Thirty wells were selected from Ochiltree, Roberts, Hansford, Lipscomb, and Hemphill Counties in Texas) 83

Fig. 4. 10 Bossier reservoir wells snapshot (Thirty wells were selected from Freestone County in Texas) 85

Fig. 4. 11 Fracturing fluid categories distribution in the selected dataset. 86

Fig. 4. 12 Minimum number of acceptable trees for the applied dataset. 87

Fig. 4. 13 The decision tree generated in the first run with 38 nodes and 29.02% OOB error. YM and LB are the abbreviations of Young's modulus and lower barrier, respectively. 89

Fig. 4. 14 The decision tree generated in the 47th run with 38 nodes and 28.54% OOB error. YM and LB are the abbreviations of Young's modulus and lower barrier, respectively. 90

Fig. 4. 15 Accuracy of the two proposed models with 38 and 19 nodes versus size of tree 91

Fig. 4. 16 Applied variables versus mean decrease accuracy (LBarrier, UBarrier and YMLB are the abbreviations of lower barrier, upper barrier, and Young's modulus of lower barrier, respectively) 91

LIST OF TABLES

Page

Table 2. 1 Composition and range of ion contents.[a] 17

Table 2. 2 Power-law parameters of prepared fracturing fluids which were loaded with different salt concentrations at 225°F (107°C) and 300 psi (2,068 kPa) 28

Table 3. 1 Chemical composition for typical seawater/formation water[a] 44

Table 4. 1 Sample of the wells properties 72

CHAPTER I

INTRODUCTION

Hydraulic fracturing is the most effective stimulation treatment in unconventional resources. One of the most important challenges in fracturing operations is the large volumes of water consumption and waste water disposal. Environmental and economical attributes of flowback fluids in the oil industry make water treatment an inevitable decision. Applications of produced water in hydraulic fracturing jobs result in low quality fracturing fluid. This is especially true for flowback fluids, which contain high polymer loading. However, seawater and flowback water, obtained either from slickwater or other treatments with low chemical loadings, can also be considered to be used as the base fluid for the hydraulic fracturing jobs. Currently, no practical operating range for produced water content is available, and applied methods are individually developed for specific jobs. Literature review indicated that use of chemical treatment techniques in reuse of produced waters has recently increased. A few practical ranges for TDS limitation were previously determined. Most of the reported ranges of TDS were based on specific jobs.

Furthermore, optimum selection of the fracturing fluid requires a profound understanding of the related reservoir properties. In this work, we developed a robust model for improved selection of fracturing fluids in tight gas sand formations. The application of the developed model can lead to reduction of the cost associated with hydraulic fracturing projects and enhancement of the ultimate production.

1.1 Background

Large amounts of produced water in the oil industry make it an international concern. More than 7 billion barrels of water were produced in 2007 in Texas alone, which was 35% of total U.S. produced water (Clark and Veil 2009). The use of five million gallons of fresh water in unconventional wells during hydraulic fracturing jobs is very common. The main sources to provide fresh water for fracturing jobs are ponds, rivers, and aquifers. Sometimes these sources are far from the location, and the shipment of the water from long distances to the well site is needed. Flowback and produced water can contain dissolved organic materials, fracturing fluid additives, and dissolved minerals from the formation (Fontenelle et al. 2013). Initial load recovery for the Pinedale Anticline field, located in southwestern Wyoming, is approximately 25 to 50% (Shafer 2011). Transportation costs is a major portion of the cost of water acquisition and handling, 56 to 84% of total costs, which can justify re-use of produced water from an economic point of view (Stepan et al. 2010).

Fracturing fluid contents can vary and include gelling agents, crosslinkers, pH adjusting agents, friction reducers, breakers, scale inhibitors, corrosion inhibitors, biocides, iron control agents, and some more additives, based on jobs requirements. The additives selection depends on location, reservoir formation and fluid, base fluid, and job design preference (Loveless et al. 2011). Required water treatments to qualify produced waters for hydraulic fracturing applications are not intensive (Blauch 2010). Harris et al. (2005) supported this by stating, “Several rheological properties directly impact a frac

fluid's performance: (1) apparent viscosity, (2) yield stress, (3) dynamic viscosity, (4) rheomalaxis (irreversible thixotropy), (5) viscoelasticity, and (6) the related issue of turbulent-drag reduction." One of the methods applied in water treatment was the electrocoagulation (EC) method. EC does not remove dissolved ions, so the salinity of the treated fluid is high (Fontenelle et al. 2013). A previous work introduced a substitute for commonly used fracturing fluid, which consists of modified guar, buffer, and crosslinker in a NaBr brine solution in ultra-deep wells. In ultra-deep fracturing stimulation, high-density brine-based fluid is needed to control hydrostatic pressures. The commonly used system is hard to break and expensive. They reported improvement in proppant transporting and a regain in conductivity in the developed fluid (Gupta et al. 2012a). Harris et al. (2005) also stated, "Proppant transport is a function of (1) wellbore and fracture geometry; (2) volumetric rate; (3) proppant size, concentration and specific density; and (4) carrier-fluid rheology

The main functions of fracturing fluids are having sufficient viscosity to generate fracture geometry and transport proppants (Harris et al. 2009a). In another work, produced water was used in fracturing fluid focusing on the good proppant transport characteristics and good regain of conductivity. The polymer/surfactant ratio, breaker effect, conductivity, and friction loop tests were applied at various temperatures and different loadings (Gupta et al. 2012a, 2012b).

The quality of flowback fluid depends on the applied treatment as well as formation and hydrocarbon characteristics. The TDS of flowback fluids can range from 100 to over 400,000 mg/l (Guerra et al. 2011). Some jobs, such as slickwater treatments,

can flow back fairly fresh waters that can be reused after some hydrocarbon and organic material removal, pH adjustment, scale removal, and bacteria removal processes. In high salt contaminated fluids it is also necessary to reduce the TDS of the fluid. This is one of the most important processes in water treatments and various techniques like evaporation, membrane filtration, distillation, electric separation, and chemical treatment have been tried by various operators (Arthur et al. 2005; Arthur et al. 2010; Veil 2010). These methods have shown limited success in some cases. This has encouraged oil and gas companies to invest more on water treatment systems and to develop new techniques to reduce costs. Onsite treatments can greatly help to reduce water acquisition, transportation, and disposal costs. Quality and quantity of flowback fluids, future job characteristics, governmental, and practicability are factors that influence the decision making process.

The idea of using seawater and produced water in hydraulic fracturing is not new (Harris and van Batenburg 1999; Le and Wood 1992). Previous works indicated that there were conflicting opinions regarding the concept of using other sources of water instead of fresh water. For example, some researchers show that high salinity can help breakers while others believe the reverse effect (Harris and van Batenburg 1999; Hassen et al. 2012). Although borate crosslinked guar-based gel has minimal shear sensitivity and gel residue (Wiskofske et al. 1997), Gupta et al. (2013) stated that despite better and faster clean up and the ability to provide good proppant pack conductivity, conventional borate crosslinkers are not good candidates at temperatures greater than 225°F. The wide

differences in these reports have resulted in uncertainty regarding the use of the methodology.

This study investigated the role of chelating agents to increase the admissibility of higher TDS in the fracturing fluids without compromising their main functions. The effect of chelating agents on multivalent cations has been widely studied (Putzig and St. Clair 2007; Blauch 2010; Fedorov et al. 2010, 2014; Gupta et al. 2013). EDTA was applied to reduce or eliminate the impact of divalent cations (Mg^{2+} and Ca^{2+}). The interference of high concentrations of monovalent cations such as Na^{+} and K^{+} with viscosity build up was reduced by using a more compatible buffer and higher pH. The suitable pH window for guar/borate crosslinker starts from 9.5 (Pezron et al. 1990). In this study, the range of pH values was 10.5 to 12.5.

The first part of this study sets the proppant transport, viscosity, and rheological properties of fracturing fluids as the main concerns to define the critical dissolved solid contents in the reuse of flowback fluid to help minimize water handling costs and footprints.

Fracturing fluid selection is a crucial element of hydraulic fracturing treatment design. Certain variables, such as reservoir pressure and temperature, thickness of fracturing interval, strength of upper and lower barriers, half-length fracture, existence of natural fractures, and formation lithology can affect efficiency of the hydraulic fracture job. Computational and statistical techniques such as empirical relationships, multivariate analysis, Artificial Neural Network (ANN), nearest neighbor algorithm have been commonly applied for optimizing hydraulic fracturing design (Ali 1994;

Anifowose et al. 2013; Sitouah et al. 2013; Voneiff et al. 2013 and 2014; Aulia et al. 2014; Mehrgini et al. 2014; Maucec et al. 2015). However, these techniques are often blindly applied, without a sufficient statistical and computational background, which can lead to inaccurate outcome. Fundamental understanding of statistical techniques can help in selection of the appropriate method for a reliable application of these techniques. A dependable model should generate high prediction accuracy without high level of computational complexity (Sitouah et al. 2013).

The ensemble learning models have showed superior performance over the other individual learning techniques in solving complex problems. After investigating and examining different methods, random forest algorithm was selected as the most appropriate technique for building a fracturing fluid selection model. Random forest is especially suitable for this case where there are discrete and continuous variables and available data are often noisy and contain missing values (Anifowose et al. 2013).

In the second part of this work, we developed a robust model for improved selection of fracturing fluids in tight gas sand formations. The application of the developed model can lead to reduction of the cost associated with hydraulic fracturing projects and enhancement of the ultimate production.

1.2 Statement of Problem

Economic production from tight sand gas reservoirs usually involves multistage hydraulic fracturing. High costs of water acquisition and waste water disposal, and the lack of available water resources near operation sites, make the reuse of produced water an unavoidable option. However, recycling produced water in hydraulic fracturing jobs result in low quality fracturing fluids, which usually have high levels of hardness and salinity. This is especially true for flowback fluids, which contain high polymer loading. The viscosity and rheological properties of fracturing fluids significantly affect leak-off rate, proppant placement, length and width of fractures, fracture conductivity, and consequently, the success of the treatment.

On the other hand, hydraulic fracturing is essential for development of tight gas sand formations. However, optimum selection of the fracturing fluid requires a profound understanding of the related reservoir properties. In this work, we developed a robust model for improved selection of fracturing fluids in tight gas sand formations. The application of the developed model can lead to reduction of the cost associated with hydraulic fracturing projects and enhancement of the ultimate production.

The objective of this study is to determine and improve the acceptable dissolved solid contents for flowback fluids to prepare fracturing fluids and introduce a reliable fluid selection method based on field data.

1.3 Research Objectives

Literature review indicated that the use of chemical treatment systems have recently received increased attention regarding TDS. The overall goal of the project is to provide industry with a viable option for the reuse of produced water. The detailed objectives of this work can be summarized as follows:

1. Investigation of the feasibility of using produced water in hydraulic fracturing stimulation in sandstone fields at reservoir temperature
2. Introduction of new techniques to evaluate the flowback fluid and to purify/qualify produced water
3. Develop a robust advisory system for selection of fracturing fluid in tight gas sand reservoirs
4. Reduction of high costs for water acquisition and produced water disposal

1.4 Method Overview

Analyses of 36 flowback fluid samples from the West Texas region were collected, and experimental studies were conducted on the analysis of the dissolved solids of produced water, which affect the application of flowback fluids and the capability of prepared fluids in proppant transport and handling. A high-pH borate crosslinked guar-based polymer was selected to determine the ranges of acceptable salt

contents. Dynamic viscosity and rheological properties tests, static proppant settling, and small-amplitude oscillation rheology were the methods used to evaluate prepared samples at low, medium, and high temperatures up to 305°F.

Some divalent cations such as calcium and magnesium have negative effects on the prepared polymers. Magnesium is the controlling ion, and approximately 30% of flowback fluids must be treated to meet the maximum acceptable concentration criterion. While monovalent cations such as sodium and potassium were tolerable at higher concentrations and the potassium contents in almost all flowback fluids met the determined acceptable value, more than 40% of samples required treatment for high sodium ion concentrations. Although the presence of other ions such as iron show no significant variation in fracturing fluid properties, they can affect treatment in special cases. Adjusting the concentrations of the polymer, buffer, and crosslinker can minimize the adverse effects of temperature and salts. The fluids prepared with the determined ranges of dissolved solids showed reasonable thermal stability and proppant transport characteristics. This work introduces the practical operating range for produced water composition and defines the ions that can adversely impact borate-crosslinked fracturing fluid characteristics at different temperatures.

The methodology part of constructing the decision rule for fluid selection is based on Random Forest learning method, which is one of the most common decision tree methods for relatively complex trees. We use this method since there is uncertainty about the structure of how covariates can enter the model. Moreover, this method has potential to reflect relatively complex forms of structure which seems hard or even

infeasible to detect with conventional methods of modeling. For instance, in this problem where predictors are a combination of factors and continuous variables.

1.5 Outline of Dissertation

Following the introductory chapter, this dissertation includes four additional chapters. Chapter II focuses on the analysis of the dissolved solid contents of produced water, which affects the application of flowback fluids and the capability of prepared fluids in proppant transport and handling. A series of laboratory experiments were conducted on a high-pH borate crosslinked guar-based polymer to determine the effects of salt species on the prepared polymer, ranges of acceptable salts contents, and ability to transport proppant. For this purpose, analyses of 36 flowback fluid samples from the West Texas region have been collected, and the maximum and minimum values of all of the contents have been determined to investigate the impact factor of each component. Dynamic rheology tests, traditional changing shear rates, the steady-shear viscosity, and small-amplitude oscillation rheology, were the methods used to evaluate prepared samples.

Chapter III objectives are to: (a) to investigate the feasibility of using produced water in hydraulic fracturing in sandstone fields at reservoir temperatures, (b) introduce new techniques to evaluate the flowback fluid and to purify/qualify produced water at high temperatures, and (c) study the use of chelating agents to expand the acceptable

range of TDS in fracturing base fluids. The effect of salts and chelating agents on the proppant transport and rheological properties of fracturing fluids was examined in detail.

Chapter IV focuses on developing a decision method to optimize selection of fracturing fluid based on extensive reservoir data obtained from tight sand fields in Texas. The influential reservoir parameters for development of this model were selected based on information obtained from literature, reservoir simulations, and outcome of surveys filled out by fracturing experts. Finding a correlation between these variables and the fracturing fluid is a challenging task.

Finally, Chapter V summarizes the concluding remarks of the research stemming from this dissertation and recommendations for future research.

CHAPTER II

EFFECT OF DISSOLVED SOLIDS ON REUSE OF PRODUCED WATER AT HIGH TEMPERATURE IN HYDRAULIC FRACTURING JOBS*

2.1 Introduction

The oil and gas industry is one of the largest fresh water consumers, as well as one of the highest contaminant water producers. More than 7 billion barrels of water were produced in Texas in 2007, more than one third of total U.S. produced water (Clark and Veil 2009). Each hydraulic fracturing job in unconventional wells usually consumes more than five million gallons of fresh water. The main sources providing fresh water for fracturing jobs are ponds, rivers, and aquifers. Sometimes these sources are far from the locations, requiring shipment of water over long distances to the well-site. Flowback and produced water can contain dissolved organic materials, fracturing fluid additives, and dissolved minerals from the formation (Fontenelle et al. 2013). The cost of water acquisition and handling in the Bakken field in 2010 ranged from 2.00 to 16.80 dollars per barrel; 56 to 84% of total costs were transportation costs, the reduction of which is a very good motivation to use produced water on site (Stepan et al. 2010).

---

*Reprinted with permission from "Effect of Dissolved Solids on Reuse of Produced Water at High Temperature in Hydraulic Fracturing Jobs" by Ashkan Haghshenas and Hisham Nasr-El-Din, 2014. *Journal of Natural Gas Science and Engineering.* **21** (2014) 316-325, Copyright 2014 by Elsevier B.V.

Fracturing fluids must have sufficient viscosity to generate fracture geometry and transport proppants (Harris et al. 2009a). Fracturing fluid contents can vary and include gelling agents, crosslinkers, pH adjusting agents, friction reducers, breakers, scale inhibitors, corrosion inhibitors, biocides, iron control agents, and some additional additives, based on job requirements. The selection of specific additives depends on the location, reservoir formation and fluid, base fluid, and job-design preference (Loveless et al. 2011). Harris et al. (2005) stated that the following rheological properties have a direct impact on the performance of a fracturing fluid: (1) apparent viscosity, (2) yield stress, (3) dynamic viscosity, (4) rheomalaxis (irreversible thixotropy), (5) viscoelasticity, and (6) the related issue of turbulent-drag reduction. In the presence of various chemical species, such as simple salts, alkalis, and surfactants, the physical and chemical nature of polymer molecules can change significantly during treatment processes (Nasr-El-Din and Taylor 1996). Gupta et al. (2012a) introduced a substitute for commonly used fracturing fluid, which consists of modified guar, buffer, and crosslinker in a NaBr brine solution for fracturing in ultra-deep wells. In ultra-deep fracturing stimulation, high-density brine-based fluid is needed to control hydrostatic pressures. The commonly used system is expensive and hard to break. The authors reported improvement in proppant transport and regaining conductivity in the developed fluid. Harris et al. (2005) stated that proppant transport is a function of (1) wellbore and fracture geometry; (2) volumetric rate; (3) proppant size, concentration and specific density; and (4) carrier-fluid rheology. Gupta et al. (2012a, 2012b) investigated the use of produced water in fracturing fluid, focusing on good proppant transport characteristics

and good restoration of conductivity. The polymer/surfactant ratio, breaker effect, conductivity, and friction loop tests were examined at various temperatures and different loadings.

This study sets forth the proppant transport and rheological properties of fracturing fluids as the main concerns to define the critical dissolved solid contents in the reuse of flowback fluid to help minimize water handling costs and footprints.

2.2 Experimental Studies

The experimental approach in this work focuses on rheological properties and proppant transport of fracturing fluids containing maximum acceptable ion contents. A guar-based gel is selected as the base fluid in this investigation. Although guar has 8 to 13% residue by weight, it actually has less residue by volume because of its high density material. Depending on the application, guar is an acceptable polymer. Also, crosslinked gel minimizes the amount of gel residue, and borate systems have minimal shear sensitivity (Wiskofske et al. 1998).

2.3 Flowback Fluid Analyses

Analyses of 36 samples from the West Texas region were collected, and maximum and minimum values of all the contents have been determined to investigate the impact factor of each component (**Table 2.1**). The first four ions in Table 2.1 (Na^+, K^+, Mg^{2+}, and Ca^{2+}) are the most influential ones in the reuse of flowback fluid; therefore, they were thoroughly examined.

2.4 Materials

A borate crosslinked galactomannan (guar/borate) was selected as the base fluid. This fluid consists of guar gum, buffer (potassium carbonate, monoethanolamine, and a mixture of potassium carbonate and potassium hydroxide), and a crosslinker (borate solution) as the base components. Deionized (DI) water was used to prepare polymer solutions. ACS Grade salts ($CaCl_2 \cdot 2H_2O$, $MgCl_2 \cdot 6H_2O$, KCl, and NaCl) were used to prepare synthetic flowback fluids.

2.5 Procedures

The following procedure was used to prepare all samples:

1. 700 (± 5) ml of fresh water or salt water was placed in a 1000 ml beaker to prepare the linear gel.

2. A blender was used at 500 rpm circulating rate, which was needed to establish a vortex shape with no air bubbles trapped.

3. A predetermined volume of the guar gum was added slowly from the shoulder of the created vortex to prepare 20, 35, and 50 pptg (pound per thousand gallons) of polymer loading.

4. The solution was mixed for 30 (± 1) minutes. An increase in the rotational speed to 700 rpm was needed during the mixing time to have a good vortex with no air bubbles.

5. Finally, the buffer was added, followed by the crosslinker (based on the tables presented by the provider company), and mixed for five seconds before loading into the viscometer.

To recreate the same test conditions for all prepared fluids, all viscosity measurements were conducted one hour after the initial mixing to avoid any viscosity changes due to polymer hydrolysis (Nasr-El-Din and Taylor 1996). Four salts, $CaCl_2 \cdot 2H_2O$, $MgCl_2 \cdot 6H_2O$, KCl, and NaCl, each in four different concentrations (calcium: 200, 400, 600, and 800 ppm, magnesium: 200, 400, 600, and 800 ppm, sodium: 5,000, 7,000, 10,000, and 12,000 ppm, potassium: 500, 1,000, 2,000, 3,000 ppm), have been selected to run the experiments. All tests were repeated three times and the two closest values were averaged and reported.

Table 2. 1— Composition and range of ion contents.[a]

Ions	Minimum Concentration (mg/l)	Maximum Concentration (mg/l)
Ca^{2+}	137	20,100
Mg^{2+}	20	1,690
K^{+}	28	5,770
Na^{+}	540	74,600
Al^{3+}	0	4.33
B^{3+}	1	192
Si^{4+}	0	40.7
Sr^{2+}	0	5,049
Ba2+	0	2,175
$Fe(^{2+},^{3+})$	0.3	114
$SO42^{-}$	0	2,000
$HCO3^{-}$	76	1,190
Cl^{-}	1,200	153,000
$CO3^{2-}$	240	430
TDS[b]	2,900	252,000
TSS[c]	10	13,762

a Samples were collected from 36 flowback fluids following hydraulic fracturing jobs from the West Texas region.
b TDS = total dissolved solids, mg/l
c TSS = total suspended solids, mg/l

In this study, fluids for well temperatures up to 305 °F (152°C) were used at a pressure of 300 psi (2,068 kPa). Two dynamic measuring methods for rheological properties of fluids and proppant support and a static method for proppant transport experiments were conducted to compare the performance of the fluid systems from a broader perspective. The methods used to evaluate the fluids were changing shear rate, rheological properties at bottomhole temperatures, small-amplitude oscillatory shear (SAOS), and static settling.

2.6 Results and Discussion

2.6.1 Viscosity Measurement Tests

Crosslinking agents, such as commonly used borate crosslinked gels, improve fracturing fluid viscosity. Although they are less sensitive to shear rate changes and can provide higher conductivity in comparison with other fracturing fluids, they are sensitive to salt content. High salt concentrations and temperatures can affect the hydration of the polymer and the process of crosslinking. The fluid system with 20 pptg of polymer, 1.75 gpt buffer, and 1.0 gpt crosslinker was selected as the base fluid at 140°F (60°C) and different concentrations of salts were added for each case. Borate gels require a pH range between 9.5 and 10.5 for optimum efficiency; the pH was measured before and after viscosity measurements. If the measured pH is less than 9.5 after the experiments,

additional buffer was added and the experiment was repeated. The apparent viscosity was measured by using a M5600 viscometer as a function of the shear rate. **Fig. 2.1** shows some precipitations in the fluid that contains 600 ppm of magnesium chloride after a viscosity measuring test using a viscometer. Salt contents reduced the solubility of the prepared polymers, especially in the presence of divalent cations. The same phenomenon was observed in the presence of excessive concentrations of calcium, potassium and sodium. The experimental approach that was utilized in this section focused on salt concentrations and the viscosity of the prepared gel. These experiments investigated the maximum salt content for acceptable viscosity development over changing shear rates.

Laboratory tests were run to determine the viscous properties of fracturing fluids prepared with DI water and varying concentrations of different salts. The viscosity of samples prepared with different salt concentrations was measured and then compared to the viscosity of the original formulation. Typically, high viscous fluids are considered suitable candidates due to their good proppant transport capability, although plots cannot directly indicate proppant transport properties (Harris et al. 2009b). **Figs. 2.2 to 2.7** show the viscosity profiles of crosslinked gels containing four various salts in different concentrations. The limiting criteria for the acceptable viscosities were 600 and 100 cp at shear rates of 40 and 170 s^{-1}, respectively (Bunger et al. 2013). The results show that the acceptable salt concentrations at the shear rate of 40 s^{-1} are less than the ones at 170 s^{-1}. In the proppant settling process, lower shear rate viscosities are more important

because the proppant settling occurs at low shear rates. The maximum tolerable concentration for each salt was determined.

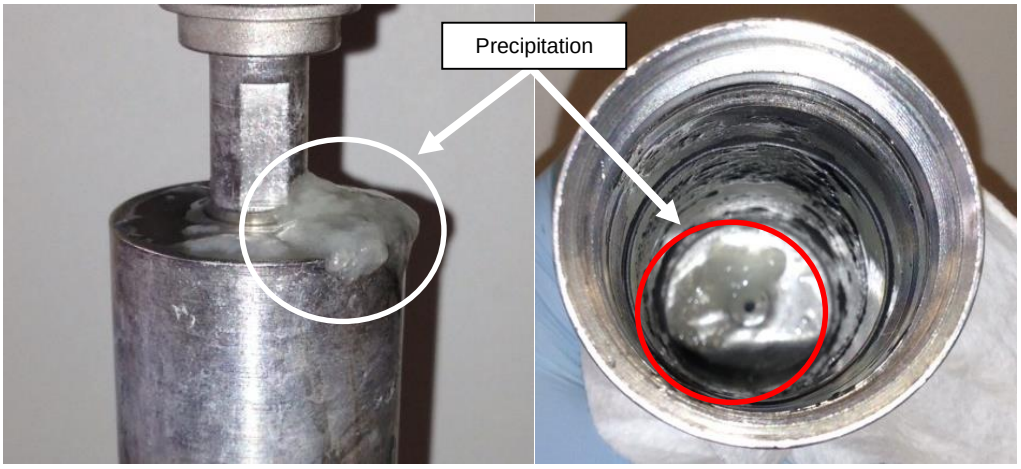

Fig. 2. 1— Precipitation of gel prepared with 35 pptg guar, 4.0 gpt buffer, 1.0 gpt crosslinker loading, and 600 ppm magnesium after a shear viscosity test at 225°F (107°C) and 300 psi (2,068 kPa). In the picture on the left, there are some precipitation on the bob, and in the picture on the right, precipitation can be seen at the bottom of the measuring cup.

Figs. 2.2 – 2.7 show the effect of various salt concentrations on the measured viscosity of the base fluid. The apparent viscosity of the borate crosslinked solution decreased as the salt concentrations was increased. The effects of divalent cations were more severe, and in smaller ranges they decreased the viscosity of the fluid significantly. The effect of temperature and salts can be controlled and compensated by tuning the concentration of the polymer, buffer, and crosslinker. To meet the minimum acceptable viscosity for the fluid and maintain the maximum acceptable salt concentrations, at higher temperatures an increase in polymer loadings was needed. In this study, 35 and 50 pptg of polymer, 4 gpt buffer and 1.0 and 2.0 gpt crosslinker were selected as the

base fluid at 225 and 305°F (107 and 152°C), respectively. The concentration for each additive was selected based on fluid preparation instructions from a local service company.

In all experiments, a similar viscosity profile trend was observed for all salt contents**. Figs. 2.8 to 2.11** show that the apparent viscosities at high shear rates (from 80 to 100 s^{-1} and higher) are almost the same. Therefore, it is difficult to interpret their behavior in that region. However, this range is wider and more realistic in near wellbore region than shear rate of 10 s^{-1}, which was reported in a previous study (Harris et al. 2009b). Guar is a bar-shaped polymer, and at low shear rates polymer chains are trapped together and are not aligned in the flow direction. Consequently, increasing the polymer concentration at low shear rates will significantly increase the resistance to flow.

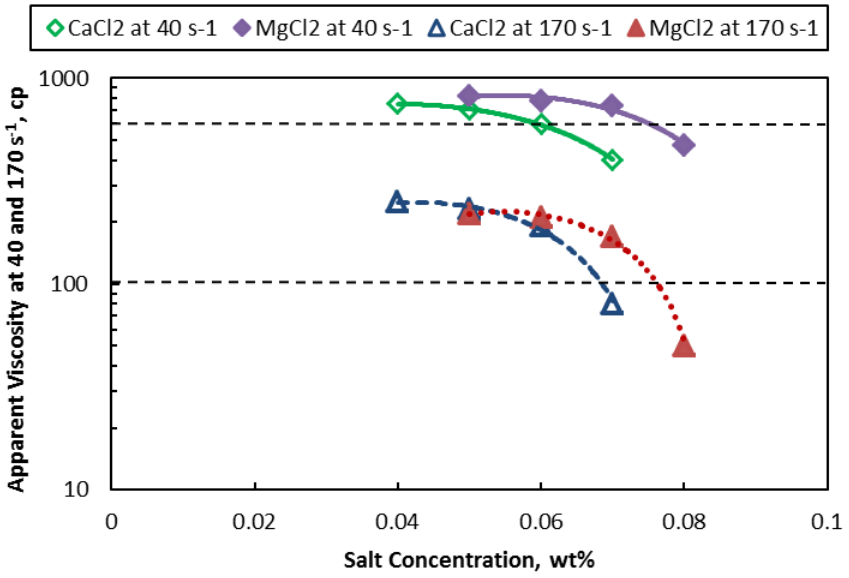

Fig. 2. 2— Comparison between gels prepared with different concentrations of divalent ions at 40 and 170 s^{-1}, 140°F (60°C), and 300 psi (2,068 kPa). The base fluid was a gel prepared with 20 pptg guar, 1.75 gpt buffer, and 1.0 gpt crosslinker loading.

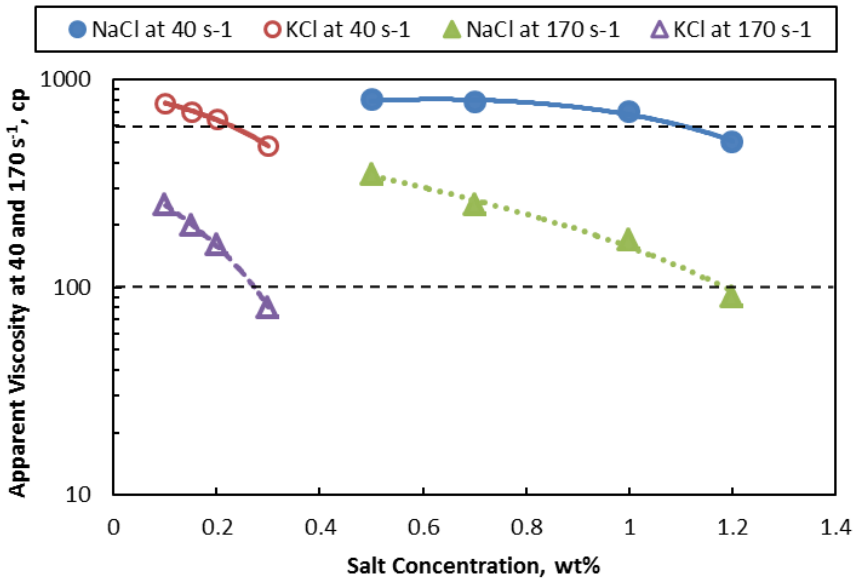

Fig. 2. 3— Comparison between gels prepared with different concentrations of monovalent ions at 40 and 170 s^{-1}, 140°F (60°C), and 300 psi (2,068 kPa). The base fluid was a gel prepared with 20 pptg guar, 1.75 gpt buffer, and 1.0 gpt crosslinker loading.

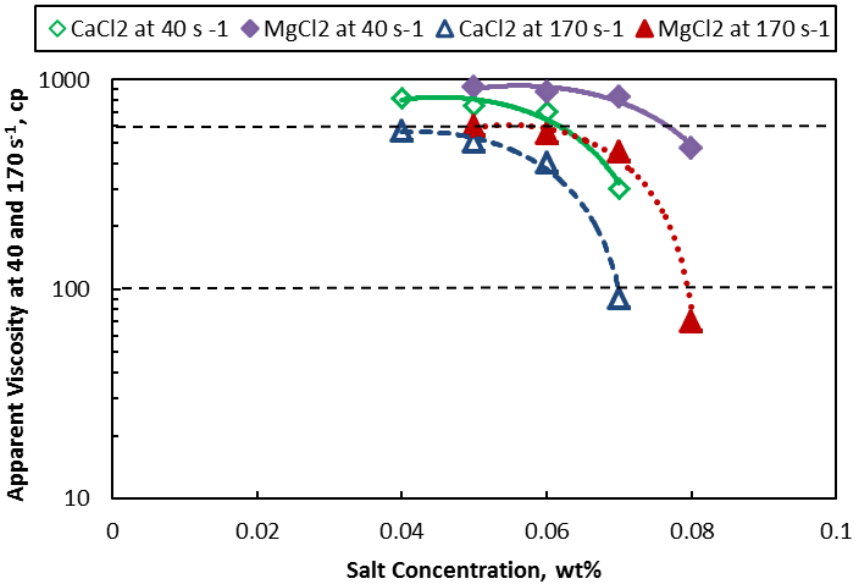

Fig. 2. 4— Comparison between gels prepared with different concentrations of divalent ions at 40 and 170 s^{-1}, 225°F (107°C), and 300 psi (2,068 kPa). The base fluid was a gel prepared with 35 pptg guar, 4 gpt buffer, and 1.0 gpt crosslinker loading.

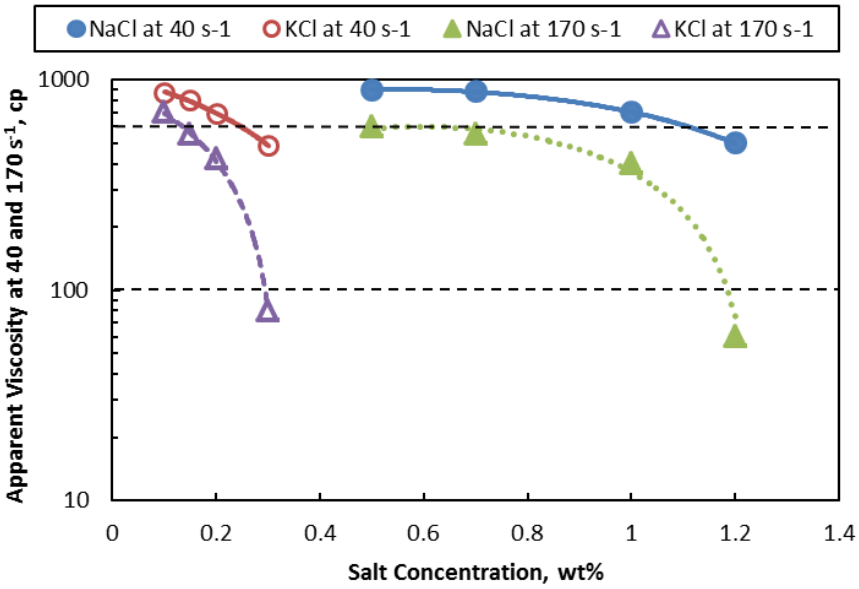

Fig. 2. 5— Comparison between gels prepared with different concentrations of monovalent ions at 40 and 170 s^{-1}, 225°F (107°C), and 300 psi (2,068 kPa). The base fluid was a gel prepared with 35 pptg guar, 4 gpt buffer, and 1.0 gpt crosslinker loading.

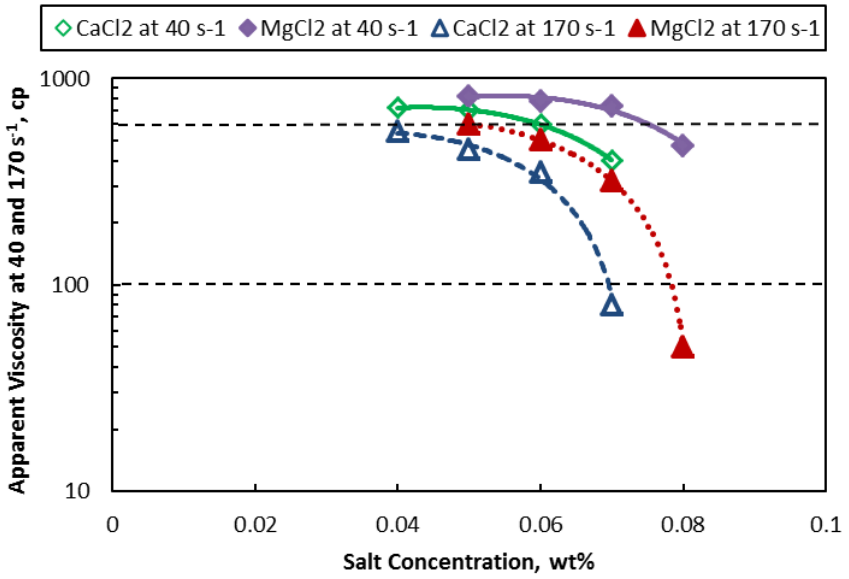

Fig. 2. 6— Comparison between gels prepared with different concentrations of divalent ions at 40 and 170 s^{-1}, 305°F (152°C), and 300 psi (2,068 kPa). The base fluid was a gel prepared with 50 pptg guar, 4 gpt buffer, and 2.0 gpt crosslinker loading.

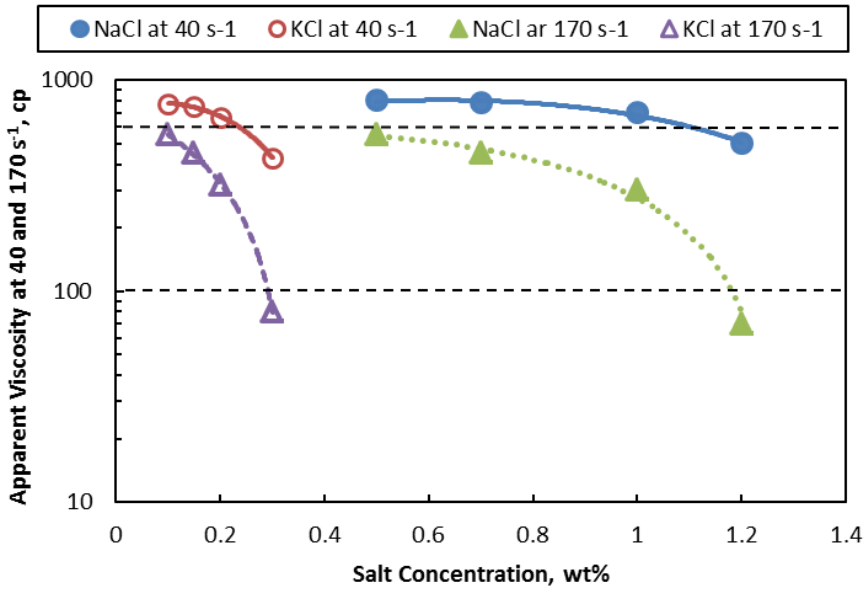

Fig. 2. 7— Comparison between gels prepared with different concentrations of monovalent ions at 40 and 170 s^{-1}, 305°F (152°C), and 300 psi (2,068 kPa). The base fluid was a gel prepared with 50 pptg guar, 4 gpt buffer, and 2.0 gpt crosslinker loading.

However, at high shear rates, the polymer chains are more aligned in the flow direction and the resistance to flow was not great. Increasing the polymer concentration at high shear rates would not significantly increase the viscosity of the polymer solution. Shear rates in the near wellbore region and in fractures vary from 100 to 10 s^{-1}; however, the tests have been run from 1 to 1,000 s^{-1} and vice versa to follow changes and trends.

In this work, the dissolved solid contents, including calcium, magnesium, sodium, and potassium, were investigated. Cationic ions can reduce the hydration of fracturing fluid viscosity. In the fluids containing Ca and Mg ions, the effects of these divalent cations were very dominant. In the presence of potassium carbonate as buffer, a significant amount of these cations precipitated in the forms of calcium carbonate and

magnesium carbonate, respectively, after the buffer was added to the solution. The insoluble contents significantly impact the crosslinking process. In some cases, monoethanolamine was used as a buffer in this work to avoid this problem and minimize precipitation. The maximum acceptable concentrations for Ca^{2+} and Mg^{2+} were approximately 600 and 750 ppm, which were higher than 75 and 71% of the measured values in the entire reported flowback fluid samples, respectively. For monovalent cations, Na^{+} and K^{+}, the maximum tolerable concentrations were much higher, 11,000 and 2,300 ppm, and these ranges cover more than 59 and 97% of analyzed samples, respectively. In some cases, the increased density helped to provide a higher viscosity in the presence of Na^{+} and K^{+}. In most of the flowback fluid analyses, the concentration of iron ions was 10 to 30 ppm. Although the results show that this concentration of iron does not affect the viscous properties of the prepared fracturing fluid, it can significantly reduce the functionality of breakers. No changes in measured viscosities were observed in the presence of 20 ppm iron ions. The viscosity/shear rate relationship for all prepared fluids follow the power-law model ($\mu = k\gamma^{n-1}$). Where μ is the apparent viscosity, mPa.s; k is the power-law constant, mpa.sn; γ is the shear rate, s^{-1}; and n is the power-law index, dimensionless. The power-law constants (n' and k) were measured every 15 minutes. Power-law constants for some of the prepared fluids are given in **Table 2.2**. The effect of the polymer concentration, temperature, and salts on the viscosity diminished at shear rates higher than 80 to 100 s^{-1}. This can be due to the rod-like shape of the polymer chain.

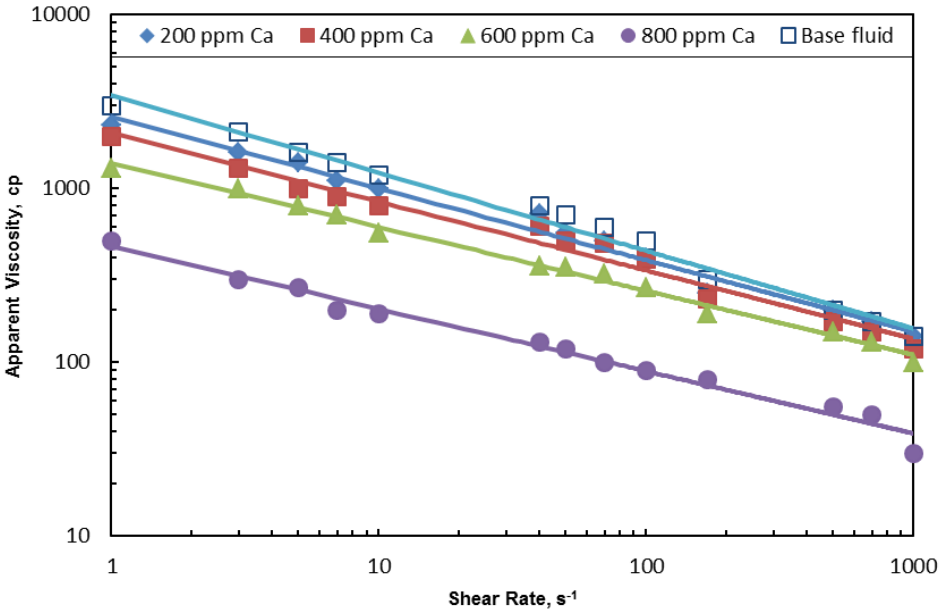

Fig. 2. 8— Comparison between gels prepared with DI water and the fluids containing different concentrations of calcium at 225°F (107°C) and 300 psi (2,068 kPa). The base fluid was a gel prepared with 35 pptg guar, 4 gpt buffer, and 1.0 gpt crosslinker loading.

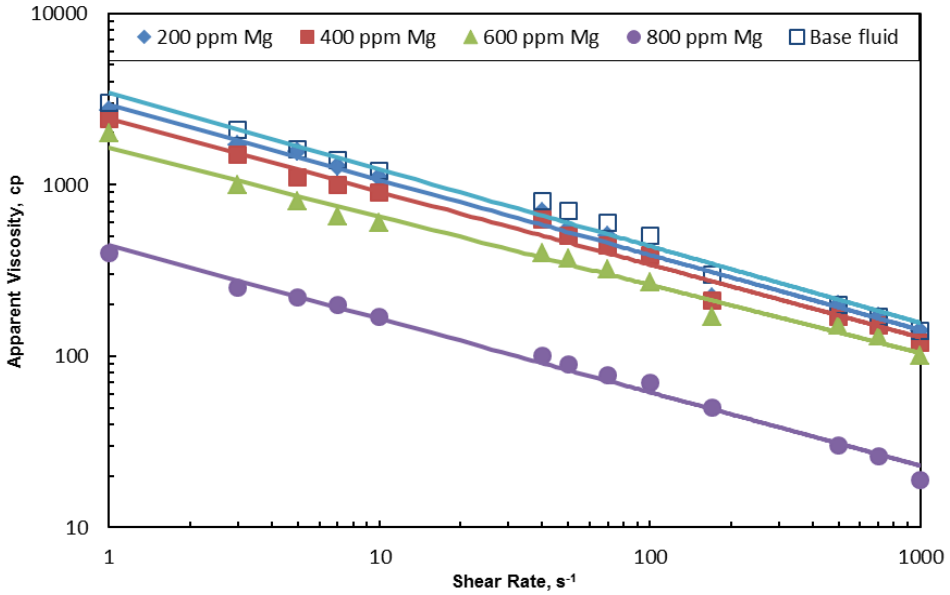

Fig. 2. 9— Comparison between gels prepared with DI water and the fluids containing different concentrations of magnesium at 225°F (107°C) and 300 psi (2,068 kPa). The base fluid was a gel prepared with 35 pptg guar, 4 gpt buffer, and 1.0 gpt crosslinker loading.

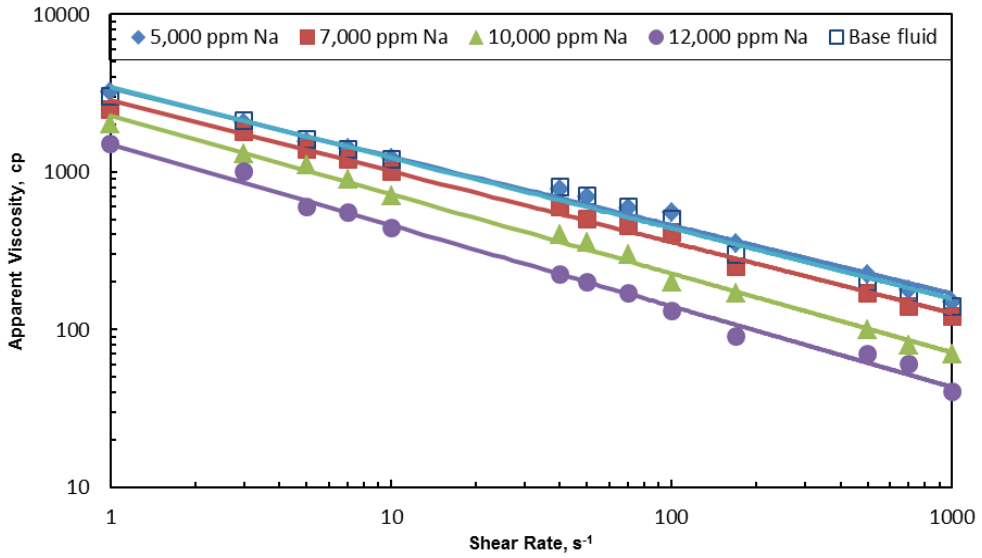

Fig. 2. 10— Comparison between gels prepared with DI water and the fluids containing different concentrations of sodium at 225°F (107°C) and 300 psi (2,068 kPa). The base fluid was a gel prepared with 35 pptg guar, 4 gpt buffer, and 1.0 gpt crosslinker loading.

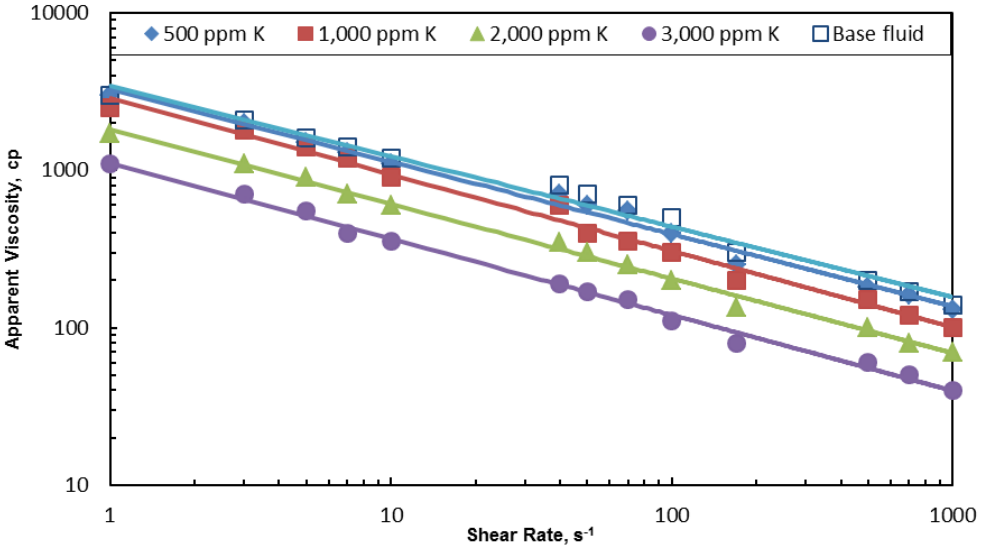

Fig. 2. 11— Comparison between gels prepared with DI water and the fluids containing different concentrations of potassium at 225°F (107°C) and 300 psi (2,068 kPa). The base fluid was a gel prepared with 35 pptg guar, 4 gpt buffer, and 1.0 gpt crosslinker loading.

Table 2. 2— Power-law parameters of prepared fracturing fluids which were loaded with different salt concentrations at 225°F (107°C) and 300 psi (2,068 kPa).

Ion concentration, ppm	Salt type	K, mPa.sn	n’	R^2
Base Fluid	—	9751.8	0.3224	0.9857
5,000	NaCl	5,935.2	0.4486	0.9897
7,000	NaCl	5,590.9	0.3951	0.9934
10,000	NaCl	3,543.8	0.4085	0.9946
500	KCl	9,663.2	0.2882	0.9898
1,000	KCl	9,875.4	0.2406	0.9909
2,000	KCl	3,970.7	0.3417	0.9958
200	CaCl2	10,679.2	0.2688	0.9851
400	CaCl2	7,333.1	0.3257	0.9781
600	CaCl2	1,836.2	0.5585	0.9928
200	MgCl2	13,116.6	0.2043	0.9844
400	MgCl2	1,0369.0	0.2403	0.9837
600	MgCl2	3,543.8	0.4087	0.9834

2.6.2 Effect of Temperature on High-pH Borate Crosslinked Guar-Based Polymer

Usually, fracturing fluids require fairly low total dissolved solids (TDS) in order not to sacrifice fluid stability and to be sure rheological properties remain stable. High TDS should not sacrifice the rheological characteristics and thermal stability of the fracturing fluid (Gupta et al. 2013). The following subsections explore how much treatment is needed to make these fluids applicable for future fracturing jobs and which

contents can affect the developed fluid more. Two hours of thermal stability tests were conducted at a single shear rate (170 s^{-1}), at reservoir temperatures (140, 225, and 305°F) (60, 107, and 152°C), and a pressure on the fluids of 300 psi (2,068 kPa) approved in the previous section to check the thermal stability of the fluids. The viscosity of the prepared base fluids which were loaded with the reported salt concentrations in the previous section are shown in **Fig. 2.12**. The results support that the viscosity profile can be adjusted by controlling the amount of dissolved solids in the polymer at bottomhole temperature.

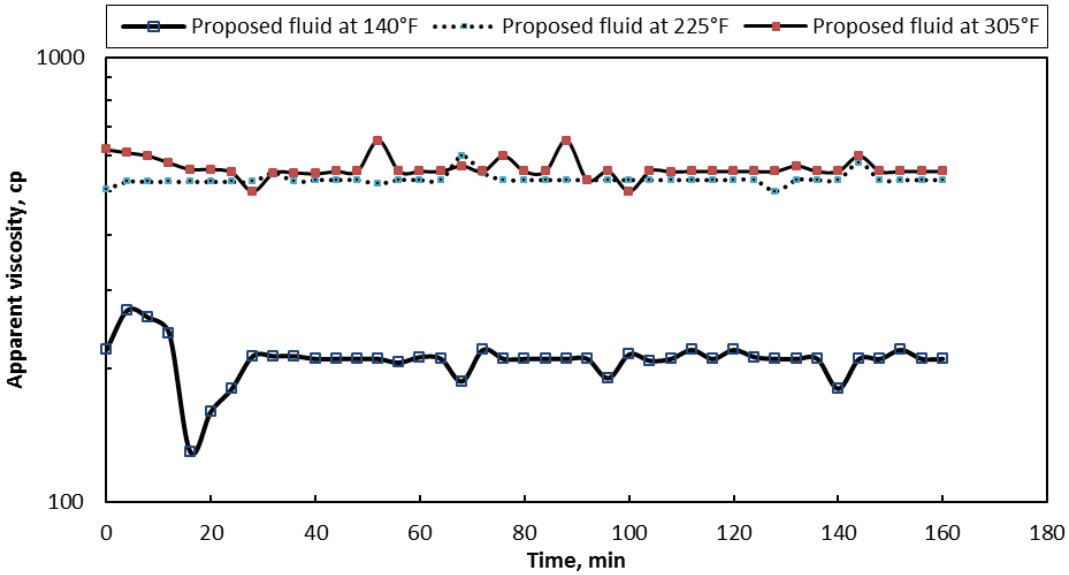

Fig. 2. 12— Single shear rate test to investigate the stability of proposed fluids at 140, 225, and 305°F (60, 107, and 152°C); 170 s^{-1}; and 300 psi (2,068 kPa). The base fluids were gels prepared with 20, 35, and 50 pptg of polymer; 1.75, 4, and 4 gpt buffer, and 1.0, 1.0 and 2.0 gpt crosslinker was selected as the base fluid at 140, 225, and 305°F (60, 107, and 152°C), respectively.

Similar viscosity profiles have been developed for different combinations of brines and the tested gels did not break. At lower temperatures (140 and 225°F) (60 and 107°C), the effect of polymer loading is more dominant than temperature and the recorded viscosity for the fluid prepared with 35 pptg of polymer at 225°F (107°C) is higher than the one prepared with 20 pptg of polymer at 140°F (60°C). At higher temperatures it is vice versa and the fluid loaded with 50 pptg of polymer at 305°F (152°C) showed viscosity value close to the one with 35 pptg of polymer at 225°F (107°C).

2.6.3 Small-Amplitude Oscillatory Shear (SAOS) Measurements

The objective of this portion of the work is to measure the elastic and viscous properties (G' and G") of prepared polymers in the near wellbore region and in fractures. Experimental studies were conducted to measure the rheological properties for prepared polymers using an oscillatory rheometer. The complex nature of the crosslinked fluid makes it more difficult to interpret the results. The storage module, G', represents the elastic response and loss modulus, and G" reflects the viscous response of the fluid. A small strain amplitude in the linear viscoelastic limit can measure the storage and loss moduli of a fluid at a given oscillation frequency. Fluids with high elasticity characteristics show better proppant suspension properties in static and dynamic conditions. This method is a nondestructive technique (Harris et al. 2009b). When storage and loss moduli cross over, the relaxation time of the network and the settling

ability of a suspended particle in the fluid increases (Yount et al. 2005; Loveless et al. 2011).

A dynamic-oscillatory viscometer, Grace M5600, at 5% applied strain was used to obtain a relationship between the rheological properties and the crosslink network structure of a fluid. **Figs. 2.13 to 2.15** show the G' and G" vs. frequency for the samples prepared with fresh water and the fluid which contained a mix of approved salt concentrations and modulus crossover at 75 and 225°F (24 and 107°C). At 75°F (24°C) the fluid contains a mix of salts that had a faster relaxation time, although the difference between them was not significant. The G' modulus for both of them showed an increase in the viscous and elastic regime values, as well as in the elastic values, and the values are very close. Therefore, we can conclude that the elasticity of the polymers increases with frequency. On the other hand, the G" modulus started to decrease when it reached the elastic regime. These values closely follow the same trend in this regime.

Fig. 2.14 shows that an increase in temperature expanded the viscous regime for both fluids. The sample prepared with fresh water had a lower crossover value, but in this case the difference was negligible and showed that temperature did not significantly affect the crossover points. The increase in temperature severely reduced the G' and G" modulus values, especially in the elastic regime. The presence of salts reduced G' and G" values but did not expand the viscous regime. In **Fig. 2.15**, the fluids with higher polymer loadings showed higher G' and G" values. However, the same behavior was also observed at 225°F (107°C).

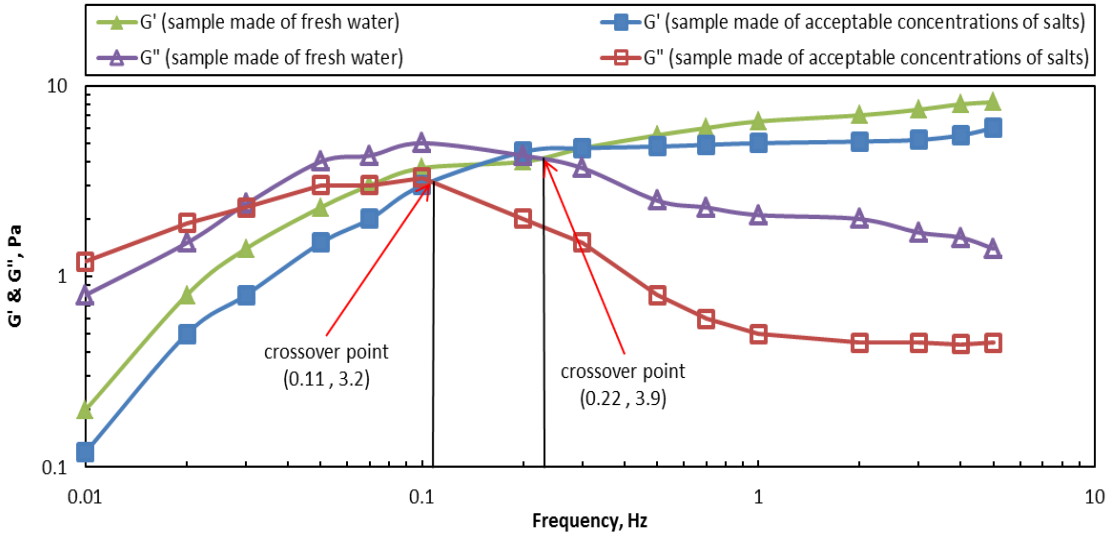

Fig. 2. 13— SAOS measurements performed on the gel prepared with fresh water and the fluid loaded with the maximum acceptable dissolved solid contents at 75°F (24°C) and 5% applied strain. The base fluid was a gel prepared with 20 pptg guar, 1.75 gpt buffer, and 1.0 gpt crosslinker loading.

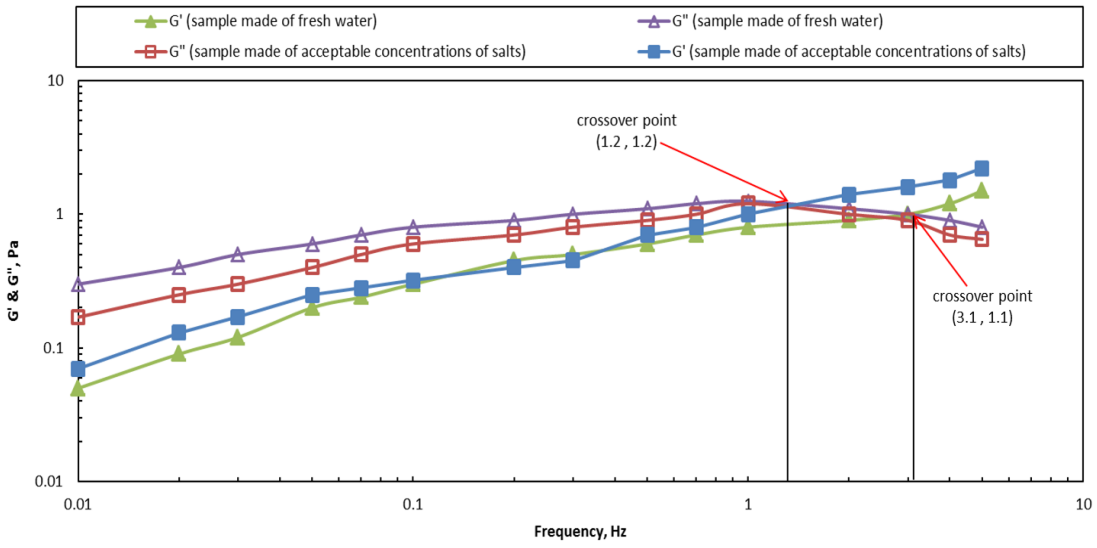

Fig. 2. 14— SAOS measurements performed on the gel prepared with fresh water and the fluid loaded with the maximum acceptable dissolved solid contents at 225°F (107°C) and 5% applied strain. The base fluid was a gel prepared with 20 pptg guar, 1.75 gpt buffer, and 1.0 gpt crosslinker loading.

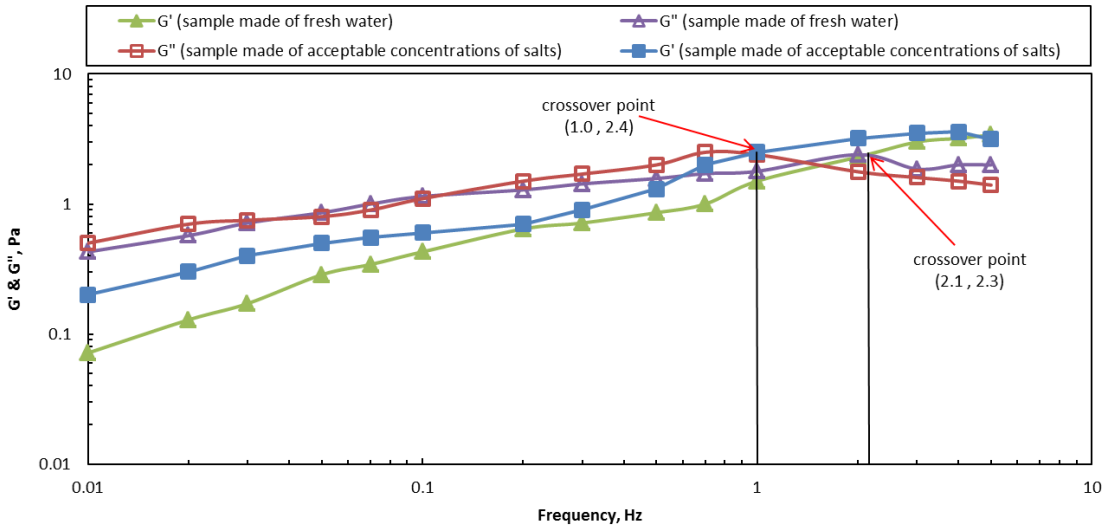

Fig. 2. 15— SAOS measurements performed on the gel prepared with fresh water and the fluid loaded with the maximum acceptable dissolved solid contents at 225°F (107°C) and 5% applied strain. The base fluid was a gel prepared with 35 pptg guar, 4.0 gpt buffer, and 1.0 gpt crosslinker loading.

2.6.4 Static Settling Tests

In hydraulic fracturing treatments, the success of the treatment strongly depends on the proper placement of proppant particles in the fracture. "Proper placement" means the packing of a fracture to achieve maximum conductivity of gas/oil through the fracture into the wellbore. The placement of the proppants along the fracture is based on design equations where sand transport velocity is related to the rheological parameters of the fracturing fluid and characteristics of the proppant particle, such as size and density. Harris et al. (2005) stated that the model for proppant placement in a hydraulic fracture should include proppant characteristics, viscous rheological parameters (K and n'), elastic parameters (complex dynamic viscosity) from the linear viscoelastic constitutive

equation, and the normal stress difference from the nonlinear viscoelastic constitutive equation. The influence of the crosslinked-polymer-gel network structure on proppant transport was also discussed. To reach a maximum horizontal distance in fractures, a sufficient vertical settling time is required.

The static settling test is conducted on the fluids with acceptable solid contents with the base fluid at 75 and 225°F (24 and 107°C). A 20/40-mesh Ottawa sand with the apparent specific gravity of 2.65 at an equivalent of 4 lbm/gal was used in these tests. This method can visually help us to compare the proppant settling for various fluids. A 100 ml graduated cylinder was filled with proppant loaded fracturing fluid and placed in a see-through cell. The see-through cell can be heated to 450°F (232°C) at a pressure of 500 psi (3,447 kPa). About 15 (± 5) minutes are required for the sample to reach to the cell temperature. The amount of precipitated particles was measured every 5 minutes continuing until all of the proppants settled down.

Proppant settling of the fluid will change as a result of an increase in temperature at downhole conditions. A rise in temperature can change the chemical equilibrium, pH, the number of crosslink bond of borate-fluid systems, and consequently, the proppant transport capacity of gel (de Kruijf 1993).

The base borate-crosslinked gel and the sample loaded with a mix of salts at approved concentrations were tested at 75 and 225°F (24 and 107°C). **Fig. 2.16** shows the process of proppant settling in the salt loaded sample at different times. **Fig. 2.17** shows that in a 200 minute observation, 73% of proppants in the fresh water sample and 68% of proppants in the salt mix sample were suspended at 75°F (24°C).

.5 minutes 30 minutes 35 minutes 50 minutes 75 minutes

Fig. 2. 16— Static proppant settling test on the fluid prepared with maximum acceptable dissolved solid contents which was loaded with 4 lbm/gal of 20/40 Ottawa sand at 225°F (107°C). The base fluid was a gel prepared with 20 pptg guar, 1.75 gpt buffer, and 1.0 gpt crosslinker loading.

Temperature has a significant effect on proppant handling characteristics of borate crosslinked fluids and as it can be seen in **Figs. 2.17 and 2.18**, all of the proppants settled at 225°F (107°C) much faster than ambient temperature. The proppants settled down after 85 and 75 min in the base fluid and the sample loaded with the mix of salts, respectively. **Fig. 2.19** shows the effect of increasing polymer loading on the proppant transport. In this case, increasing polymer loading from 20 pptg to 35 pptg at 225°F (107°C), improved the proppant handling in the fresh water sample by 10% and in the sample made of acceptable concentrations of salts by 2%.

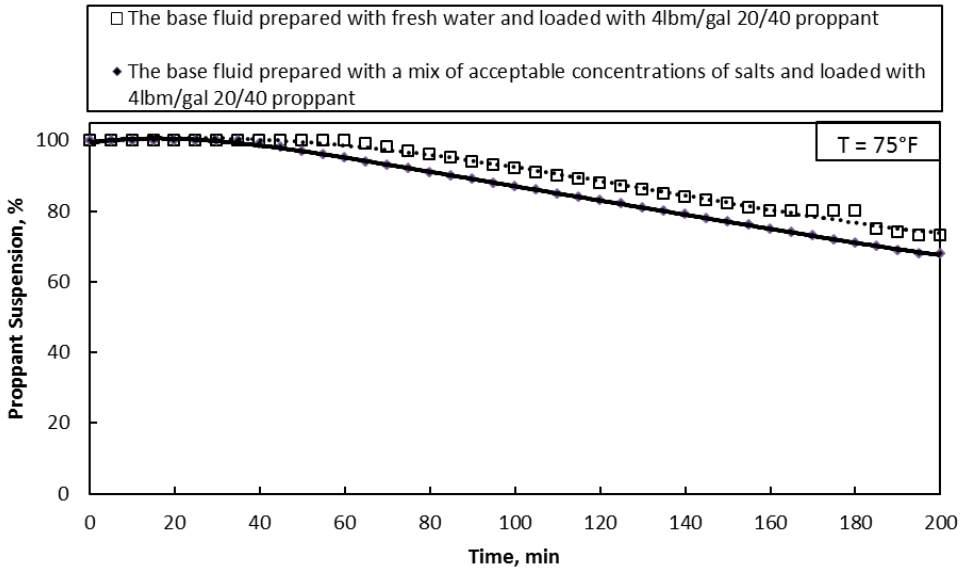

Fig. 2. 17— Comparison between proppant settling of sample prepared with fresh water and the fluid prepared with the maximum acceptable dissolved solid contents which were loaded with 4 lbm/gal of 20/40 Ottawa sand at 75°F (24°C). The base fluid was a gel prepared with 20 pptg guar, 1.75 gpt buffer, and 1.0 gpt crosslinker loading.

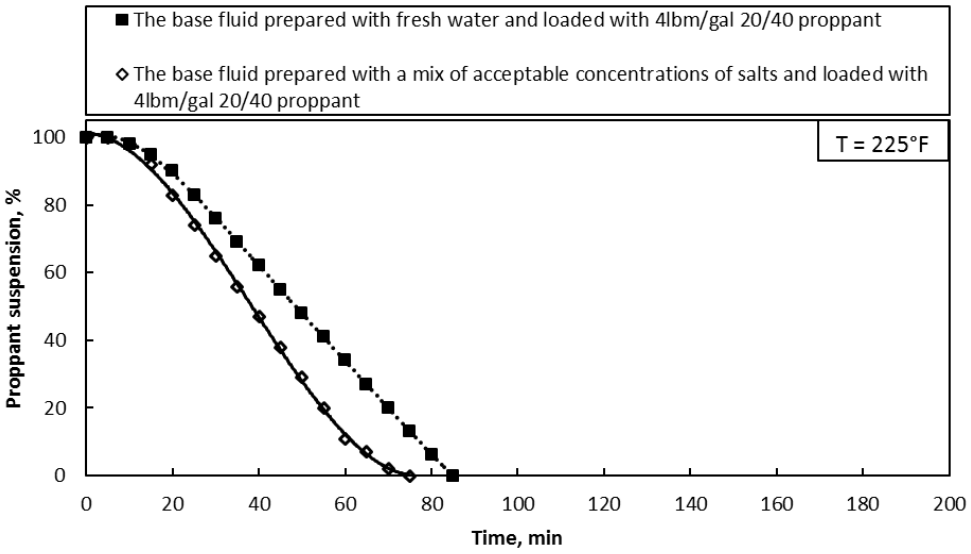

Fig. 2. 18— Comparison between proppant settling of sample prepared with fresh water and the fluid prepared with the maximum acceptable dissolved solid contents which were loaded with 4 lbm/gal of 20/40 Ottawa sand at 225°F (107°C). The base fluid was a gel prepared with 20 pptg guar, 1.75 gpt buffer, and 1.0 gpt crosslinker loading.

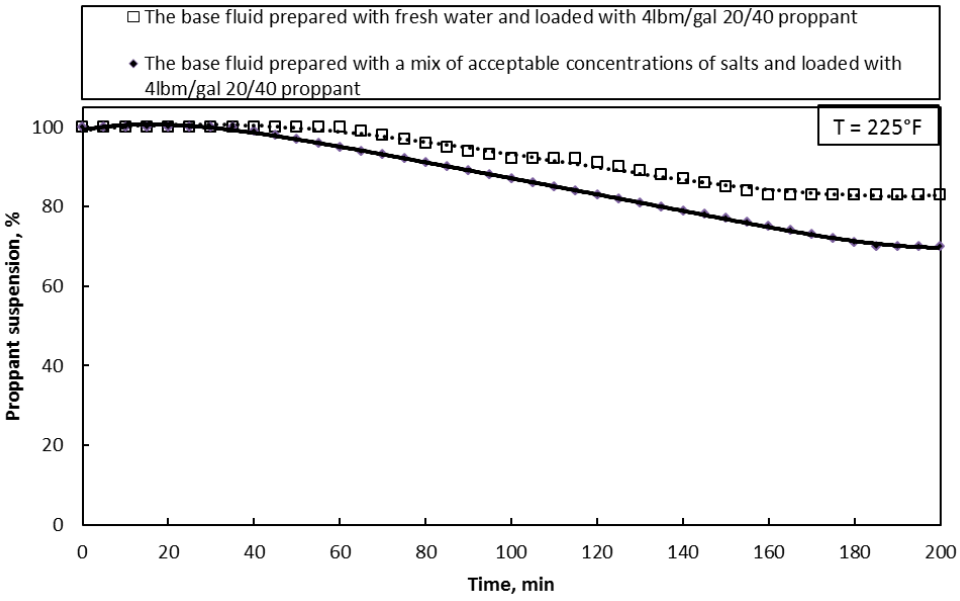

Fig. 2. 19— Comparison between proppant settling of sample prepared with fresh water and the fluid prepared with the maximum acceptable dissolved solid contents which were loaded with 4 lbm/gal of 20/40 Ottawa sand at 225°F (107°C). The base fluid was a gel prepared with 35 pptg guar, 4.0 gpt buffer, and 1.0 gpt crosslinker loading.

2.7 Conclusions

The effects of mono and divalent cations on the rheological properties of high-pH borate crosslinked guar-based polymer were examined in detail. Based on the results obtained, the following conclusions can be drawn:

1. The determined maximum acceptable concentration values for four dominant ions (Na^{2+}, K^{2+}, Mg^{2+}, and Ca^{2+}) in flowback fluids show that the high-pH borate

crosslinked guar-based polymer fluid has a reasonable quality without compromising the required functionality at temperatures up to 305 °F (152 °C).

2. Potassium and calcium ions have more tolerable limits, and more than 97 and 75% of reported samples had acceptable ion concentrations at temperatures up to 305 °F (152 °C), respectively.
3. Magnesium and sodium are the controlling ions, and about 30 and 40% of flowback fluids need treatment to reduce the concentrations of these ions at temperatures up to 305 °F (152 °C), respectively.
4. The viscosity measurements are valid in shear rates up to 80-100 s^{-1}. This range is more applicable in decision making in comparison with previous reported value (10 s^{-1}). The apparent viscosities at higher shear rates are very close and indistinguishable.
5. The proposed fluid with the maximum acceptable TDS from flowback fluids performs very well in SAOS and static settling tests and show acceptable proppant transport and handling capability of the fluid.

These results show that it is technically feasible to reuse flowback fluids with minimum treatments regarding ion contents up to the high temperatures.

CHAPTER III

A FEASIBILITY STUDY OF REUSING FLOWBACK FLUIDS IN HYDRAULIC FRACTURING TREATMENTS*

3.1 Introduction

Produced water management, historically, has been a concern in the oil and gas industry. Produced water in some mature oil fields is 7 or 8 times greater than the hydrocarbon production and the large amount of produced water is not the only issue of concern. Most of these waters are highly contaminated, and it is necessary to safely dispose them to ensure they will not harm the environment. Water injections and use in secondary and enhanced oil recovery methods have increased the water demand in the oil and gas industry. The importance of the subject became even more critical with the introduction of horizontal drilling and multi-stage fracturing. A tremendous volume of required and produced water made its management an important subject of concern for economic and environmental reasons.

---

*Reprinted with permission from "Fracturing Fluids: A Feasibility Study of Reusing Flowback Fluids in Stimulation Treatments" by Ashkan Haghshenas and Hisham Nasr-El-Din, 2014. *Hydraulic Fracturing Journal.* **1** (4) 8-20, Copyright 2014 by Petrodomain.

Produced water issues can be addressed using any or all of the following methods:

1- Reduce the amount of required water in jobs (Shipman et al. 2013; Bryant and Haggstrom 2012)
2- Develop more environmentally friendly treatment techniques (Loveless et al. 2011; Blauch 2010)
3- Recycle and reuse the flowback fluids (Haghshenas and Nasr-El-Din 2014; Fontenelle et al. 2013)
4- Dispose of flowback fluids by safer methods (Veil 2010; Arthur et al. 2005)

In this research the reuse of produced water was explored. Literature survey (Arthur et al. 2010) shows that 15 - 50% of injected water is flowed back to the surface. While this may seem like a small volume, in absolute terms this can be quite significant, especially in drought prone regions. Water can be supplied from surface water, groundwater, municipal water suppliers, or recycled flowback fluid; depending on availability, accessibility, cost, and regulations. The quality of flowback fluid depends on the applied treatment as well as formation and hydrocarbon characteristics. The TDS of flowback fluids can range from 100 to over 400,000 mg/l (Guerra et al. 2011). Some jobs, such as slickwater treatments, can flow back fairly fresh waters that can be reused after some hydrocarbon and organic material removal, pH adjustment, scale removal, and bacteria removal processes. In high salt contaminated fluids it is also necessary to reduce the TDS of the fluid. This is one of the most important processes in water treatments and various techniques like evaporation, membrane filtration, distillation,

electric separation, and chemical treatment have been tried by various operators (Arthur et al. 2005; Arthur et al. 2010; Veil 2010). These methods have shown limited success in some cases. This has encouraged oil and gas companies to invest more on water treatment systems and to develop new techniques to reduce costs. Onsite treatments can greatly help to reduce water acquisition, transportation, and disposal costs. Quality and quantity of flowback fluids, future job characteristics, governmental, and practicability are factors that influence the decision making process.

The idea of using seawater and produced water in hydraulic fracturing is not new (Harris and van Batenburg 1999; Le and Wood 1992). Previous works indicated that there were conflicting opinions regarding the concept of using other sources of water instead of fresh water. For example, some researchers show that high salinity can help breakers while others believe the reverse effect (Harris and van Batenburg 1999; Hassen et al. 2012). Although borate crosslinked guar-based gel has minimal shear sensitivity and gel residue (Wiskofske et al. 1997), Gupta et al. (2013) stated that despite better and faster clean up and the ability to provide good proppant pack conductivity, conventional borate crosslinkers are not good candidates at temperatures greater than 225°F. The wide differences in these reports have resulted in uncertainty regarding the use of the methodology.

This study investigated the role of chelating agents to increase the admissibility of higher TDS in the fracturing fluids without compromising their main functions. The effect of chelating agents on multivalent cations has been widely studied (Putzig and St. Clair 2007; Blauch 2010; Fedorov et al. 2010, 2014; Gupta et al. 2013). EDTA was

applied to reduce or eliminate the impact of divalent cations (Mg^{2+} and Ca^{2+}). The interference of high concentrations of monovalent cations such as Na^{+} and K^{+} with viscosity build up was reduced by using a more compatible buffer and higher pH. The suitable pH window for guar/borate crosslinker starts from 9.5 (Pezron et al. 1990). In this study, the range of pH values was 10.5 to 12.5.

3.2 Experimental Studies

The experimental approach in this work focuses on providing sufficient viscosity to create a sufficiently wide fracture and transport proppants as the key functions of fracturing fluids (Harris and Heath et al. 2009). In the viscosity measurements, different salts were tested to investigate the maximum acceptable concentrations of the most common salts in the flowback fluids. Viscosity measurements were also conducted to determine the fluid behavior at field conditions.

According to Harris and Heath (2009), a simple viscosity measurement is not sufficient to measure the proppant transport characteristic of the polymer solutions. Viscoelastic property measurements are needed to investigate the stability of the mixed saline fluid and to measure the rheological properties, (storage, G', and loss, G", moduli) of the proposed fluid and compare them to the fracturing fluid prepared with fresh water.

Finally, the proppant transport ability of the proposed fluid was examined and compared to the selected base fluid. Tests were run at temperatures up to 305°F.

3.3 Materials

Size, shape, and length of polymers affect their physical properties. A borate crosslinked galactomannan (guar /borate) is selected as the base fluid. This fluid consists of guar gum, buffer (monoethanolamine and a mixture of potassium carbonate and potassium hydroxide), ethylenediaminetetraacetic acid, diammonium salt (EDTA), and crosslinker (a borate solution) as the base components. Calcium chloride dihydrate, magnesium chloride hexahydrate, potassium chloride, and sodium chloride (all American Chemical Society Grade) were used as sources of monovalent and divalent cations in the test fluids.

Analyses of 36 samples from the West Texas region were collected to determine the maximum and minimum values of all the contents **(Table 2.1)**. This study attempted to represent produced waters as much as possible. The applied limits surpassed TDS of seawater **(Table 3.1)**.

A Barnstead EASY pure PoDi-model D13321was used to obtain deionized (DI) water. The DI water had a resistivity of 18.2 MΩ.cm at room temperature. It was used in all polymer preparations. For other chemicals and additives no further purification was necessary. A Thermo Scientific Orion 950 ROSS® FAST QC™ titrator was used to measure the pH value. Shear viscosity and G' and G" measurements were conducted by using an M5600 HP/HT Rheometer with a R1/B5 and a R1/HB5 rotor-bob system, respectively, at 140, 225, and 305°F and a pressure of 300 psi.

Table 3. 1— Chemical composition for typical seawater/formation water[a]

Component	Danish North Sea (mg/l)	Mediterranean Sea (mg/l)	Offshore Angola (mg/l)	South China Sea (mg/l)	Gulf of Mexico (mg/l)	GOM Formation (mg/l)
Sodium	8,800	12,300	14,200	9,900	11,000	42,700
Potassium	400	380	210	400	470	1,350
Calcium	420	500	300	420	650	6,120
Magnesium	1550	1,790	630	1,170	1,220	560
Strontium	6	-	5	7	10	1,800
Chloride	22,000	22,000	15,000	18,000	19,700	81,000
Bicarbonate	140	140	95	110	90	370
Carbonate	-	-	-	-	40	0
Sulfate	3,300	2,900	1,400	2,500	3,130	0

[a] Harris and van Batenburg (1999)

3.4 Chelating Agent

Ethylenediaminetetraacetic acid (EDTA) is an aminopolycarboxylic acid. The stability constants for chelates of EDTA with multivalent cations are higher than those with monovalent cations, and it makes them capable of forming more stable chelates (Martell and Calvin 1952). It also shows very good performance at high pH values (8.5 – 13) (Fredd and Fogler 1998). Chelating agents grab multivalent cations and help to build better crosslinks. This phenomenon improves the stability of the solution at higher temperatures (Gupta et al. 2013). Sufficient amounts of EDTA could prevent

precipitation or help the dissolution of multivalent cations into the solution by complexation. The down side of this chelating agent is that it is not readily biodegradable (Frenier et al. 2003). EDTA is commonly used in stimulation processes to prevent scale precipitation and corrosion of tubulars in acid treatments (Shaughnessy and Kline 1983; Ali et al. 2002). EDTA is also effective in hydraulic fracturing fluids at low concentrations of potassium and calcium and low temperatures (Fischer et al. 2001; Khair et al. 2011). In this work diammonium EDTA was used in fluids containing high concentrations of divalent (Ca^{2+} and Mg^{2+}) and monovalent (K^{+} and Na^{+}) cations at temperatures up to 305°F. The chelating solution was nearly 45.9 wt% active and had a pH of 5.72. It should be noted that all EDTA concentrations are based on as received solution.

3.5 Preparation of Base Fluids

The following procedure was used in preparation of samples:

1. In the preparation of linear gel, 700 ml of fresh or salt water was added to a 1,000 ml beaker.

2. Before adding polymer, the circulating rate for the blender was set at 500 rpm to establish a vortex with no air bubbles trapped.

3. A predetermined volume of the guar gum was slowly added to the shoulder of the vortex in order to prepare a polymer solution with a specific concentration. Three polymer concentrations were tested: 20, 30, and 50 pptg (pound per thousand gallons) of polymer loading.

4. The solution continuously mixed for half an hour. An increase in the rotational speed to 700 rpm was needed to maintain good vortex without air entrapment.

5. In the final stage and in the case of gels prepared in fresh water, 2.0-4.0 gpt buffer was added followed by the crosslinker. In the case of brines, 2 wt% EDTA and 16 to 20 gpt (gallon per thousand gallons) buffer were added. Then, based on the tables presented by the provider company, the crosslinker was added and mixed for five seconds before loading into the viscometer. At high temperatures a delayed crosslinker was used.

All tests were repeated three times and the reported value is the average of two closest to each other. The measurements were conducted one hour after the preparation of the fluids to minimize the effect of polymer hydrolysis on the viscosity of polymer solutions (Nasr-El-Din and Taylor 1996).

3.6 Results and Discussion

3.6.1 Viscosity Measurements

A series of viscosity measurements was conducted at different temperatures to investigate the effect of shear rate on the prepared fluids. The viscosity was measured as a function of shear rate from 1 to 1,000 s^{-1} at 140, 225, and 305°F and 300 psi pressure. pH measurements were conducted before and after each test to ensure that the pH values were higher than 9.5. This is the minimum acceptable pH to reach a reasonable crosslinking stage. No pH less than 10.5 was recorded and, in high monovalent cation concentrations, the pH values increased to between 12 and 12.5.

Properties of polymers can significantly change in the presence of various chemical species, such as alkalis, simple salts, and surfactants (Nasr-El-Din and Taylor 1996). The effect of salt type and concentration on the viscosity of prepared gels was studied in detail. Three concentrations of each salt were selected from Table 1 in order to cover 70% of reported values. Then, based on the viscosity values, the fourth concentration was selected. In the potassium chloride case, the third value was the maximum reported value; therefore, the fourth test was not run. In all cases, viscosity measurements for a base fluid prepared with fresh water was conducted as well. If the salt concentrations were excessively high, the presence of cations could have interfered with the hydration and crosslinking process (Gupta et al. 2013). A solution of 2 wt%

EDTA was added before and after adding salts. The outcomes were similar. Therefore, the EDTA was added to saline solutions to simulate field conditions.

The base fluids consisted of 20, 30, and 50 pptg of polymer solutions; 2 wt% EDTA; 16, 19, and 20 gpt buffer; and 1.0, 1.25, and 3.0 gpt crosslinker at 140, 225, and 305°F, respectively. **Figs. 3.1 to 3.4** show the effect of different concentrations of Ca^{2+}, Mg^{2+}, K^{+}, and Na^{+} on the apparent viscosity of the samples at 225°F. After a certain salt concentration, the viscosity dropped significantly. The recorded values at shear rate of 40 s^{-1} were taken as controlling values. It is reasonable to set the viscosities lower than 600 cp at shear rate of 40 s^{-1}, as the limiting criterion (Bunger et al. 2013). To determine the exact values, in **Figs. 3.5 to 3.10** the viscosity was plotted versus salt concentration and the figures were compared at different temperatures. It is necessary to increase the polymer loading at higher temperatures to keep up with the set criterion.

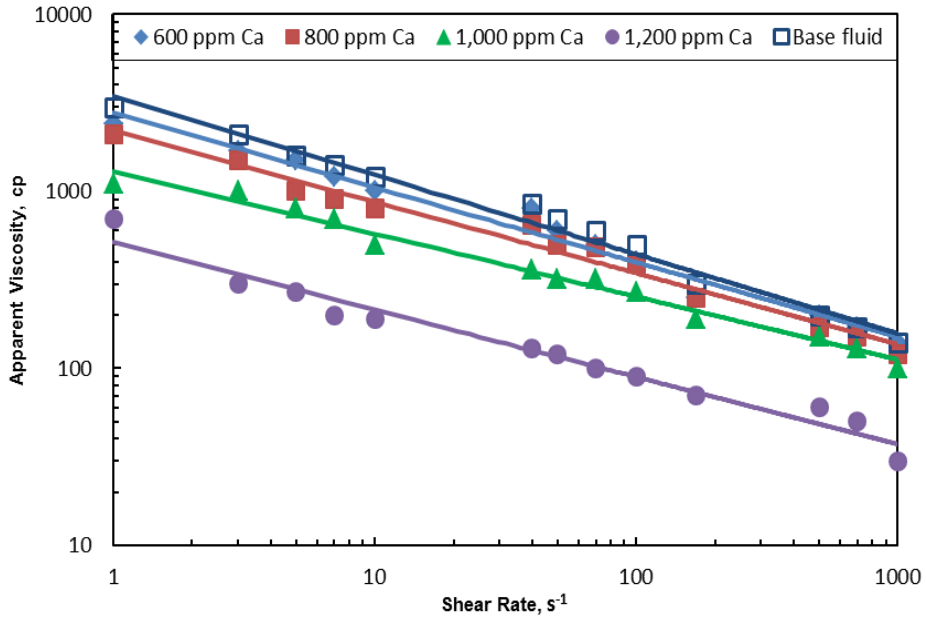

Fig. 3. 1— Comparison between gels prepared with DI water and the fluids containing different Ca^{++} concentrations at 225°F and 300 psi. The base fluid was a gel prepared with 30 pptg guar, 2 wt% EDTA, 19 gpt buffer, and 1.25 gpt crosslinker loading.

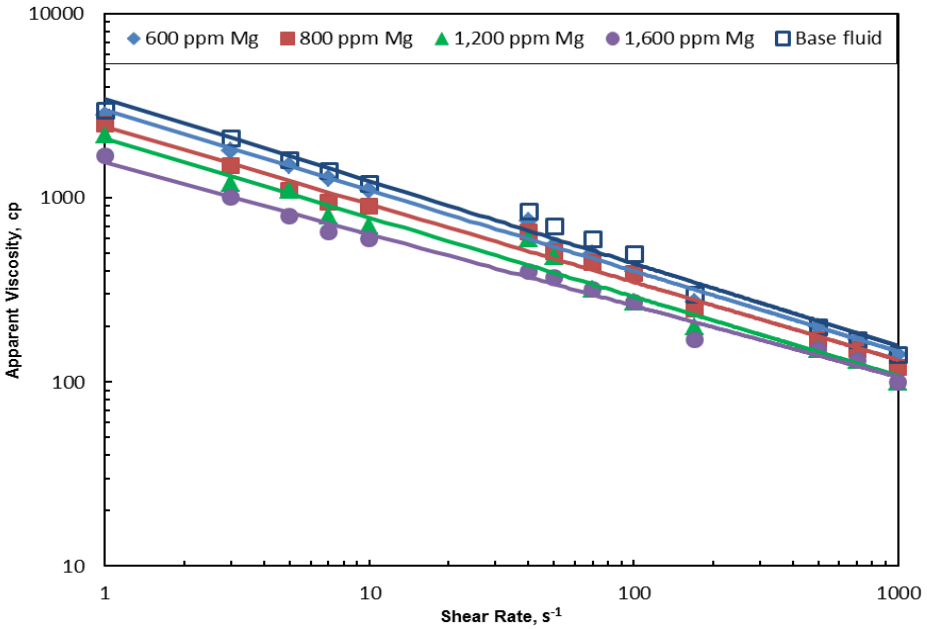

Fig. 3. 2— Comparison between gels prepared with DI water and fluids containing different Mg^{++} concentrations at 225°F and 300 psi. The base fluid was a gel prepared with 30 pptg guar, 2 wt% EDTA, 19 gpt buffer, and 1.25 gpt crosslinker loading.

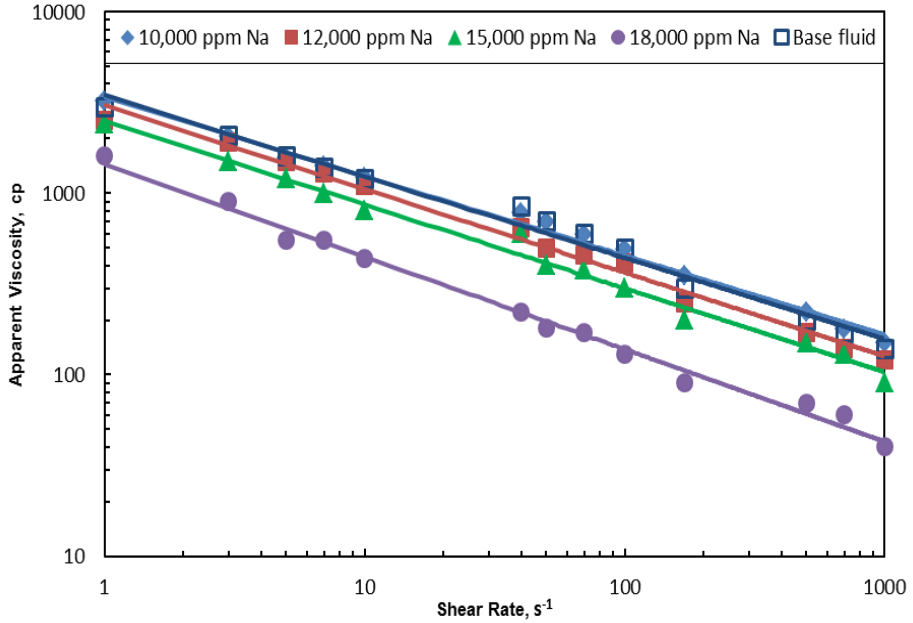

Fig. 3. 3— Comparison between gels prepared with DI water and fluids containing different Na^+ concentrations at 225°F and 300 psi. The base fluid was a gel prepared with 30 pptg guar, 2 wt% EDTA, 19 gpt buffer, and 1.25 gpt crosslinker loading.

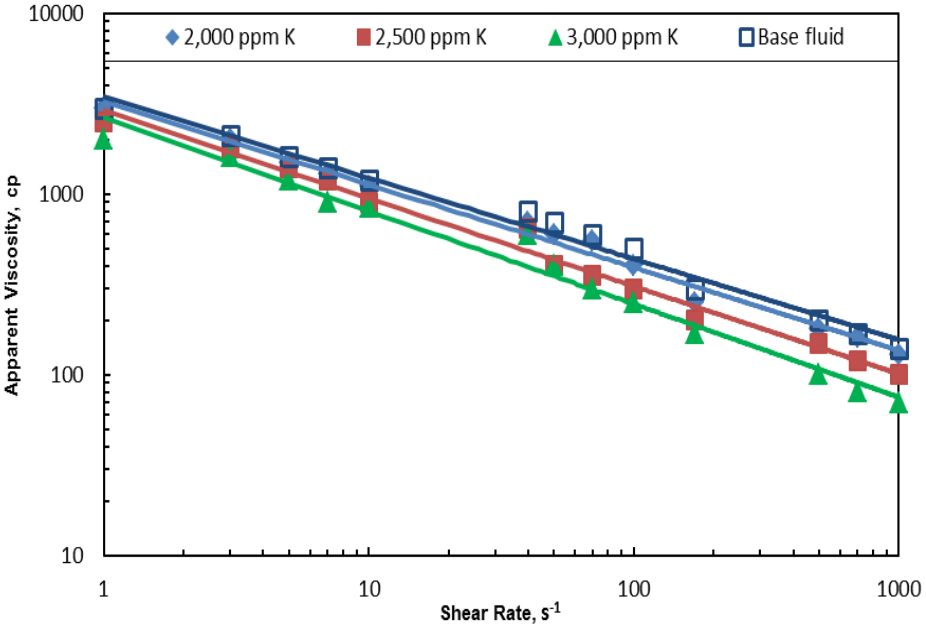

Fig. 3. 4— Comparison between gels prepared with DI water and fluids containing different K^+ concentrations at 225°F and 300 psi. The base fluid was a gel prepared with 30 pptg guar, 2 wt% EDTA, 19 gpt buffer, and 1.25 gpt crosslinker loading.

The chelating agent increased the maximum tolerable values up to 82.7%. As illustrated in **Figs. 3.5, 3.7, and 3.9**, EDTA improved the maximum acceptable Ca^{2+} and Mg^{2+} concentrations from 600 and 750 ppm to 960 and 1,370 ppm, respectively. These 60% and 82.7% increases covered 86% and 92% of the Ca^{2+} and Mg^{2+} concentrations of analyzed samples. In **Figs. 3.6, 3.8 and 3.10**, the samples containing Na^{+} and K^{+} showed better performance at higher pH values (12 to 12.5). High pH fluids increased the maximum Na^{+} concentration from 11,000 to 16,200 ppm, which was a 47.3% improvement, and all reported potassium concentrations were acceptable. These concentrations of salts were the maximum acceptable in the presence of EDTA.

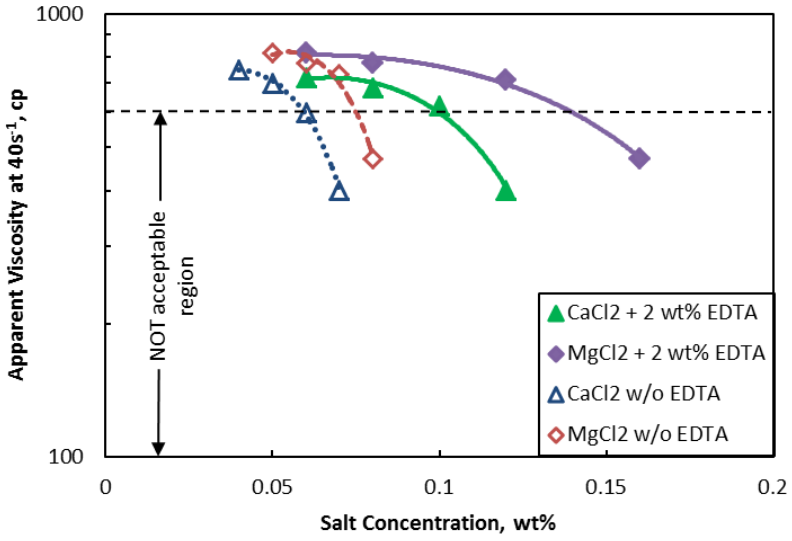

Fig. 3. 5— Comparison between gels prepared with different concentrations of divalent ions at 40 s^{-1}, 140°F, and 300 psi. The base fluid was a gel prepared with 20 pptg guar, 2 wt% EDTA, 16 gpt buffer, and 1.0 gpt crosslinker loading. The gels without EDTA were prepared with 20 pptg guar, 2.0 gpt buffer, and 1.0 gpt crosslinker loading.

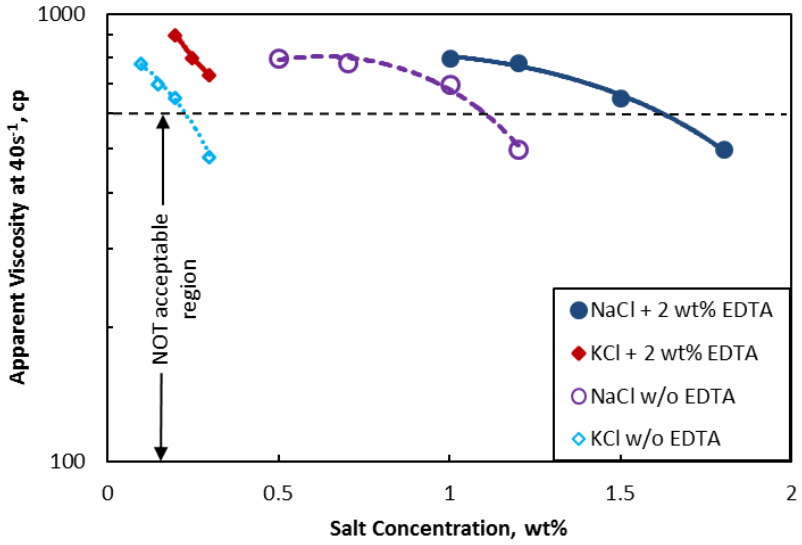

Fig. 3. 6— Comparison between gels prepared with different concentrations of monovalent ions at 40 s^{-1}, 140°F, and 300 psi. The base fluid was a gel prepared with 20 pptg guar, 2 wt% EDTA, 16 gpt buffer, and 1.0 gpt crosslinker loading. The gels without EDTA were prepared with 20 pptg guar, 2.0 gpt buffer, and 1.0 gpt crosslinker loading.

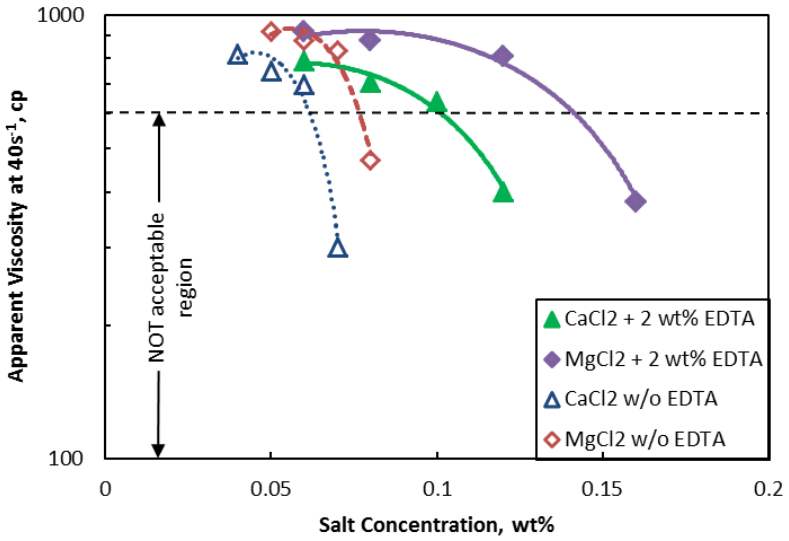

Fig. 3. 7— Comparison between gels prepared with different concentrations of divalent ions at 40 s^{-1}, 225°F, and 300 psi. The base fluid was a gel prepared with 30 pptg guar, 2 wt% EDTA, 19 gpt buffer, and 1.25 gpt crosslinker loading. The gels without EDTA were prepared with 35 pptg guar, 4.0 gpt buffer, and 1.0 gpt crosslinker loading.

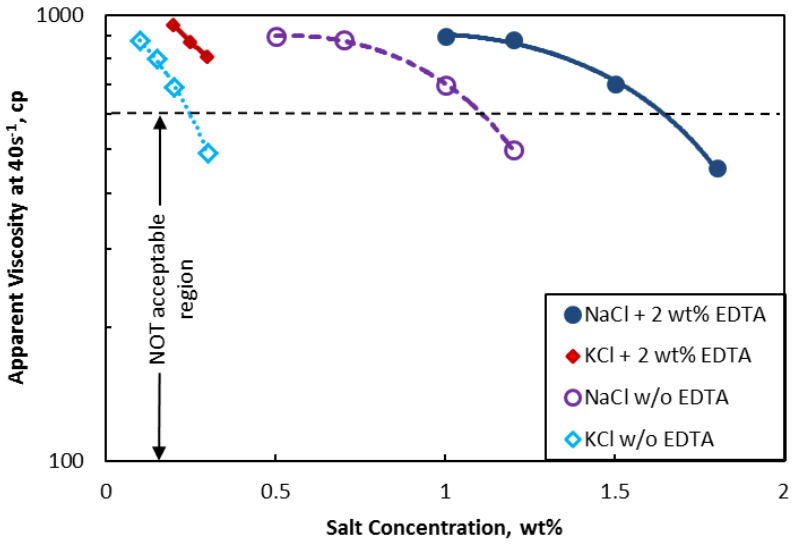

Fig. 3. 8— Comparison between gels prepared with different concentrations of monovalent ions at 40 s^{-1}, 225°F, and 300 psi. The base fluid was a gel prepared with 30 pptg guar, 2 wt% EDTA, 19 gpt buffer, and 1.25 gpt crosslinker loading. The gels without EDTA were prepared with 35 pptg guar, 4.0 gpt buffer, and 1.0 gpt crosslinker loading.

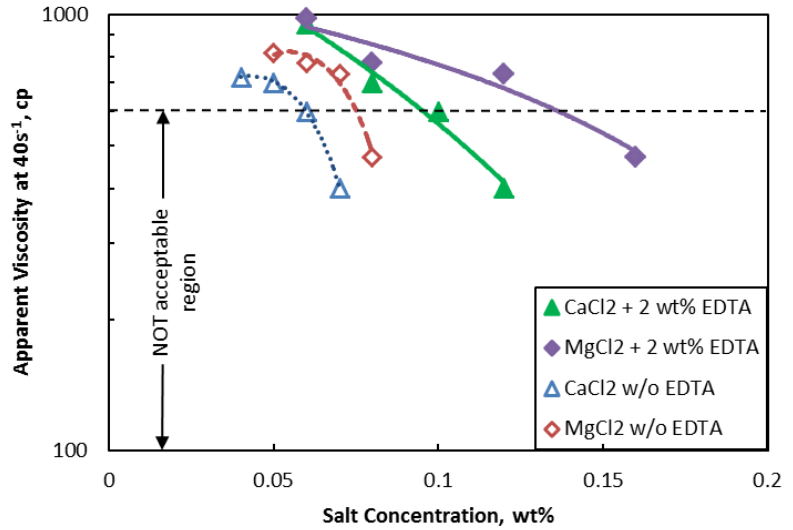

Fig. 3. 9— Comparison between gels prepared with different concentrations of divalent ions at 40 s^{-1}, 305°F, and 300 psi. The base fluid was a gel prepared with 50 pptg guar, 2 wt% EDTA, 20 gpt buffer, and 3.0 gpt crosslinker loading. The gels without EDTA were prepared with 50 pptg guar, 4.0 gpt buffer, and 3.0 gpt crosslinker loading.

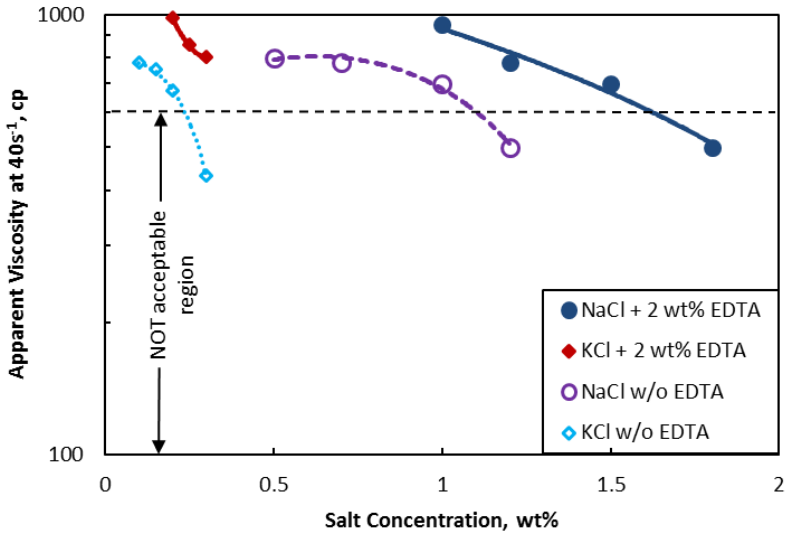

Fig. 3. 10— Comparison between gels prepared with different concentrations of monovalent ions at 40 s^{-1}, 305°F, and 300 psi. The base fluid was a gel prepared with 50 pptg guar, 2 wt% EDTA, 20 gpt buffer, and 3.0 gpt crosslinker loading. The gels without EDTA were prepared with 50 pptg guar, 4.0 gpt buffer, and 3.0 gpt crosslinker loading.

3.6.2 Thermal Stability at Bottomhole Temperatures

In the previous section, the results showed that EDTA helped the fluid to tolerate high salinity, much higher than seawater, and build a very good viscosity over a wide range of shear rates. It is a good sign that this fluid can be a viable candidate for fracturing fluids, but it is not enough. The proposed fluid should display acceptable thermal stability over at least a two-hour single shear rate test at bottomhole temperature. High concentrations of divalent cations, such as calcium and magnesium, can increase the risk of fracturing fluid failure. The fluids were prepared with the same procedure and specifications. **Fig. 3.11** illustrates the apparent viscosity over time. The experiments

were run at a shear rate of 170 s^{-1}, temperatures 140, 225, and 305°F, and a pressure of 300 psi in all experiments. The power-law constants (n' and K) were measured every 15 minutes. All gels did not break over time and the recorded viscosities were very stable. Determining the lowest possible polymer loading was the other part of the test. At 140 and 305°F, 20 and 50 pptg guar were the minimum polymer loadings which, show acceptable viscosities, respectively. However, EDTA enabled us to reduce the polymer loading from 35 to 30 pptg at 225°F. The gel loaded with 30 pptg guar and 2 wt% EDTA could build better viscosity than the one loaded with 35 pptg guar and no EDTA at 225°F.

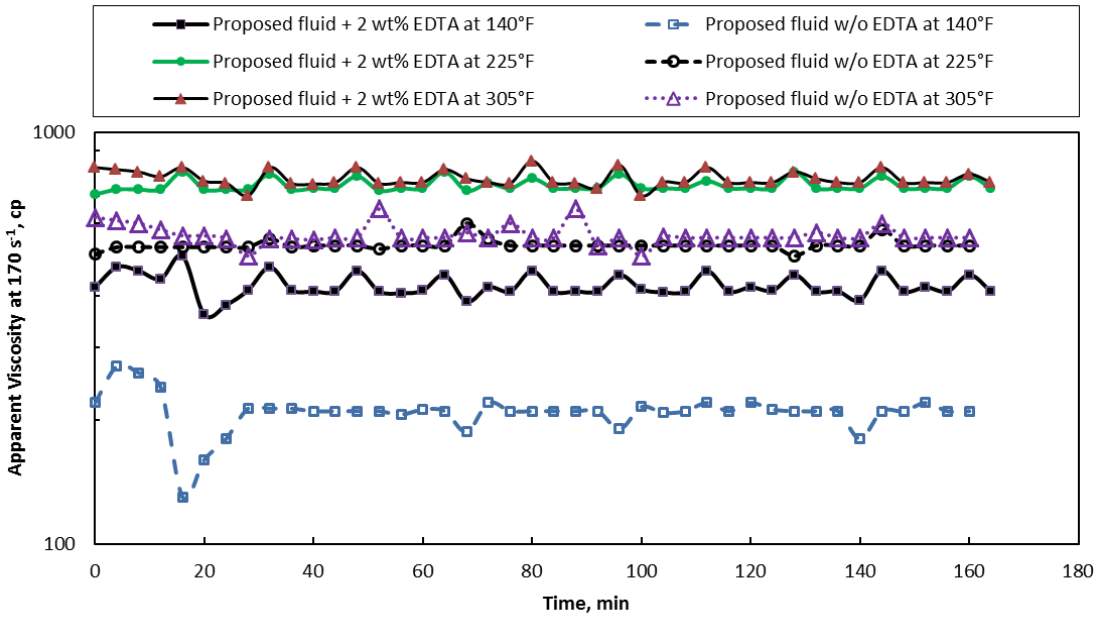

Fig. 3. 11— Single shear rate test to investigate the stability of proposed fluids at 140, 225, and 305°F; 170 s^{-1}; and 300 psi. The base fluids were gels prepared with 20, 30, and 50 pptg of polymer; 2 wt% EDTA, 16, 19, and 20 gpt buffer; and 1.0, 1.25 and 3.0 gpt crosslinker was selected as the base fluid at 140, 225, and 305°F, respectively. The gels without EDTA were prepared with 20, 35, and 50 pptg guar, 2.0, 4.0, and 4.0 gpt buffer, and 1.0, 1.0, and 3.0 gpt crosslinker loading at 140, 225, and 305°F, respectively.

High salinity can act as a breaker in post fracturing treatments (Fischer et al. 2001). However, high TDS in high pH crosslinked guar/borate systems causes several problems. The main issues are reduction in the hydration level, weak viscosity development, pH reduction, and interference with the crosslinking process. When all salts were added in the fluids, although KCl increased the ionic strength of the solution and the performance of the fluid improved, NaCl decreased the rate of dissolution of calcium and magnesium precipitations (Fredd and Fogler 1998).

3.6.3 Small-Amplitude Oscillatory Shear (SAOS) Measurements

Although polymer-based fracturing fluids have been used in the oil and gas industry for a long time, most of the time the rheological properties of the viscoelastic fluids are not very well understood. The change in viscoelastic properties during the treatment should be observed. For this purpose, the elastic and viscous properties of the prepared fluids were studied at different temperatures. All measurements were conducted at ambient and 225°F temperatures.

The high pH crosslinked guar/borate system is a viscoelastic fluid, and G' and G" represent its elastic and viscous properties. In Small-Amplitude Oscillatory Shear (SAOS) measurement, a small strain amplitude (5% in this case) in the linear viscoelastic limit can measure the storage (G') and loss (G") moduli of a fluid at a given oscillation frequency. This is a nondestructive technique. The relaxation time is when G' and G" crossover. The higher the relaxation time, the better the proppant suspension

properties in static and dynamic conditions (Harris et al. 2009). In this part, SAOS tests were applied to the proposed fluids from the previous sections and the effects of EDTA, polymer loading, and high pH were investigated on the viscoelastic properties and, consequently, on the proppant transport of the fracturing fluid. **Figs. 3.12 through 3.14** indicate the change of G' and G" as a function of frequency at ambient and 225°F. In all figures, the G" values are higher than G' at the beginning of the experiments. This is because crosslinked guar/borate gel is more of a viscous fluid than it is elastic.

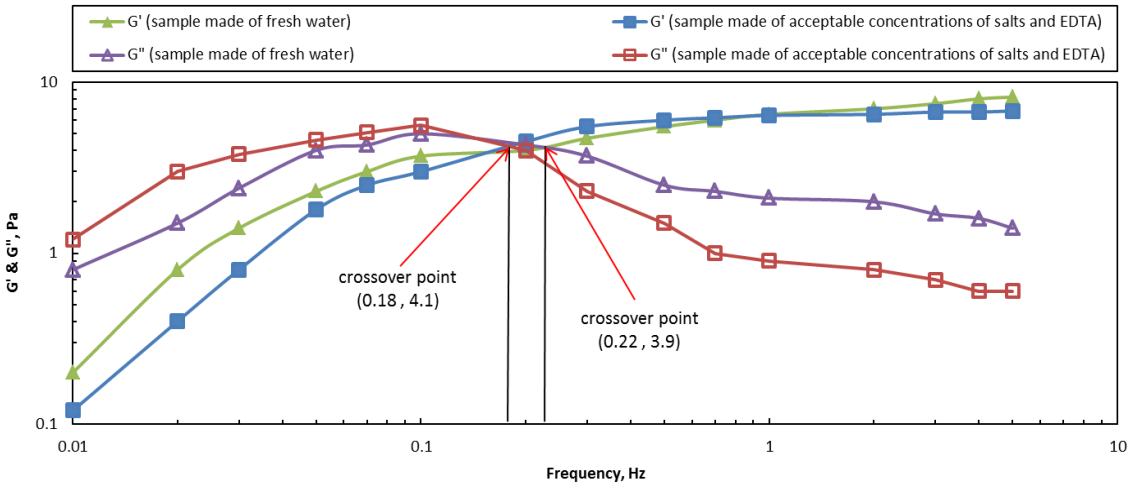

Fig. 3. 12— SAOS measurements performed on the gel prepared with fresh water and the fluid loaded with the maximum acceptable dissolved solid contents at 75°F and 5% applied strain. The base fluid was a gel prepared with 20 pptg guar, 2 wt% EDTA, 16 gpt buffer, and 1.0 gpt crosslinker loading.

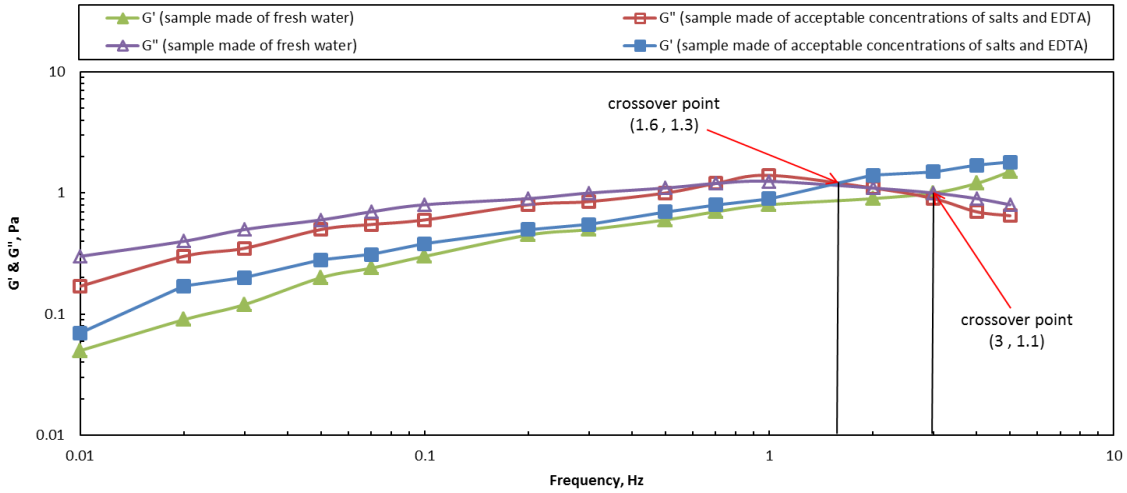

Fig. 3. 13— SAOS measurements performed on the gel prepared with fresh water and the fluid loaded with the maximum acceptable dissolved solid contents at 225°F and 5% applied strain. The base fluid was a gel prepared with 20 pptg guar, 2 wt% EDTA, 19 gpt buffer, and 2.0 gpt crosslinker loading.

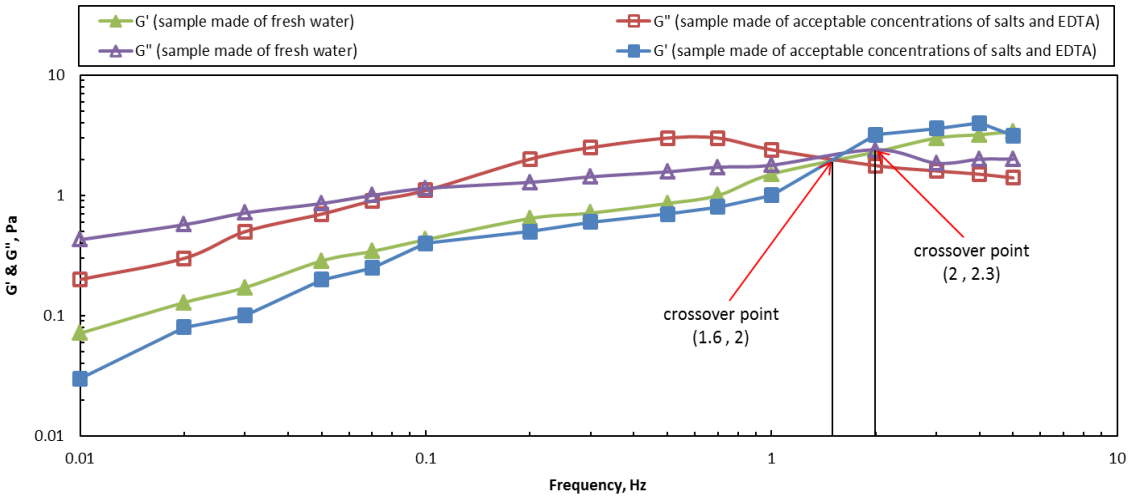

Fig. 3. 14— SAOS measurements performed on the gel prepared with fresh water and the fluid loaded with the maximum acceptable dissolved solid contents at 225°F and 5% applied strain. The base fluid was a gel prepared with 30 pptg guar, 2 wt% EDTA, 19 gpt buffer, and 1.25 gpt crosslinker loading.

The main characteristic of Figs. 3.12 through 3.14 is that the crossover points are very close in value and even in frequency at both temperatures. This fact indicates that EDTA was effective in maintaining the main functionality of the fracturing fluid. Also, both followed the same trend in viscous and elastic regions. This included a little buildup for G" in the viscous region and as soon as it reached the relaxation point it started to decrease. On the other hand, G' started to build up from the beginning and continued all the way until it almost reached a plateau at high frequencies in the elastic region. **Figs. 3.13 and 3.14** show that, regardless of polymer loading, the increase in the temperature expands the viscous region. So, these fluids have more dominant viscous properties than elastic fluids at higher temperatures. It was noticeable that G' and G" values are higher by one order of magnitude at ambient temperatures. The same trend was also observed at higher polymer loading at 225°F.

3.6.4 Static Settling Tests

The static settling test is a simple but practical method which visually enables a comparison between proppant settling in different fluids. Fracturing fluid should be able to provide adequate transport of proppants in the fracture. The further the proppant moves inside the fracture and the higher its conductivity, the more successful the job. After the linear gel was prepared, a 20/40-mesh Ottawa sand was added to the fluid before the crosslinking process. The proppant had a specific gravity of 2.65 and was added at a concentration of 4 lb_m/gal. The fluid/proppant mixture was placed in a 100 ml

graduated cylinder in a see-through cell that could be heated up to 450°F at a pressure of 500 psi. The level of proppant settlement through the fluid was recorded every 5 minutes for 200 minutes or until all of the proppant had settled to the bottom of the test chamber. This experiment would simulate near wellbore conditions where the shear rates are low.

Fig. 3.14 illustrates the test results at ambient temperatures. Suspension in both tests was approximately 70%. To imitate downhole conditions, the tests were also conducted at a temperature of 225°F. The samples needed 15 (± 5) minutes to reach the cell temperature. **Figs. 3.16 and 3.17** confirm that increasing the polymer loading from 20 to 30 pptg at 225°F significantly increased the performance of both fluids. The base fluid was prepared with fresh water and the sample loaded with maximum salt concentrations and EDTA showed very good suspension, and 83% and 75% of the proppants remained in suspension after about 200 minutes, respectively. **Fig. 3.18** shows the hourly levels of proppant settling in a sample loaded with salts and EDTA at 225°F.

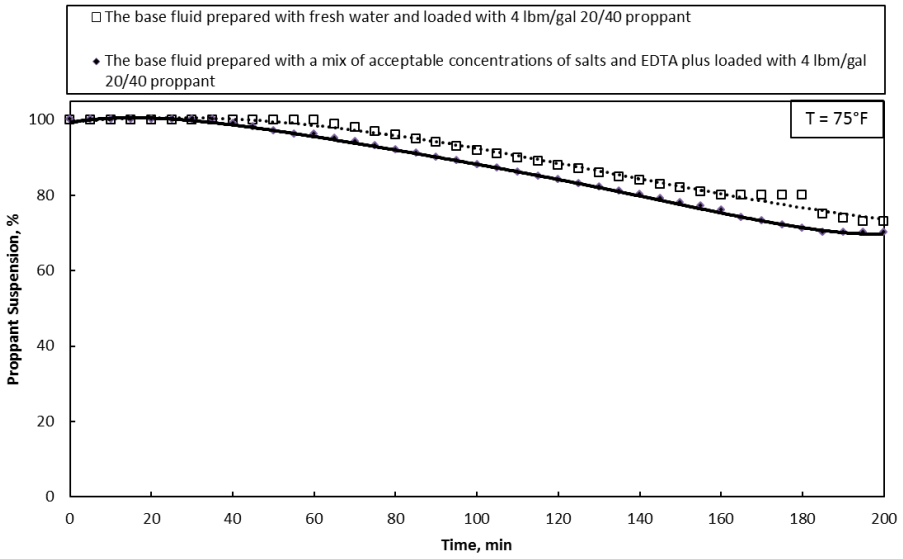

Fig. 3. 15— Comparison between proppant settling of sample prepared with fresh water and the fluid prepared with the maximum acceptable dissolved solid contents which were loaded with 4 lb_m/gal of 20/40 Ottawa sand at 75°F. The base fluid was a gel prepared with 20 pptg guar, 2 wt% EDTA, 16 gpt buffer, and 1.0 gpt crosslinker loading.

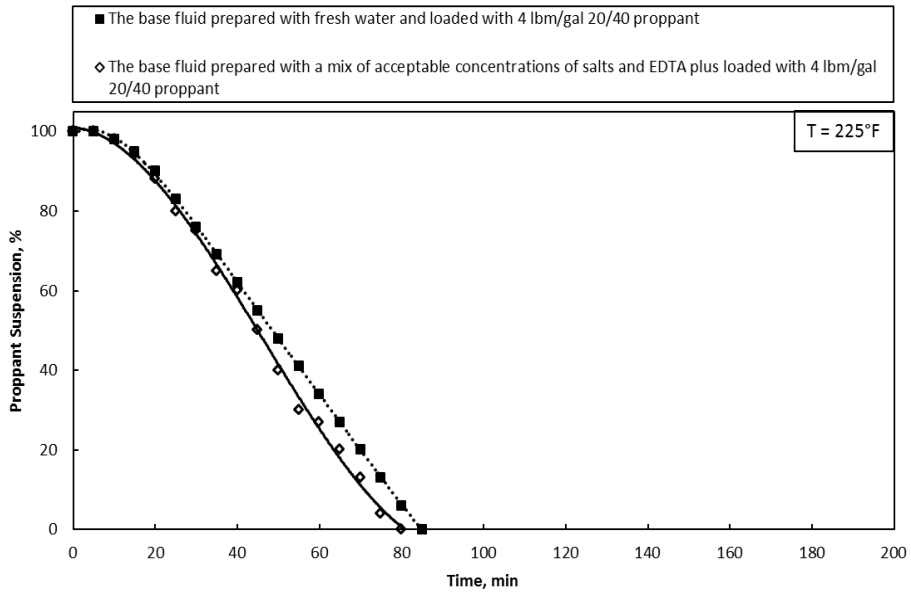

Fig. 3. 16— Comparison between proppant settling of sample prepared with fresh water and the fluid prepared with the maximum acceptable dissolved solid contents which were loaded with 4 lb_m/gal of 20/40 Ottawa sand at 225°F. The base fluid was a gel prepared with 20 pptg guar, 2 wt% EDTA, 19 gpt buffer, and 2.0 gpt crosslinker loading.

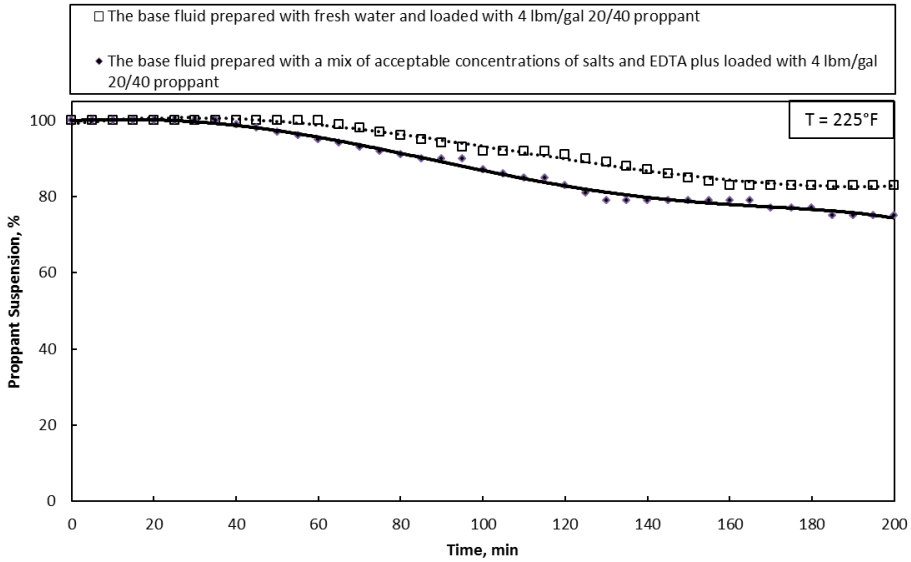

Fig. 3. 17— Comparison between proppant settling of sample prepared with fresh water and the fluid prepared with the maximum acceptable dissolved solid contents which were loaded with 4 lb_m/gal of 20/40 Ottawa sand at 225°F. The base fluid was a gel prepared with 30 pptg guar, 2 wt% EDTA, 19 gpt buffer, and 1.25 gpt crosslinker loading.

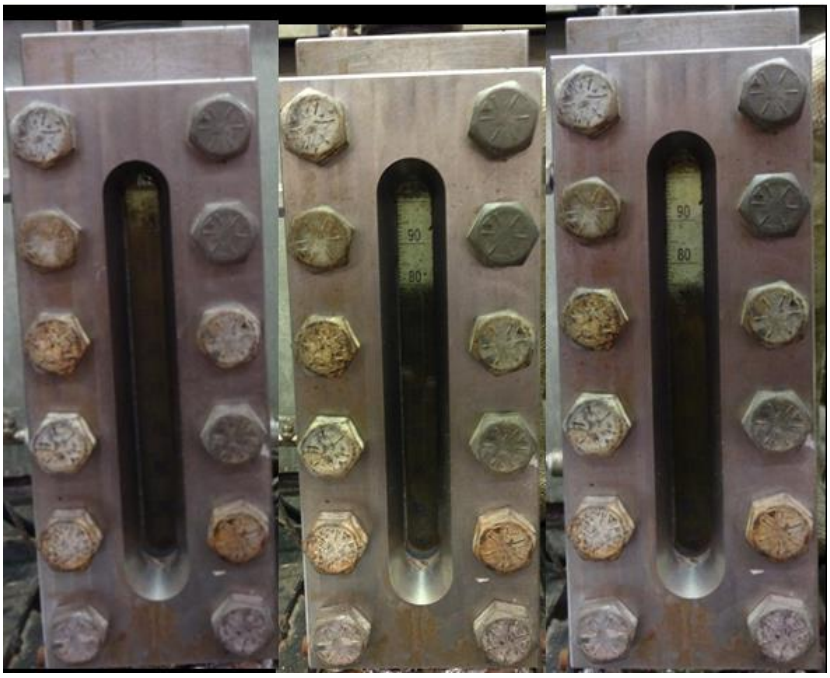

60 minutes 120 minutes 180 minutes

Fig. 3. 18— Static proppant settling test on the fluid prepared with maximum acceptable dissolved solid contents which was loaded with 4 lbm/gal of 20/40 Ottawa sand at 225°F. The base fluid was a gel prepared with 30 pptg guar, 2 wt% EDTA, 19 gpt buffer, and 1.25 gpt crosslinker loading.

3.7 Conclusions

Static and dynamic rheological measurements and proppant static settling tests were conducted using a high-pH guar/borate crosslinked system. Two monovalent cations (Na^+ and K^+) and two divalent cations (Ca^{2+} and Mg^{2+}) were tested at temperatures up to 305°F. Based on the results, the following conclusions can be drawn:

1. EDTA, polymer loading, and high pH improved the tolerable salinity of the base hydraulic fracturing fluid.
2. Adding 2 wt% EDTA enhanced the viscosity of the fracturing fluid and the maximum acceptable concentrations of calcium and magnesium were increased 60% and 82.7%, respectively.
3. Fluids containing sodium and potassium performed better at higher pH values.
4. EDTA resulted in 15% reduction in polymer loading at 225°F.
5. The thermal stability of the fluids containing EDTA was higher and apparent viscosities also increased from ~36% to 95% at different temperatures.
6. Presence of the chelating agent increased the G' and G" values by an order of magnitude at 225°F.
7. Proppant settling characteristics of the proposed fluid were very similar to the fluid prepared with fresh water.

Therefore, it is technically practicable to use EDTA in the reuse of flowback fluids in hydraulic fracturing jobs.

CHAPTER IV

A ROBUST ADVISORY SYSTEM FOR SELECTION OF FRACTURING FLUID IN TIGHT GAS SAND RESERVOIRS

4.1 Introduction

Fracturing fluid selection is a crucial element of hydraulic fracturing treatment design. Certain variables, such as reservoir pressure and temperature, thickness of fracturing interval, strength of upper and lower barriers, half-length fracture, existence of natural fractures, and formation lithology can affect efficiency of the hydraulic fracture job. Computational and statistical techniques such as empirical relationships, multivariate analysis, Artificial Neural Network (ANN), nearest neighbor algorithm have been commonly applied for optimizing hydraulic fracturing design (Ali 1994; Anifowose et al. 2013; Sitouah et al. 2013; Voneiff et al. 2013 and 2014; Aulia et al. 2014; Mehrgini et al. 2014; Maucec et al. 2015). However, these techniques are often blindly applied, without a sufficient statistical and computational background, which can lead to inaccurate outcome. Fundamental understanding of statistical techniques can help in selection of the appropriate method for a reliable application of these techniques. A dependable model should generate high prediction accuracy without high level of computational complexity (Sitouah et al. 2013).

Hydraulic fracturing has been the most effective stimulation technique, extensively applied in thousands of wells that have been drilled in tight gas sand

reservoirs in Texas over the years. Completion and production data from five tight gas sand reservoirs in Texas were extracted and collected from a public domain (i.e., drillinginfo website) to develop a reliable fracturing fluid selection model for tight gas sand reservoirs. The objectives of this chapter are to investigate the effect and weight factor of some of the main variables in fracturing fluid selection process and to correlate the significant variables that affect the decision making process and develop a fracturing fluid selection model for tight gas sand reservoirs from the available data. The ensemble learning models have showed superior performance over the other individual learning techniques in solving complex problems. After investigating and examining different methods, random forest algorithm was selected as the most appropriate technique for building a fracturing fluid selection model. Random forest is especially suitable for this case where there are discrete and continuous variables and available data are often noisy and contain missing values (Anifowose et al. 2013).

4.2 Methodology

When it comes to data analysis there are several available techniques that are commonly applied in the industry. The first question to ask is "which technique is the most appropriate for a specific case of study?". Selection of a suitable data analysis tool can result in an accurate and a reliable outcome. For this selection, it is recommended to

have a general understanding of the cons and pros of the various data analysis tools, as well as the properties of the case understudy.

The next step is to determine which properties of the case study are most important for fine-tuning the proposed model for accurate and reliable prediction. In this work, first we applied several techniques including regression method, conversion of categorical variables into numeric variables, ANN, and considered all features and pick machine learning algorithm to investigate the feasibility and validity of these methods. None of those techniques converged to reliable result, therefore, we used the random forest technique (Breiman 2001).

Several random tree methods have been previously introduced such as subspace method for decision forests (Ho 1995and1998), shape recognition (Amit and Geman 1997), random split selection (Dietterich 2000), and perfect random tree ensembles (Cutler and Zhao 2001). In this work, we applied one of the latest and the most reliable random forest techniques, developed by Breiman (2001). We used random forest package in the R programming language and software, which is an accessible open source software for statistical computations.

Random forest method is a highly versatile ensemble method that integrates several decision-making models into one. Random forests models are built from aggregating decision trees and they can be used for regression and classification problems (Breiman 2001). They can also be applied for building prediction models based on dependent variables or for classifying a categorical dependent variable on the basis of the observable independent covariance. In all decision tree learning algorithms,

a random vector Θ_k is generated for the k^{th} tree. This independent random vector has the same distribution of the other previously generated vectors $\Theta_{1, \ldots,} \Theta_k$-1. These random vectors form a classifier consists of a collection of tree-structured classifiers $\{h(x,\Theta_k), k=1, \ldots\}$ where x is an input factor. In this technique, each tree votes for the most popular class (Breiman 2001). One of the most dominant characteristics of the random forest method is that it has less tendency to overfit compared to other learning techniques and can handle large number of features. Also random forest can provide a list of most influential features in the predicting process.

Random forest incorporates the method of bagging and the random selection of features in order to build a selection of decision trees with controlled variance (Ho 1995and1998; Geman 1997; Breiman 1996). Bagging produces an aggregated predictor based on multiple versions of a predictor by averaging over the versions in the case of a numerical outcome. The multiple versions are created by making bootstrap duplicates of the learning set. The combination of learning models increases the classification accuracy. In addition, bagging averages noisy and unbiased models in order to create a model with low variance in terms of classification. The key factor in the bagging technique is the instability of the prediction technique. Bagging can improve accuracy, where perturbing the learning set could result in significant different predictor models. Despite a low associated bias, deep decision trees that are required for complex data analysis have a high variance, due to the large degree of freedom in these trees (Breiman 1996). Thus, bagging takes a low-bias-high-variance predictor and transforms it into a stable and a more accurate ensemble learner. However, if there are a large number of

variables in the dataset, bagging cannot adequately reduce the variance. Alternatively, a random forest can create a predictor by bagging and randomizing a deep tree, in order to reduce the associated variance.

Furthermore, one of the random forest advantages is to rank the importance of variables in a natural way. For this purpose, random forest permutes each variable while the rest of variables are left untouched. Then, it estimates the importance of the permuted variables by calculating at how much prediction error increased for that variable (Liaw and Weiner 2002). In the following sections, we will discuss classification of trees and how to incorporate them into the random forest model.

4.3 Random Forest Algorithm

Determining and defining input and output variables is the first step in applying random forest for analyzing and prediction purposes. The second step is pre-processing the data, which includes removing outliers, de-noising, and treating the inconsistent and incomplete data such as predicting the missing values in a set of variables. Random forest is a binary recursive partitioning. In a binary splitting process the parent node is always split into two child nodes and each child node becomes a parent node for the next splitting level. Therefore, the third step is calculating the optimal tree depth. In a classification tree, splitting is based on maximized entropy or Gini's index. For a dataset T, which contains examples from n classes, Gini index is defined as

$$Gini(T) = 1 - \sum_{i}^{n} p^2(i) \quad \ldots \ldots \ldots \ldots \ldots \ldots \ldots \ldots \ldots \ldots \ldots \ldots \ldots \ldots \ldots \ldots \ldots (4.1)$$

where p(i) is the relative frequency of class i in T. In splitting process of dataset T into two subsets T_1 and T_2 with two different sizes N_1 and N_2 respectively, the gini index (T) is defined as

$$Gini_{split}(T) = \frac{N_1}{N} gini(T_1) + \frac{N_2}{N} gini(T_2) \quad \ldots \ldots \ldots \ldots \ldots \ldots \ldots \ldots \ldots \ldots \ldots (4.2)$$

The attribute value that provides the smallest split gini (T) will be chosen to split the node. This process can become very complex and it is very important to reach to an optimum tree before using it for classification and prediction purposes (Breiman 2001). The last step is measuring the contribution of each variable and quantifying its importance. The misclassification probability for a dataset with *v* sub samples of equal size N_1, N_2, …, N_v and the V-fold cross-validation error **(ε_{CV})** ε_{cv} for the classification tree is defined as

$$\varepsilon_{cv} = \frac{1}{N_v} \sum_{i=1}^{N_v} I(\hat{y}_{i(N-N_v)} \neq y_i) \quad \ldots \ldots \ldots \ldots \ldots \ldots \ldots \ldots \ldots \ldots \ldots \ldots (4.3)$$

where $\hat{y}_{i(N-N_v)}$ is the predicted value of the sample computed from the tree that is constructed using *N-Nv* samples (Maucec et al. 2015).

The training set in random forest algorithm consists of two-third of the data which will be selected randomly to build a tree. This process will be repeated for all trees in the analysis. The remaining one-third of the dataset in each tree is the testing set. The Out-Of-Bag (OOB) error estimate is calculated based on the overall misclassification in the test datasets of all trees. Thus, evaluation of the OOB error performed by the random forest model eliminates the requirement of a cross-validation test and identifies the best decision tree (Breiman 2001).

4.4 Data Gathering

We reviewed completion and production reports from 164 wells in Olmos, Bossier, Morrow, Cotton Valley, and Canyon Sand reservoirs, in Texas, that were completed using six different fracturing fluid categories. These reservoirs have different characteristics and completion designs. At least 30 wells from each reservoir were selected for the analysis in order to ensure that the dataset is representative of the variability in the reservoirs. **Fig. 4.1** illustrates the locations of the reservoirs.

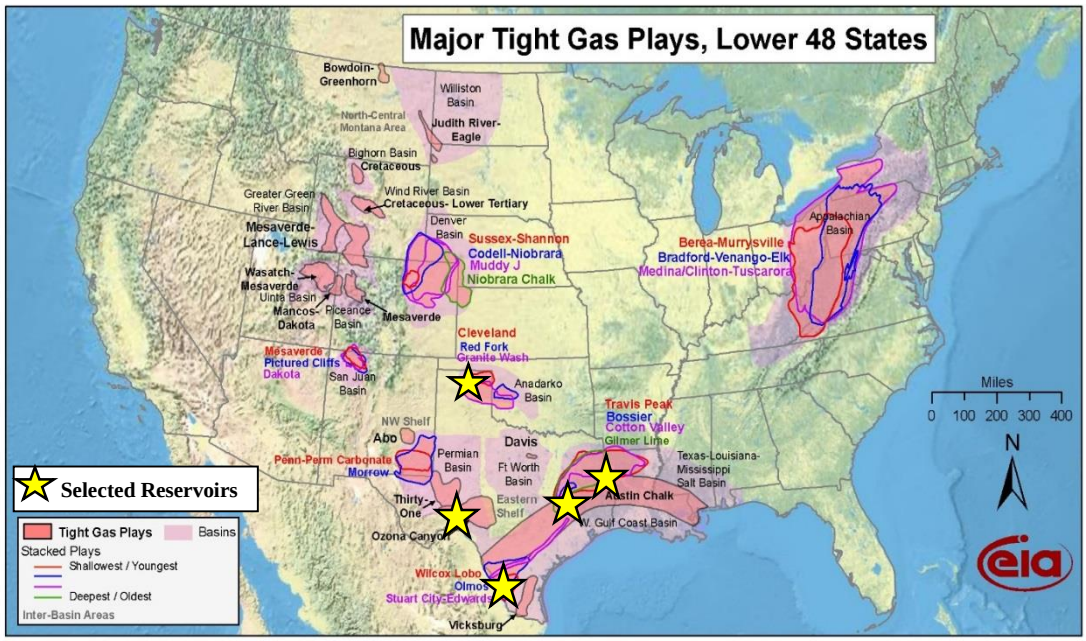

Source: Energy Information Administration based on data from various published studies
Updated: June 6, 2010

Fig. 4. 1— Reservoirs selected for the study (the red stars on the map show the location of the reservoirs).

Six predictor variables were selected based on hydraulic fracturing literature, outcomes of reservoir simulations, and surveys of fracturing experts' opinions. The continuous predictor variables in this study included bottomhole temperature (BHT), bottomhole pressure (BHP), and pay zone thickness. The discrete variables were lower and upper barrier strength and Young's modulus of lower barrier. The response variable was calculated by extracting the pause and resume events for a particular job from the event job table, and then the duration between the pause and resume was summed for a particular job, resulting in optimum tree. Five hundred trees were generated and the process repeated 100 times. The sample data is shown in **Table 4.1**.

Table 4. 1— Sample of the wells properties

	API#	County	Total Depth	Field Name	Reservoir Name	depth (ft)	PI Top (ft)	PI Bottom (ft)	wellhead pressure (psi)	Cumulative Gas (MCF)
1	42-183-31341	Gregg	10,680	WILLOW SPRINGS (COTTON VALLEY)	COTTON VALLEY	7400	7386	10498	1200	2,421,201
2	42-423-31584	Smith	12,060	OVERTON (COTTON VALLEY SAND)	COTTON VALLEY SAND	11600	11544	11760	3475	1,512,510
3	42-183-31547	Gregg	10,650	WILLOW SPRINGS (COTTON VALLEY)	COTTON VALLEY	7400	7441	10473	3300	1,216,000
4	42-423-31658	Smith	11,950	OVERTON (COTTON VALLEY SAND)	COTTON VALLEY SAND	12000	11690	11783	3350	1,038,042
5	42-423-31604	Smith	11,954	OVERTON (COTTON VALLEY SAND)	COTTON VALLEY SAND	11600	11582	11724	4350	970,911
6	42-423-31622	Smith	12,035	OVERTON (COTTON VALLEY SAND)	COTTON VALLEY SAND	11700	11584	11846	3215	910,779
7	42-183-31643	Gregg	10,750	EASTON, N. (COTTON VALLEY)	COTTON VALLEY	9900	9153	10635	4115	825,575
8	42-423-31680	Smith	11,912	OVERTON (COTTON VALLEY SAND)	COTTON VALLEY SAND	11600	11482	11724	2265	784,555
9	42-423-31576	Smith	12,252	OVERTON (COTTON VALLEY SAND)	COTTON VALLEY SAND	11800	11704	11998	3650	761,156
10	42-183-31653	Gregg	10,850	EASTON, N. (COTTON VALLEY)	COTTON VALLEY	10000	9265	10718	1615	731,433
11	42-183-31605	Gregg	10,825	WHITE OAK (COTTON VALLEY SAND)	COTTON VALLEY SAND	10500	10382	10666	4658	695,601
12	42-183-31573	Gregg	10,938	GLENWOOD (COTTON VALLEY)	COTTON VALLEY	10700	10640	10815	4650	668,421
13	42-183-31565	Gregg	10,795	WHITE OAK (COTTON VALLEY SAND)	COTTON VALLEY SAND	10600	10514	10646	4415	640,407
14	42-423-31695	Smith	12,028	OVERTON (COTTON VALLEY SAND)	COTTON VALLEY SAND	11700	11544	11804	3215	589,977
15	42-183-31606	Gregg	10,825	GLENWOOD (COTTON VALLEY)	COTTON VALLEY	10600	10505	10687	4888	555,293

4.5 Properties and Characteristics of the Selected Reservoirs

Most of completion and production data used in this study are accessible on public domains (e.g., drillinginfo website). Among the selected reservoir properties, BHT, BHP, and pay zone thickness were presented and published on public domains. The distributions of these input parameters are illustrated in **Fig. 4.2 to 4.5**.

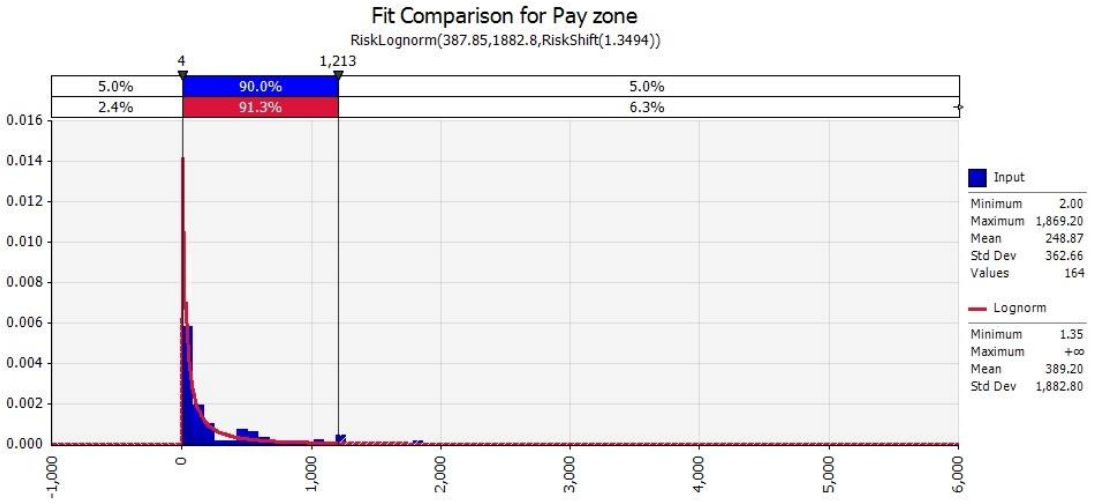

Fig. 4. 2— Distribution of pay zone thickness for all selected wells.

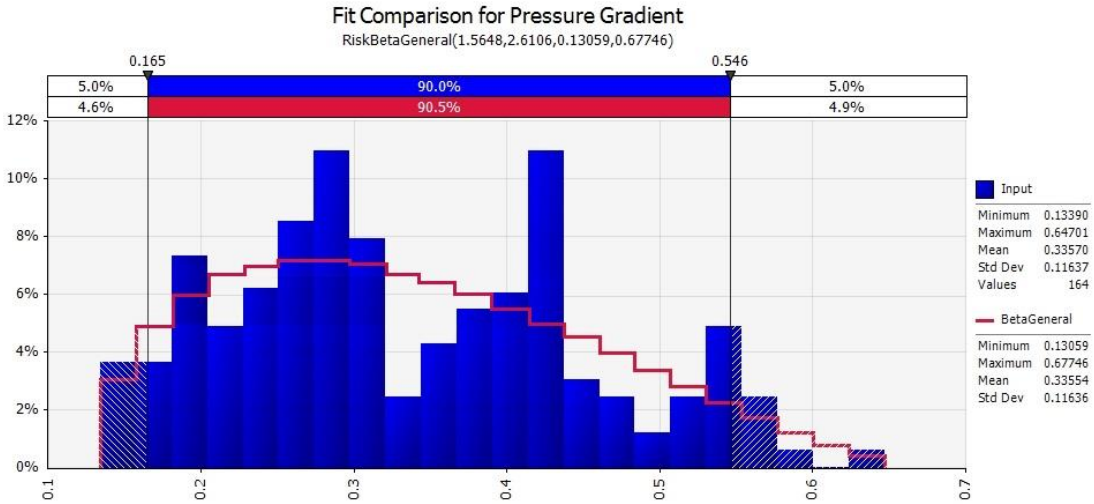

Fig. 4. 3— Distribution of pressure gradient for all selected wells.

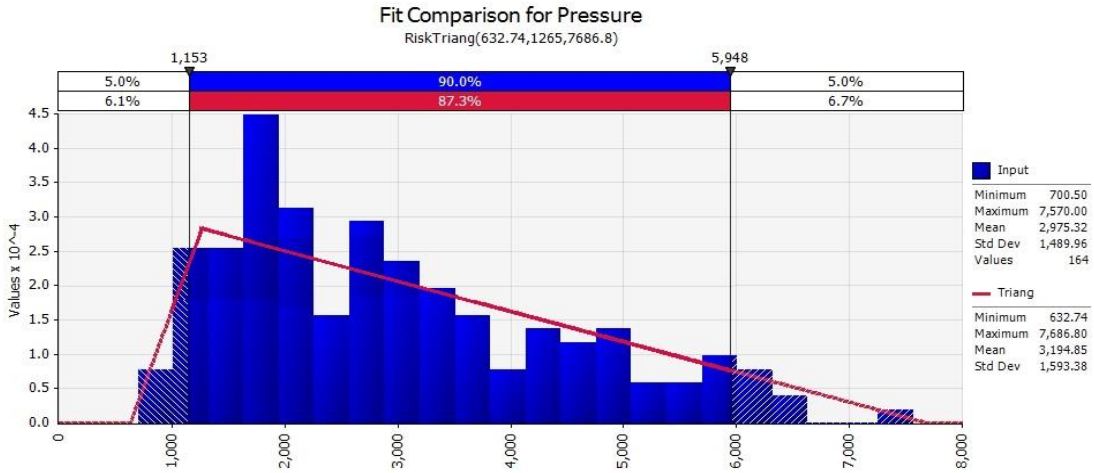

Fig. 4. 4— Distribution of bottomhole pressure for all selected wells.

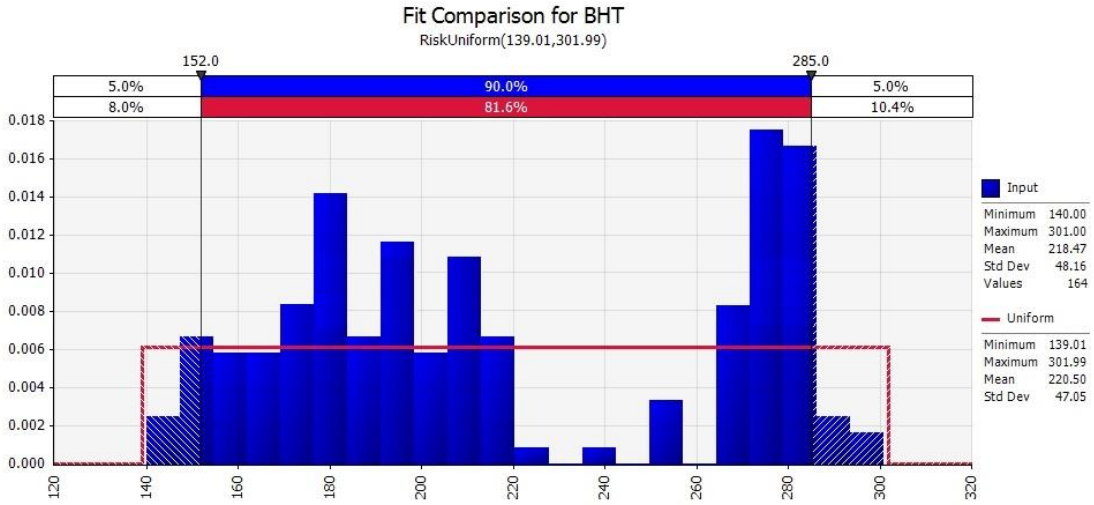

Fig. 4. 5— Distribution of bottomhole temperature for all selected wells.

On the other hand, lower and upper barrier strengths and Young's modulus of lower barrier are not reported on public domains. Thus, we used an indirect approach to estimate these properties. In cases where sonic logs were available, we used compressional and shear wave velocity measurements to estimate dynamic elastic moduli (Zhixi et al. 1997) via

$$E_d = \rho v_s^2(3v_p^2 - 4v_s^2)/(v_p^2 - v_s^2) \quad \text{.....} \quad (4.4)$$

where E_d is the dynamic elastic modulus, Gpa, V_p is the compressive wave velocity, m/s, V_s is the shear wave velocity, m/s, and ρ is the bulk density, kg/m.

In the absence of sonic logs, we estimated the elastic properties by incorporating mineralogy and shapes of rock constituents using an effective medium theory called self-consistent approximation (Mavko et al. 2009). We first used gamma ray log to estimate the clay and non-clay (sand) content in the reservoir. We then applied the self-consistent approximation to estimate the effective bulk and shear moduli by

$$\sum_{i=1}^{N} X_i(K_i - K_{sc}^*)P^{*i} = 0 \quad \text{.....} \quad (4.5)$$

and

$$\sum_{i=1}^{N} X_i(\mu_i - \mu_{sc}^*)Q^{*i} = 0 \quad \text{.....} \quad (4.6)$$

where K^*_{SC} and μ^*_{SC} are the effective bulk and shear moduli of the rock, X_i is the volumetric concentration of the rock component i, K_i and μ_i are the bulk and the shear moduli of the rock component, and P^{*i} and Q^{*i} correspond to the shape geometry of each rock component. Young's modulus and Poisson's ratio were then calculated from the estimates of bulk and shear moduli. Next, the brittleness index introduced by Rickman et al. (2008) was calculated based on the estimates of Young's modulus and Poisson's ratio via

$$Britt_{index} = \left(\frac{E_{Britt}+v_{Britt}}{2}\right)100 \quad \text{..... (4.7)}$$

where E_{Britt} and υ_{Britt} are normalized Young's modulus and Poisson's ratio and

$$E_{Britt} = \left(\frac{E-E_{min}}{E_{max}-E_{min}}\right) \quad \text{..... (4.8)}$$

and

$$v_{Britt} = \left(\frac{v-v_{min}}{v_{min}-v_{max}}\right) \quad \text{..... (4.9)}$$

where E_{max} and E_{min} are the maximum and the minimum Young's moduli, and υ_{max} and υ_{min} are the maximum and the minimum Poisson's ratios.

4.6 Reservoirs Selection

There are several tight gas sand reservoirs in Texas that operators have been attempting to optimize their completion and production. To date, thousands of wells have been drilled by industry in Texas and a wide variety of completion designs have been employed in tight gas sand reservoirs in Texas. We analyzed public domain completion and production data on 164 wells in five tight gas sand reservoirs in Texas to investigate the influence of reservoir parameters on completion design and build a fracturing fluid selection model based on previous successful jobs. In this section we have presented a brief history and description of each selected reservoir.

4.6.1 Cotton Valley Reservoir

Cotton Valley reservoir, located in the East Texas, is one of the largest and the oldest reservoirs which has been completed by various hydraulic fracturing treatments using different types of fracture fluids such as crosslinked gel and slick water. The typical completion designs in this reservoir have two to four stage fracture treatments. Starting from the deepest interval, the producing intervals are usually fracture stimulated one at a time. Then, all stimulated intervals are placed on production after flowback (Malpani 2006).

This reservoir mainly consists of tightly cemented, very fine to fine-grained sandstone interbedded with mudstone, carbonate, and siltstone. It is extended from

Northeast Texas to Northwest Louisiana (Spain et al. 2011). Production interval of this reservoir ranges from approximately 750 ft to more than 15,000 ft subsea along the southern margins of the East Texas Basin and Louisiana-Mississippi Salt Basins Provinces (Dyman and Condon 2006).

For this work, 31 wells in Cotton Valley reservoir from Gregg and Smith Counties in Texas were selected. Some of the most important characteristics of these wells are as follows:

- All wells are active vertical gas wells with at least 7 years of production history.
- The completion and production interval is from 7,386 to 11,998 ft.
- Pay zone thickness is from 8 to 1,244.8 ft.
- Pressure gradient is from 0.23 to 0.57 psi/ft.
- BHT is from 207 to 290°F.
- Cumulative gas production is from 137,951 to 2,427,017 MCF.

Fig. 4.6 illustrates the location of the selected wells on the map.

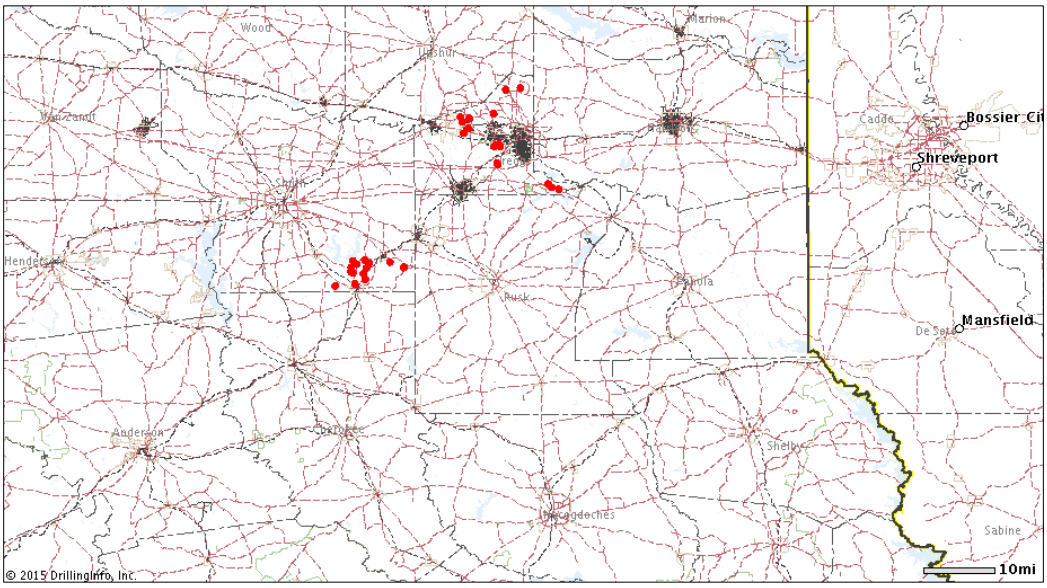

Fig. 4. 6— Cotton Valley reservoir wells snapshot (Thirty one wells were selected from Gregg and Smith Counties in Texas)

4.6.2 Olmos Reservoir

The Olmos formations of the Rio Grande Embayment area is a gas reservoir throughout Webb, LaSalle, McMullen, and Dimmit counties of South Texas. Most of the best quality reservoir facies are extended from west-southwest to east and south of Texas. The reef line continues towards south-southwest and through Webb County extends down into Mexico. Improvements in hydraulic fracturing technologies, application of modern high-resolution logs, large scale slick water fracturing, and horizontal drilling in the mid ’90s have resulted in exceptional well performance within Olmos reservoir and boosted the production, which was initially marginally profitable (Condon and Dyman 2003).

For this work, 40 wells in Olmos reservoir from Webb County in Texas were selected. Some of the most important characteristics of these wells are as follows:

- All wells are active vertical gas wells with at least 10 years of production history.
- The completion and production interval is from 4,458 to 7,366 ft.
- Pay zone thickness is from 2 to 152 ft.
- Pressure gradient is from 0.14 to 0.47 psi/ft.
- BHT is from 148 to 220°F.
- Cumulative gas production is from 103,450 to 602,751 MCF.

Fig. 4.7 illustrates the location of the selected wells on the map.

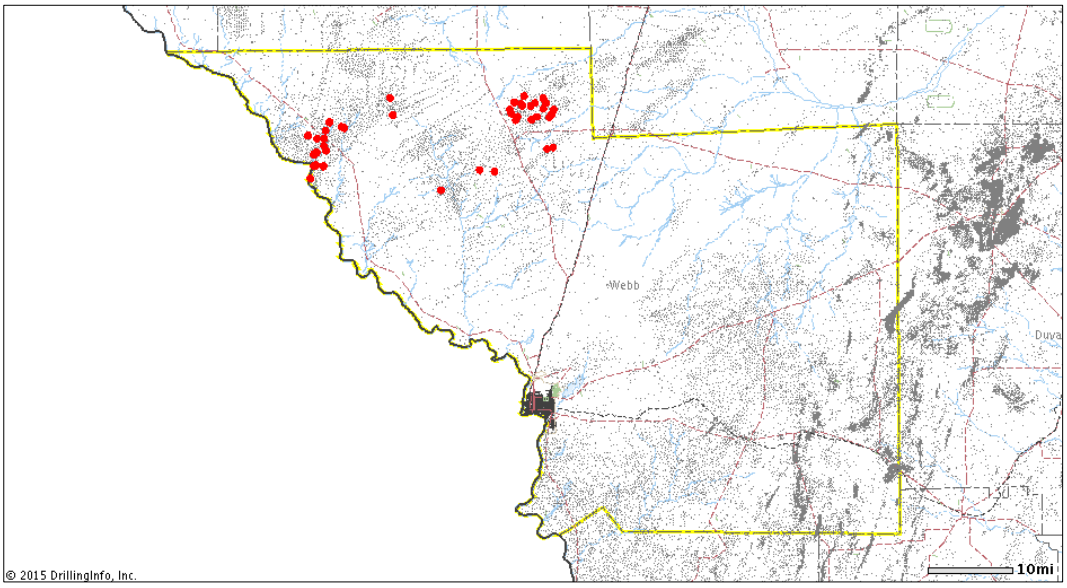

Fig. 4. 7— Olmos reservoir wells snapshot (Forty wells were selected from Webb County in Texas)

4.6.3 Canyon Sand Reservoir

The origin of Canyon Sands are Upper Pennsylvanian deposits found on the Permian Basin eastern shelf, Texas and in the Val Verde basin, located in Val Verde, Sutton, and western Edwards counties in Texas. The Canyon group has deposited during Missourian time on the eastern shelf.

The Canyon Sand has been active for more than three decades with commercial gas production. Top and bottom of the reservoir are at 2,000 to10,000 ft, respectively. The reservoir has produced approximately 2 TCF of gas. This reservoir covers more than 10 counties in South Central Texas. Average estimated quartz content for this reservoir ranges from 77 to 85%. Rock fragments consist of quartzites, limestone, phyllites, siltstone, slates, and shale clasts. Clay grains are present and consist of more than 20% of the rock matrix (Trabelsi 1994).

For this work, 33 wells in Canyon Sand reservoir from Crockett County in Texas were selected. Some of the most important characteristics of these wells are as follows:

- All wells are active vertical gas wells with at least 10 years of production history.
- The completion and production interval is from 3,839 to 9,558 ft.
- Pay zone thickness is from 12.8 to 1,375.2 ft.
- Pressure gradient is from 0.17 to 0.43 psi/ft.
- BHT is from 159 to 250°F.
- Cumulative gas production is from 112,521 to 889,098 MCF.

Fig. 4.8 illustrates the location of the selected wells on the map.

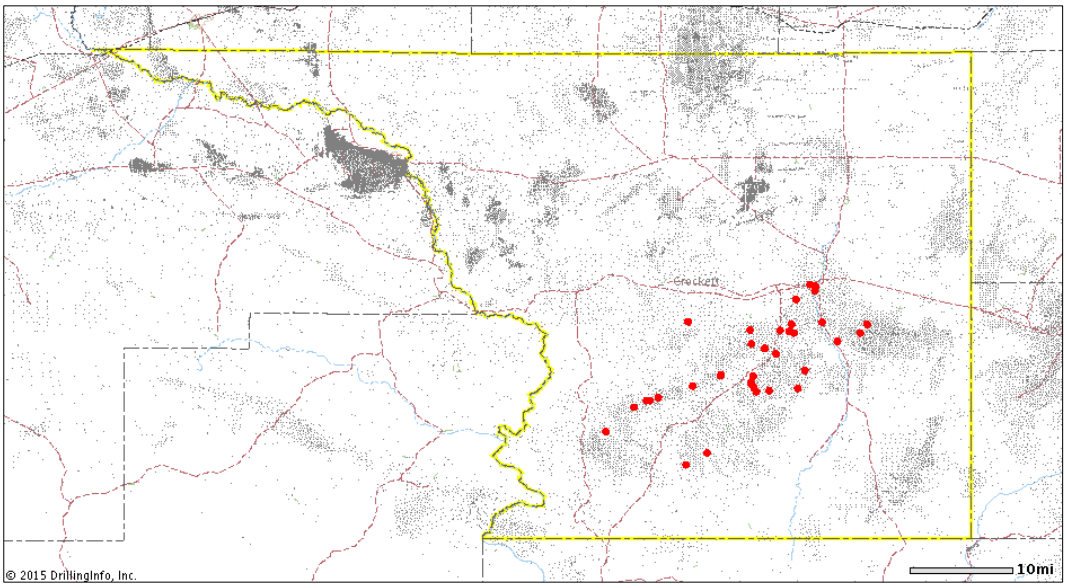

Fig. 4. 8— Canyon Sand reservoir wells snapshot (Thirty three wells were selected from Crockett County in Texas)

4.6.4 Morrow Reservoir

The Denver Basins and Lower Pennsylvanian Morrow formation of the Anadarko consists of shale and sandstone and it has about 1,800 ft thickness. The Morrow reservoir produces gas in Oklahoma, Texas, Kansas, and Colorado. The dominant mineralogy in the Morrow is sandstone. Morrow reservoir has been divided into three categories based on their differences in terms of depositional setting and geographic properties: deltaic, shallow marine, and incised valley-fill (Turner et al. 2008).

For this work, 30 wells in Olmos reservoir from Ochiltree, Roberts, Hansford, Lipscomb, and Hemphill Counties in Texas were selected. Some of the most important characteristics of these wells are as follows:

- All wells are active vertical gas wells with at least 7 years of production history.
- The completion and production interval is from 6,742 to 15,082 ft.
- Pay zone thickness is from 3.2 to 1,861.6 ft.
- Pressure gradient is from 0.13 to 0.65 psi/ft.
- BHT is from 140 to 270°F.
- Cumulative gas production is from 259,976 to 4,040,402 MCF.

Fig. 4.9 illustrates the location of the selected wells on the map.

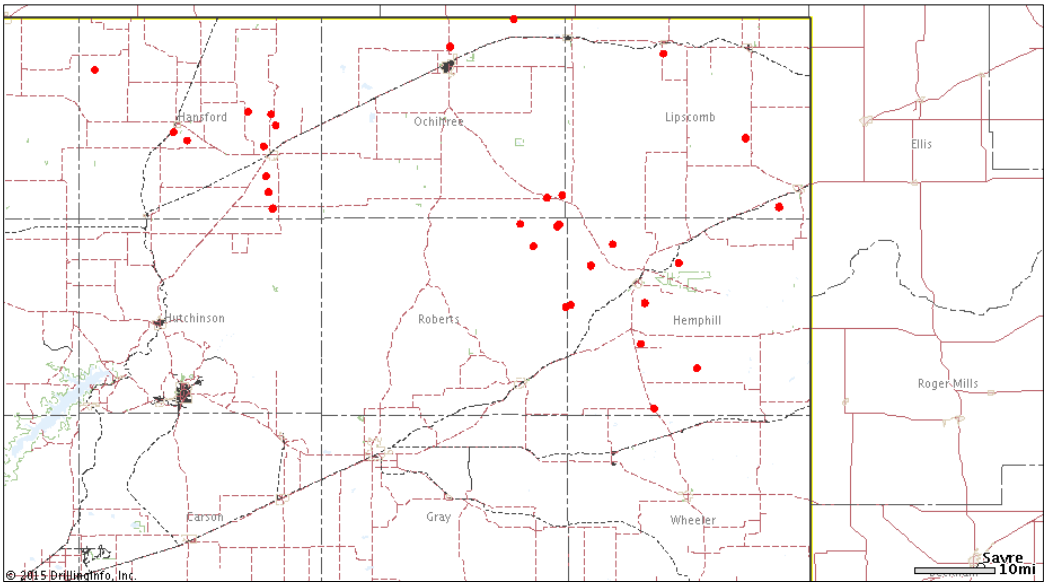

Fig. 4. 9— Morrow reservoir wells snapshot (Thirty wells were selected from Ochiltree, Roberts, Hansford, Lipscomb, and Hemphill Counties in Texas)

4.6.5 Bossier Reservoir

The Jurassic-age Bossier sands were located in the East Central part of Texas and deposited in the East Texas Basin. This sedimentary basin is one of the three major salt provinces in the US and one of the most active tight gas sands plays in the North America over the last decade (Newsham and Rushing 2009). The western shelf margin of the East Texas Basin has been the most active section of Bossier sand in the past and current developments. The Bossier interval is a thick lithological complex composed of black to gray-black shale inter bedded with fine grained argillaceous sandstone. The sand-body thickness varies from tens to several hundred feet (Rushing et al. 2008).

For this work, 30 wells in Olmos reservoir from Freestone County in Texas were selected. Some of the most important characteristics of these wells are as follows:

- All wells are active vertical gas wells with at least 7 years of production history.
- The completion and production interval is from 8,397 to 13,070 ft.
- Pay zone thickness is from 42.4 to 1,869.2 ft.
- Pressure gradient is from 0.25 to 0.60 psi/ft.
- BHT is from 270 to 301°F.
- Cumulative gas production is from 285,692 to 2,611,435 MCF.

Fig. 4.10 illustrates the location of the selected wells on the map.

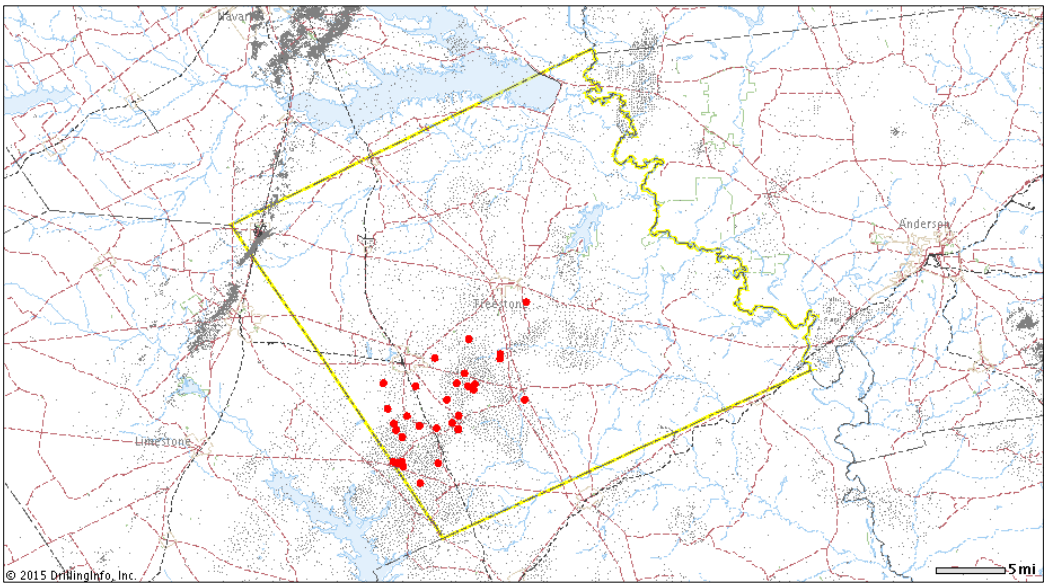

Fig. 4. 10— Bossier reservoir wells snapshot (Thirty wells were selected from Freestone County in Texas)

4.7 Results and Discussion

In this section, we explain the decision making model developed for tight gas sand reservoirs. As mentioned before, there are several crucial parameters in fracturing fluid selection which are selected based on experts' opinions. We provided details on the process of variable selection in the data gathering section of this chapter. The objective of this study was to predict fracturing fluid in tight gas sand reservoirs. The step by step process for this purpose was as follow:

After variables affecting the decision tree were selected, similar fluid types were lumped into general categories, in order to improve prediction capability of the model.

Lumping reduced the fluid types from 31 to 5 general categories: CO_2/N_2/foam, CO_2/N_2/foam assisted hybrid, low concentrate gel, slick water, hybrid gel, and crosslinked gel. The distribution of the fluid categories is illustrated in **Fig. 4.11.** Crosslinked gel and slick water treatments were the most and the least applied fracturing fluid categories, respectively, among the selected wells.

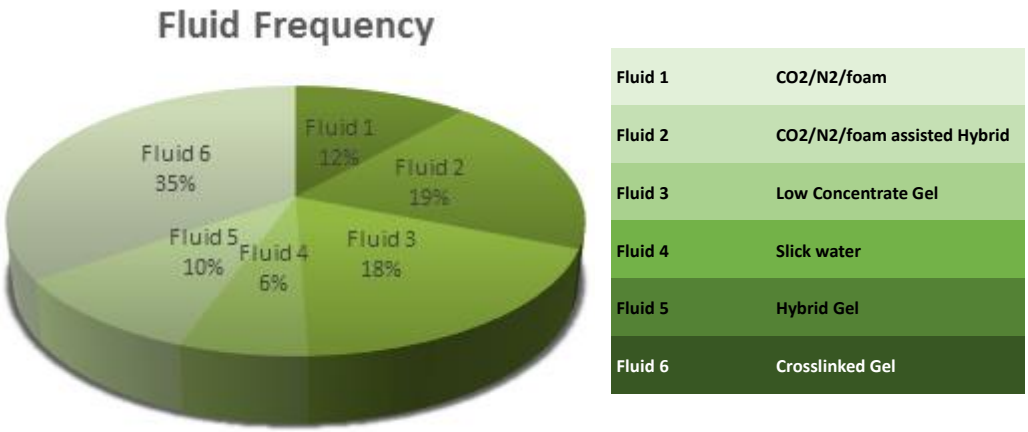

Fig. 4. 11— Fracturing fluid categories distribution in the selected dataset.

There is a minimum acceptable number of trees for each case to reach a reliable outcome. Although in our case this value is approximately 50 trees, we generated 500 trees to ensure the stabilization of OOB error (**Fig. 4.12**). The performance for a smaller number of variables can usually be improved by increasing the number of trees. As a rule of thumb, 500 to 1,000 trees were generated in each random forest run. We generated 500 trees in each run and then repeated this procedure 100 times.

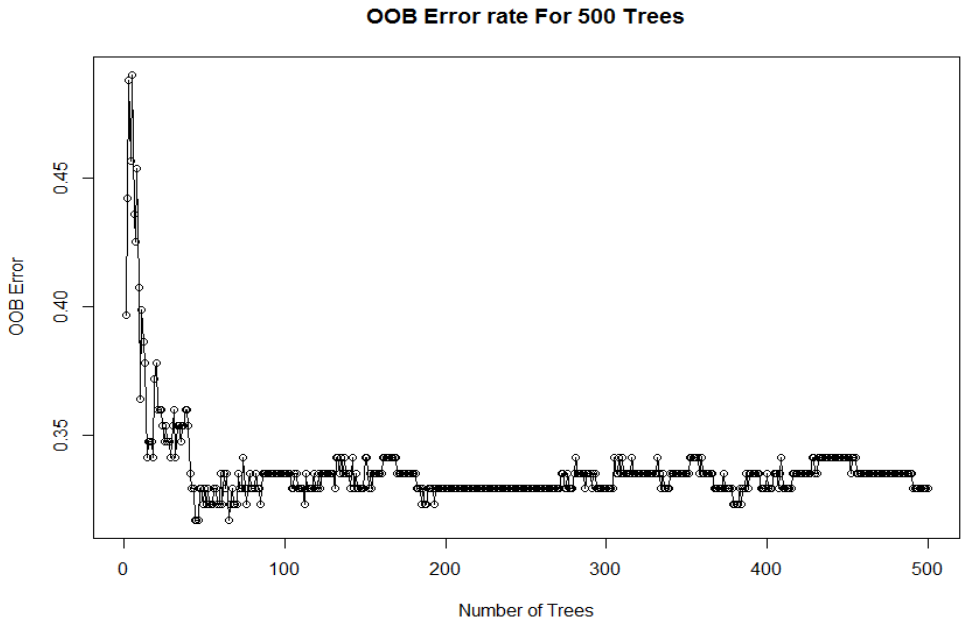

Fig. 4. 12— Minimum number of acceptable trees for the applied dataset.

Two trees with the lowest OOB error were nominated for the selection of the best decision tree in predicting the appropriate hydraulic fracturing fluids in tight gas sand reservoirs. **Fig. 4.13** illustrates the first tree, which was generated in the first run. This tree has 38 nodes and the OOB error in this case was 29.02%. In **Fig. 4.14** shows the other candidate tree with 19 nodes and 28.54% OOB error. The OOB errors in these cases are similar and additional analysis is required to select the best decision tree. The calculated OOB in each case shows the deviation from dataset. There is a possibility that the selected fracturing fluids in some wells were not the most appropriate treatments, although they have resulted in production enhancement. Therefore, the calculated OOB

error identifies the deviation from the dataset. Experts' opinions are required for improving the accuracy of the result produced by a decision tree.

The next step was to check the validity and reliability of the proposed decision trees. In general, the more nodes in the tree leads to less accuracy in prediction by the tree. As the number of nodes increases, the risk of overfitting also increases (Breiman 2001). **Fig. 4.15** illustrates the accuracy of the models versus number of nodes in each tree. The result shows that the tree with 19 nodes is more accurate and reliable based on the prepared dataset.

The final step was to calculate the variables importance and to determine the most important variables in the process of fracturing fluids selection in tight gas sand reservoirs. **Fig. 4.16** shows that the BHT and Young's modulus of the lower barrier are the most and the least important variables in this process, respectively.

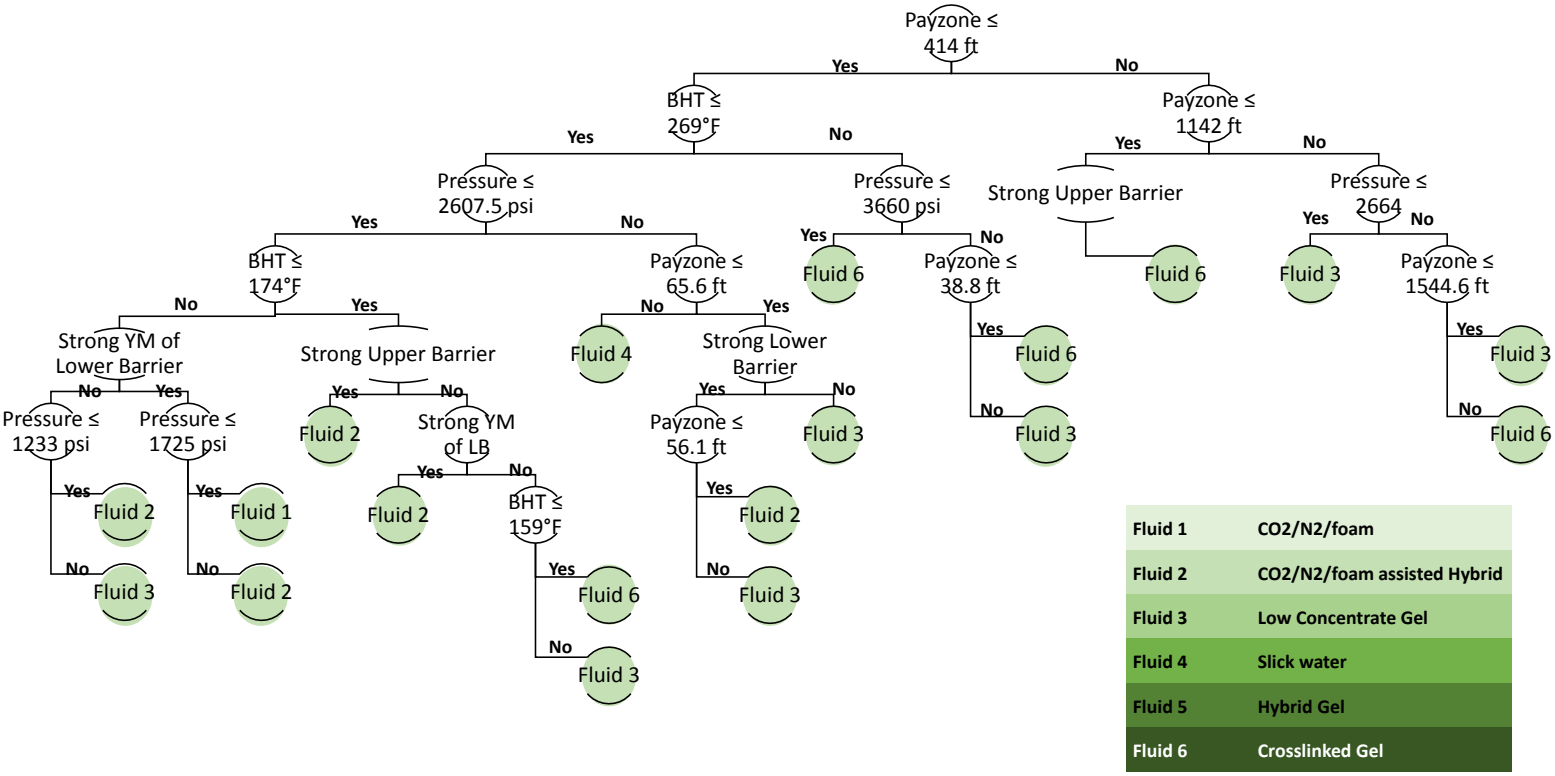

Fig. 4. 13— The decision tree generated in the first run with 38 nodes and 29.02% OOB error. YM and LB are the abbreviations of Young's modulus and lower barrier, respectively.

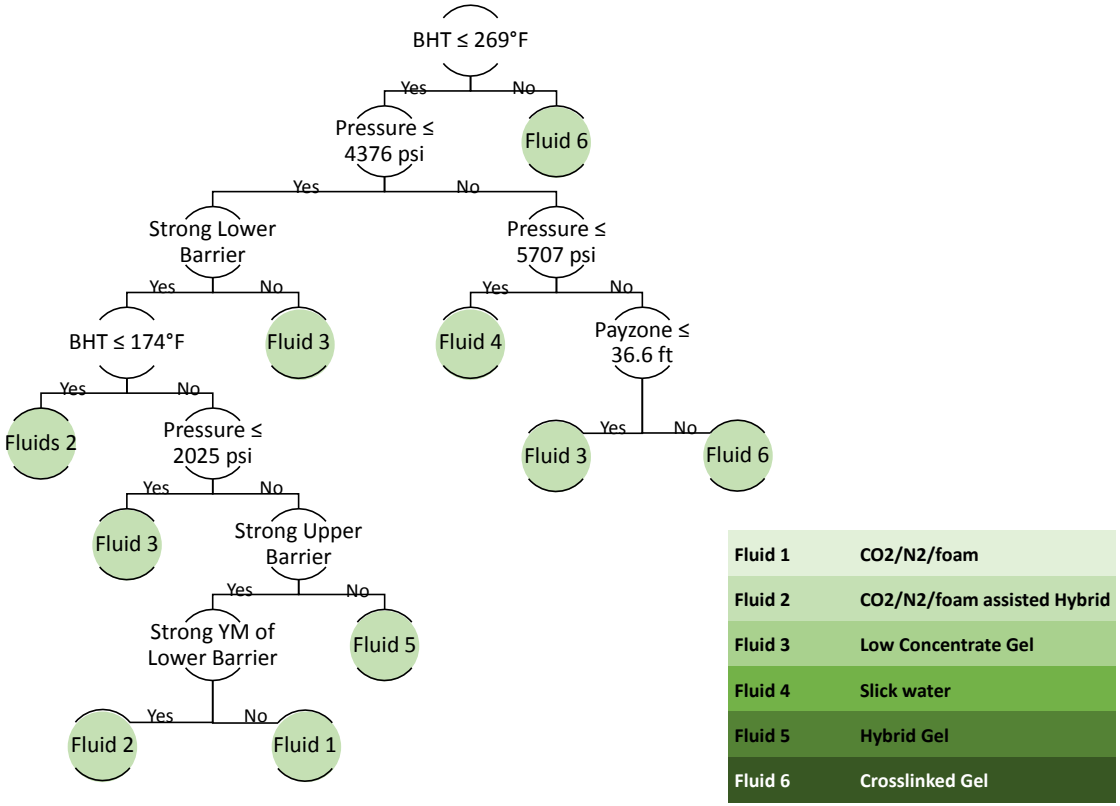

Fig. 4. 14— The decision tree generated in the 47th run with 38 nodes and 28.54% OOB error. YM and LB are the abbreviations of Young's modulus and lower barrier, respectively.

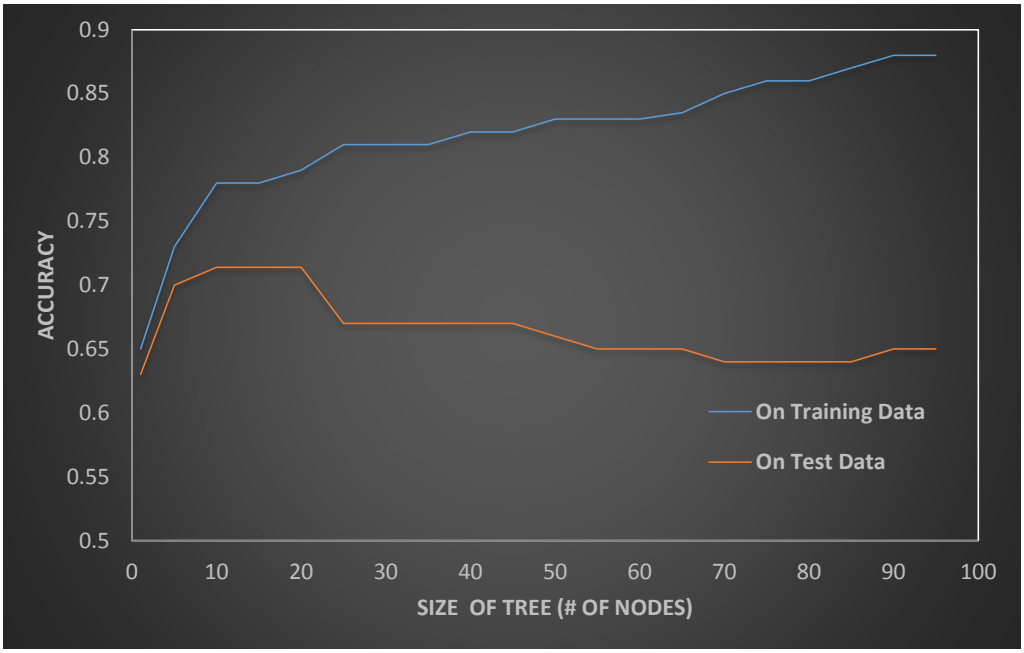

Fig. 4. 15— Accuracy of the two proposed models with 38 and 19 nodes versus size of tree

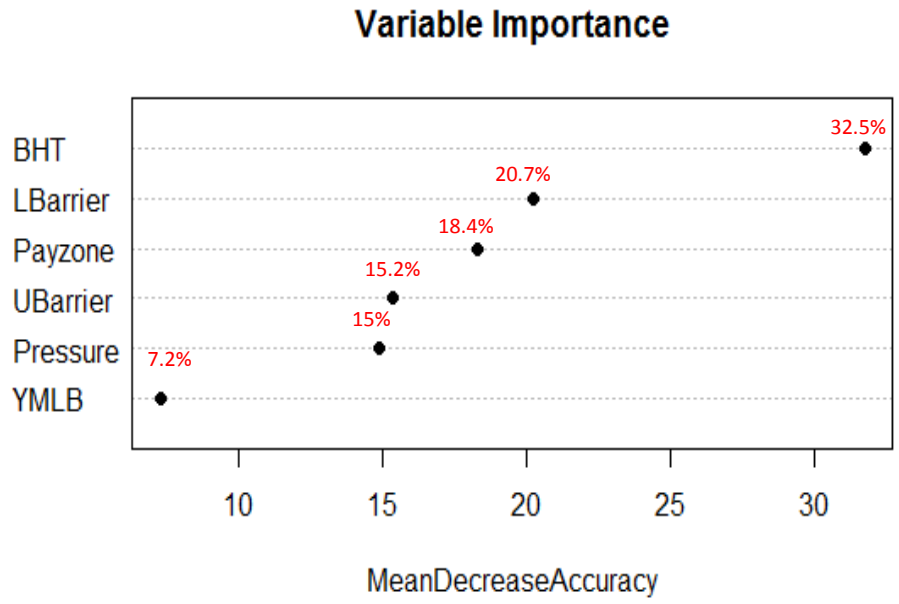

Fig. 4. 16— Applied variables versus mean decrease accuracy (LBarrier, UBarrier and YMLB are the abbreviations of lower barrier, upper barrier, and Young's modulus of lower barrier, respectively)

4.8 Conclusions

The application of random forest on the dataset of 164 wells from five different tight gas sand reservoirs in Texas, showed that random forest could be successfully applied to develop a decision tree for selection of hydraulic fracturing fluids. The random forest technique is powerful in its ability to break up complex data and handle various types of data that includes categorical, continuous, and missing values. The following conclusions can be drawn from the results observed in this study:

1. The model statistically inferred from a set of well data can be successfully applied to hydraulic fracturing fluid selection, to enhance hydraulic fracturing design.
2. The advantage of the developed model based on random forest algorithm, compared to conventional statistical approaches is its ability to cope with complex datasets by randomization.
3. The tree with 19 nodes was more reliable than the one with 39 nodes.
4. This model can handle a combination of factors and continuous variables for fracturing fluid selection.
5. With data from 164 well and 6 selected influential variables, we reached the OOB error of 28.54%.
6. Bottom-hole temperature, pay zone thickness, and mechanical strength of lower barrier were found to be the most influential parameters for fluid selection which complied with our expectation.

7. Pressure gradient and mechanical strength of the upper barrier were only marginally important in this fracturing fluid selection.
8. CO_2/N_2/foam assisted hybrid fluid was the best predicted by our model with an error of approximately 20%.

CHAPTER V

CONCLUSIONS AND RECOMMENDATIONS

This work can be categorized into 3 main sections. In the first part, the effects of mono and divalent cations on the rheological properties of high-pH borate crosslinked guar-based polymer were examined at high temperature conditions. The second part of this dissertation described the application of EDTA in flowback fluids for enhanced TDS tolerance of the base fluid in future hydraulic fracturing jobs. Finally, in the last section we constructed a decision making model for fracturing fluid selection for optimized hydraulic fracturing in tight gas sand reservoirs. This section reiterates important conclusions from each chapter of the dissertation. Main conclusions are reiterated, and recommendations regarding future research are provided.

5.1 Effect of Dissolved Solids on Reuse of Produced Water at High Temperature in Hydraulic Fracturing Jobs

1. The results show that the high-pH borate crosslinked guar-based polymer fluid has a reasonable quality without compromising the required functionality at temperatures up to 305 °F (152 °C).
2. Potassium and calcium ions exhibit tolerable limits for the reuse of flowback fluids in future hydraulic fracturing jobs.

3. More than 97 and 75% of reported samples had acceptable ion concentrations at temperatures up to 305 °F (152 °C), respectively.
4. Magnesium and sodium are the controlling ions, and about 30 and 40% of flowback fluids need treatment to reduce the concentrations of these ions at temperatures up to 305 °F (152 °C), respectively.
5. The viscosity measurements are valid in shear rates up to 80-100 s^{-1}. This range is more applicable in decision making in comparison with previous reported value (10 s^{-1}). The apparent viscosities at higher shear rates are very close and indistinguishable.
6. The proposed fluid with the maximum acceptable TDS from flowback fluids shows acceptable proppant transport and handling capability of the fluid. This fluid performs very well in SAOS and static settling tests.

Results show that flowback fluids can be reused in hydraulic fracturing with minimum treatments regarding ion contents at low and high temperatures.

5.2 A Feasibility Study of Reusing Flowback Fluids in Hydraulic Fracturing Treatments

Static and dynamic rheological measurements and proppant static settling tests were conducted using a high-pH guar/borate crosslinked system. Two monovalent cations (sodium and potassium) and two divalent cations (calcium and magnesium) were

tested at temperatures up to 305°F. EDTA, polymer loading, and high pH improved the tolerable salinity of the base hydraulic fracturing fluid. Conclusions from this section is as follows:

1. Viscosity of the fracturing fluid was enhanced by adding 2 wt% EDTA and tolerance for the maximum acceptable concentrations of calcium and magnesium was increased to 60% and 82.7%, respectively.
2. Increasing pH of the base fluid allows for higher concentrations of sodium and potassium in the fluid.
3. EDTA resulted in 15% reduction in polymer loading at 225°F.
4. The thermal stability of the fluids containing EDTA was higher compared to fluids without EDTA.
5. Apparent viscosities of base fluids containing EDTA were increased by approximately 36-95%, compared to base fluids without EDTA, at different temperatures.
6. Presence of the chelating agent increased the G' and G" values by an order of magnitude at 225°F.
7. Proppant settling characteristics of the proposed fluid were similar to the fluid prepared with fresh water.
8. It is technically practicable to use EDTA in the reuse of flowback fluids in hydraulic fracturing jobs.

5.3 A Robust Advisory System for Selection of Fracturing Fluid in Tight Gas Sand Reservoirs

The application of random forest on the dataset of 164 wells from five different tight gas sand reservoirs in Texas, showed that random forest could be successfully applied to develop a decision tree for selection of hydraulic fracturing fluids. The following conclusions can be drawn from the results observed in this chapter:

1. The model built using well data can be successfully applied for enhanced decision making in hydraulic fracturing fluid selection.
2. The benefit of the developed model based on random forest algorithm, compared to conventional statistical approaches, is its ability to cope with complex datasets by randomization.
3. Between the two candidate decision trees that were selected based on prediction statistics, the tree constructed using19 nodes was more reliable than the one with 39 nodes.
4. The developed model is capable of handling a combination of factors and continuous variables for fracturing fluid selection.
5. With data from 164 well and 6 selected influential variables, an OOB error of 28.54% was obtained.
6. Bottom-hole temperature, pay zone thickness, and mechanical strength of lower barrier were among the most influential parameters for fluid selection.

7. Pressure gradient and mechanical strength of the upper barrier were only marginally important in the fracturing fluid selection.
8. CO_2/N_2/foam assisted hybrid fluid was the best predicted by our model with an error of approximately 20%.

5.4 Recommendations

Although this dissertation contributes to the reuse of flowback fluids as a viable practice in hydraulic fracturing jobs and focuses on optimizing fracturing fluid selection, there remains many areas in hydraulic fracturing that requires further research. The following lists the recommendations for possible future research:

1. An investigation of the impact of bacteria, dissolved/soluble organic, dispersed hydrocarbons, and other flowback contents on the feasibility of flowback fluids reuse in hydraulic fracturing.
2. Construction of a robust advisory model for selection of optimum treatments to enhance reuse of flowback fluids in hydraulic fracturing jobs.
3. An investigation on the impact of different types of chelating agents on TDS tolerance alterations of flowback fluids used as a base fluid in hydraulic fracturing.
4. Enhancement of the developed fracturing fluid selection model by incorporating additional parameters such as presence of natural fractures and fracture half-

length, as well as inclusion of more accurate data on mechanical and elastic properties of the barriers.

5. Performing experiments to measure viscosity for an analysis on the effect of additives in flowback fluid on the breaking process of hydraulic fracture fluids.
6. Selection of compatible breakers for the reuse of flowback fluids in hydraulic fracturing.
7. Conducting coreflood experiments to investigate the effect of additives in flowback fluid on fracture conductivity and formation damage.
8. Development of fracturing fluid selection advisory model for enhanced hydraulic fracture jobs in other unconventional resources such as organic-rich shale reservoirs.

REFERENCES

Ali, J.K. 1994. Neural networks: a new tool for the petroleum industry. *paper SPE, 27561*: 15-17.

Ali, A.H.A., Frenier, W.W., Xiao, Z., and Ziauddin, M. 2002. Chelating Agent-Based Fluids for Optimal Stimulation of High-Temperature Wells. Presented at the SPE Annual Technical Conference and Exhibition, San Antonio, Texas, 29 September-2 October. SPE-77366-MS. doi:10.2118/77366-MS.

Amit, Y. and Geman, D. 1997. Shape quantization and recognition with randomized trees. *Neural computation* **9** (7): 1545-1588.

Anifowose, F.A. 2013. Ensemble Machine Learning: The Latest Development in Computational Intelligence for Petroleum Reservoir Characterization. Society of Petroleum Engineers. doi:10.2118/168111-MS

Arthur, J.D., R., Bohm, B., Layne, M., and Shaiebly, T. 2010. Mixing and Scale Affinity Model for Hydraulic Fracturing Fluids. Presented to the International Petroleum and Bio-fuels Environmental Conference, San Antonio, TX August 31-September 2.

Arthur, J.D., Langhus, B.G., and Patel, C. 2005. Technical Summary of Oil & Gas Produced Water Treatment Technologies. ALL Consulting, LLC. 53 p.

Aulia, A., Rahman, A., and Quijano Velasco, J.J. 2014. Strategic Well Test Planning Using Random Forest. Society of Petroleum Engineers. doi:10.2118/167827-MS

Blauch, M.E. 2010. Developing Effective and Environmentally Suitable Fracturing Fluids Using Hydraulic Fracturing Flowback Waters. Presented at the SPE Unconventional Gas Conference, Pittsburg, Pennsylvania, 23-25 February. SPE-131784-MS. doi:10.2118/131784-MS.

Bryant, J.E. and Haggstrom, J. 2012. An Environmental Solution to Help Reduce Freshwater Demands and Minimize Chemical Use. Presented at the SPE/EAGE European Unconventional Resources Conference and Exhibition, Vienna, Austria, 20-22 March. SPE-153867-MS.doi:10.2118/153867-MS.

Bunger, A.P., McLennan, J., and Jeffrey, R. 2013. *Effective and Sustainable Hydraulic Fracturing*. Brisbane: InTech. doi: 10.5772/45724.

Breiman, L. 2001. Random forests. *Machine learning*, **45** (1): 5-32.

Breiman, Leo. 1996. Bagging predictors. *Machine learning* **24** (2): 123-140.

Clark, C.E. and Veil, J.A. 2009. Produced Water Volumes and Management Practices in the United States. No. ANL/EVS/R-09-1. Argonne National Laboratory (ANL), Chicago, Illinois.

Condon, S.M. and Dyman, T.S. 2003. 2003 Geologic assessment of undiscovered conventional oil and gas resources in the Upper Cretaceous Navarro and Taylor Groups, Western Gulf Province, Texas.

Cutler, A. and Zhao, G. 2001. Pert-perfect random tree ensembles. *Computing Science and Statistics*, **33**: 490-497.

de Kruijf, A.S., Roodhart, L.P., and Davies, D.R. 1993. Relation between Chemistry and Flow Mechanics of Borate Crosslinked Fracturing Fluids. *SPE Prod & Fac*. **8** (3): 165-170.

Dietterich, T.G. 2000. An experimental comparison of three methods for constructing ensembles of decision trees: Bagging, boosting, and randomization. *Machine learning*, **40** (2): 139-157.

Dyman, T.S. and Condon, S.M. 2006. *Assessment of undiscovered conventional oil and gas resources--Upper Jurassic-Lower Cretaceous Cotton Valley group, Jurassic Smackover interior salt basins total petroleum system, in the East Texas basin and Louisiana-Mississippi salt basins provinces* (No. 69-E-2).

Fedorov, A., Carrasquilla, J., and Cox, A. 2014. Avoiding Damage Associated to Produced Water Use in Hydraulic Fracturing. Presented at the SPE International Symposium and Exhibition on Formation Damage Control, Lafayette, Louisiana, 26-28 February. SPE-168193-MS. doi:10.2118/168193-MS.

Fedorov, A.V., Fu, D., Mullen, K., Kochmar, L., Lungwitz, B.R., and Dessinges, M.N. 2010. Efficient Hydraulic Fracturing Treatments in Western Siberia Using Produced Formation Water. Presented at the SPE Russian Oil & Gas Technical Conference and Exhibition, Moscow, Russia, 26-28 October. SPE-131729-MS. doi:10.2118/131729-MS.

Fischer, C.C., Navarrete, R.C., Constien, V.G., Coffey, M.D., and Asadi, M. 2001. Novel Application of Synergistic Guar/Non-Acetylated Xanthan Gum Mixtures in Hydraulic Fracturing. Presented at the SPE International Symposium on

Oilfield Chemistry, Houston, Texas, 13-16 February. SPE-65037-MS. doi:10.2118/65037-MS.

Fontenelle, L.K., Weston, M., Lord, P., and Haggstrom, J. 2013. Recycling Water: Case Studies in Designing Fracturing Fluids Using Flowback, Produced, and Nontraditional Water Sources. Presented at the SPE Latin American and Caribbean Health, Safety, Social Responsibility, and Environment Conference, Lima, Peru, 26-27 June. SPE-165641-MS. doi:10.2118/165641-MS.

Fredd, C.N. and Fogler, H.S. 1998. Alternative Stimulation Fluids and Their Impact on Carbonate Acidizing. *SPE J.* **13** (1): 34-41. SPE-57469-PA. doi:10.2118/31074-PA.

Frenier, W.W., Rainey, M., Wilson, D., Crump, D., and Jones, L. 2003. A Biodegradable Chelating Agent is Developed for Stimulation of Oil and Gas Formations. Presented at the SPE/EPA/DOE Exploration and Production Environmental Conference, San Antonio, Texas, 10-12 March. SPE-80597-MS. doi:10.2118/80597-MS.

Guerra, K., Dahm, K., and Dundorf, S. 2011. Oil and Gas Produced Water Management and Beneficial Use in the Western United States, U.S. Department of Interior Bureau of Reclamation, September.

Gupta, D.V.S., Carman, P., and Nguyen, S. 2013. Does Lack of Fresh Water Restrict Unconventional Gas Exploration in the Middle East? Can we Frac with Seawater? Paper 293 was presented at the ADIPEC Technical Conference, Abu Dhabi, UAE, 10-13 November.

Gupta, D.V.S., Carman, P., and Venugopal, R. 2012a. High-Density Brine-Based Fracturing Fluid for Ultra-Deep Fracturing Stimulation. Paper SPE 159822 presented at the SPE Annual Technical Conference and Exhibition, San Antonio, Texas, USA, 8-10 October 2012.

Gupta, D.V.S., Carman, P., and Venugopal, R. 2012b. A Stable Fracturing Fluid for Produced Water Applications. Paper SPE 159837 presented at the SPE Annual Technical Conference and Exhibition, San Antonio, Texas, USA, 8-10 October.

Haghshenas, A. and Nasr-El-Din, H.A. 2014. Effect of Dissolved Solids on Reuse of Produced Water at High Temperature in Hydraulic Fracturing Jobs. *Journal of Natural Gas Science and Engineering*, **21**, 316-325. doi: 10.1016/j.jngse.2014.08.013.

Harris, P.C. and Heath, S. 2009. Proppant Transport of Fracturing Gels is Influenced by Proppant Type. Presented at the SPE Hydraulic Fracturing Technology Conference, The Woodlands, Texas, 19-21 January. SPE-118717-MS. doi: 10.2118/118717-MS.

Harris, P.C., Walters, H.G., and Bryant, J. 2009. Prediction of Proppant Transport from Rheological Data. *SPE Prod & Oper Journal*. **24** (4): 550-555. SPE-115298-PA. http://dx.doi.org/10.2118/115298-PA.

Harris, P.C., Morgan, R.G., and Heath, S.J. 2005. Measurement of Proppant Transport of Frac Fluids. Paper SPE 95287 presented at the SPE Annual Technical Conference and Exhibition, Dallas, Texas, USA, 9-11 October, doi: 10.2118/95287-MS.

Harris, P.C. and van Batenburg, D. 1999. A Comparison of Freshwater- and Seawater-Based Borate-Crosslinked Fracturing Fluids. Presented at the SPE International Symposium on Oilfield Chemistry, Houston, Texas, 16-19 February. SPE-50777-MS. doi:10.2118/50777-MS.

Ho, T.K. 1998. The random subspace method for constructing decision forests. *Pattern Analysis and Machine Intelligence, IEEE Transactions on,* **20** (8): 832-844.

Ho, T.K. 1995. Random decision forests. In *Document Analysis and Recognition, 1995., Proceedings of the Third International Conference on* (Vol. 1, pp. 278-282). IEEE.

Hassen, B. R., Zotskine, Y., and Gulewicz, D. 2012. Hydraulic Fracture Containment in the Bakken with a Synthetic Polymer Water Based Fracture Fluid. Presented at the SPE Canadian Unconventional Resources Conference, Calgary, Alberta, 30 October-1 November. SPE-162670-MS. doi:10.2118/162670-MS.

Khair, E.M.M., Shicheng, Z., Shanbo, M., and Mei, Z. 2011. Performance and Application of New Anionic D3F-AS05 Viscoelastic Fracturing Fluid. *Journal of Petroleum Science and Engineering*, **78** (1): 131-138.

Le, H. and Wood, R. 1992. New frac fluid enhances options for offshore wells. *Ocean industry* **27** (2): 49-52.

Liaw, A. and Wiener, M. 2002. Classification and regression by randomForest.*R news*, **2** (3): 18-22.

Loveless, D., Holtsclaw, J., Saini, R., Harris, P., and Fleming, J. 2011. Fracturing Fluid Comprised of Components Sourced Solely from the Food Industry Provides

Superior Proppant Transport. Paper SPE 147206 presented at the SPE Annual Technical Conference and Exhibition, Denver, Colorado, USA, 30 October-2 November.

Malpani, R.V. 2007. *Selection of fracture fluid for stimulating tight gas reservoirs* (Doctoral dissertation, Texas A&M University).

Martell, A.E. and Calvin, M. 1952. Chemistry of Metal Chelate Compounds, Chap. 10, 471 – 513. Englewood Cliffs, New Jersey: Prentice-Hall Chemistry Series, Prentice-Hall.

Mavko, G., Mukerji, T., and Dvorkin, J. 2009. *The rock physics handbook: Tools for seismic analysis of porous media*. Cambridge university press.

Maucec, M., Singh, A.P., Bhattacharya, S., Yarus, J. M., Fulton, D.D., and Orth, J.M. 2015. Multivariate Analysis and Data Mining of Well-Stimulation Data by Use of Classification-and-Regression Tree with Enhanced Interpretation and Prediction Capabilities. Society of Petroleum Engineers. doi:10.2118/166472-PA

Mehrgini, B., Memarian, H., Fotouhi, A., and Moghanian, M. 2014. Recognising the Effective Parameters and their Influence on Candidate-Well Selection for Hydraulic Fracturing Treatment by Decision Making Method. International Petroleum Technology Conference. doi:10.2523/IPTC-17768-MS

Nasr-El-Din, H.A. and Taylor K.C. 1996. Rheology of Water-Soluble Polymers used for Improved Oil Recovery. In *Multiphase Rea3ctor and Polymerization System Hydrodynamics*, ed. N.P. Cheremisinoff, Chap. 24, 615-668. Houston: Gulf Publishing Company.

Newsham, K.E., Rushing, J.A., Chaouche, A. and Bennion, D.B. 2002. Laboratory and Field Observations of an Apparent Sub Capillary-Equilibrium Water Saturation Distribution in a Tight Gas Sand Reservoir. *paper SPE,75710*: 5-8.

Pezron, E., Ricard, A., and Leibler, L. 1990. Rheology of galactomannan-borax gels. *J. Polym. Sci. B Polym. Phys*. **28** (13): 2445–2461. doi: 10.1002/polb.1990.090281301.

Putzig, D.E. and St. Clair, J.D. 2007. A New Delay Additive for Hydraulic Fracturing Fluids. Presented at the SPE Hydraulic Fracturing Technology Conference, College Station, Texas, 29-31 January. SPE-105066-MS. doi:10.2118/105066-MS.

Rickman, R., Mullen, M.J., Petre, J.E., Grieser, W.V., and Kundert, D. 2008. A practical use of shale petrophysics for stimulation design optimization: All shale plays are not clones of the Barnett Shale. In *SPE Annual Technical Conference and Exhibition*. Society of Petroleum Engineers.

Rushing, J. A., Newsham, K.E., and Blasingame, T.A. 2008. Rock Typing: Keys to Understanding Productivity in Tight Gas Sands. Society of Petroleum Engineers. doi:10.2118/114164-MS

Shaughnessy, C.M. and Kline, W.E. 1983. EDTA Removes Formation Damage at Prudhoe Bay. *Journal of Petroleum Technology*, **35** (10): 1783-1791. SPE-11188-PA. doi:10.2118/11188-PA.

Shipman, S., McConnell, D., Mccutchan, M.P., and Seth, K. 2013. Maximizing Flowback Reuse and Reducing Freshwater Demand: Case Studies from the

Challenging Marcellus Shale. Presented at the SPE Eastern Regional Meeting, Pittsburg, Pennsylvania, 20-22 August. SPE-165693-MS. doi:10.2118/165693-MS.

Sitouah, M., Salmeen, M., Oyemakinde, S., Anifowose, F., and Abdullatif, O. 2013. Permeability Prediction from Specific Area, Porosity and Water Saturation using Extreme Learning Machine and Decision Tree Techniques: A Case Study from Carbonate Reservoir. Society of Petroleum Engineers. doi:10.2118/164161-MS

Spain, D.R., Liu, S., and Devier, C. 2011. Petrophysical rock typing in tight gas sands: Beyond porosity and saturation—An example from the Cotton Valley formation. In *East Texas: Middle East Unconventional Gas Conference and Exhibition, SPE* (Vol. 142808).

Stepan, D.J., Shockey, R.E., Kurz, B.A., Kalenze, N.S., Cowan, R.M., Ziman, J.J., and Harju, J.A. 2010. Bakken Water Opportunities Assessment-Phase 1. The University of North Dakota's Energy and Environmental Research Center (EERC), Grand Forks, North Dakota, April.

Trabelsi, A. 1994. Canyon sand--SW Texas example of a low permeability gas reservoir. *Oil and Gas Journal;(United States)*, **92** (19).

Turner, C.E., Peterson, F., Dyman, T.S., and Cook, T. 2008. *Geologic Controls on the Growth of Petroleum Reserves*. US Geological Survey.

Veil, J.A. 2010. Water Management Technologies Used by Marcellus Shale Gas Producers. Final Report. Presented for the United States Department of Energy, National Energy Technology Laboratory. DOE Award NO.: FWP 49462. July.

Voneiff, G., Sadeghi, S., Bastian, P., Wolters, B., Jochen, J., Chow, B., … Gatens, M. 2014. Probabilistic Forecasting of Horizontal Well Performance in Unconventional Reservoirs Using Publicly-Available Completion Data. Society of Petroleum Engineers. doi:10.2118/168978-MS

Voneiff, G., Sadeghi, S., Bastian, P., Wolters, B., Jochen, J., Chow, B., … Gatens, M. 2013. A Well Performance Model Based on Multivariate Analysis of Completion and Production Data from Horizontal Wells in the Montney Formation in British Columbia. Society of Petroleum Engineers. doi:10.2118/167154-MS

Wiskofske, M., Wiggins, M., and Yaritz, J. 1997. Low-Polymer Borate Frac Fluid Cleans Up Thoroughly, *Oil and Gas Journal*, **95** (37): 42-45.

Yount, W.C., Loveless, D.M., and Craig, S.L. 2005. Small-Molecule Dynamics and Mechanisms Underlying the Macroscopic Mechanical Properties of Coordinatively Cross-Linked Polymer Networks. *Journal of American Chemical Society*, **127** (41): 14488-14496.

Zhixi, C., Mian, C., Yan, J., and Rongzun, H. 1997. Determination of rock fracture toughness and its relationship with acoustic velocity. *International Journal of Rock Mechanics and Mining Sciences*, **34** (3): 49-e1.